N73-18011
NASA CR-2188

NASA CONTRACTOR REPORT

NASA CR-2188

ANALYTICAL PARAMETRIC INVESTIGATION OF LOW PRESSURE RATIO FAN NOISE

by F. B. Metzger, D. B. Hanson, R. W. Menthe, and G. B. Towle

Prepared by
HAMILTON STANDARD
Windsor Locks, Conn. 06096
for Langley Research Center

NATIONAL AERONAUTICS AND SPACE ADMINISTRATION • WASHINGTON, D. C. • MARCH 1973

1. Report No.	2. Government Accession No.	3. Recipient's Catalog No.
NASA CR-2188		

4. Title and Subtitle	5. Report Date
Analytical Parametric Investigation of Low Pressure Ratio Fan Noise	March 1973
	6. Performing Organization Code
7. Author(s)	8. Performing Organization Report No.
F. B. Metzger, D. B. Hanson, R. W. Menthe, G. B. Towle	HSER 5990
	10. Work Unit No.
9. Performing Organization Name and Address	11. Contract or Grant No.
Hamilton Standard Division of United Aircraft Corporation Windsor Locks, Connecticut 06096	NAS1-10896
	13. Type of Report and Period Covered
12. Sponsoring Agency Name and Address	Contractor Report
National Aeronautics and Space Administration Washington, D.C. 20546	14. Sponsoring Agency Code

15. Supplementary Notes

16. Abstract

The results of an analytical study are reported which shows the effect of various physical and operating parameters on noise produced by low pressure ratio propulsive fans operating at subsonic top speeds. Acoustical duct lining effects are included in the study. The concepts used to develop the noise theory used in the study, as well as the correlation between the theory and model test results are also presented. It is shown that good correlation has been established between theory and experiment. Using the theory, it is shown that good aerodynamic design, maximum acceptable fan solidity, low tip speed operation and use of few blades and vanes leads to the lowest noise levels. Typical results of the study indicate that a fan operating at 1.2 fan pressure ratio and 700 ft/second tip speed with 12 blades and 7 vanes and including modest acoustic treatment on the duct walls would produce levels allowing a 100,000 lb. STOL aircraft to meet a noise level objective of 95 PNdB at 500 ft at takeoff.

17. Key Words (Suggested by Author(s))	18. Distribution Statement
Acoustical Duct Lining Low Pressure Ratio Fan Noise STOL Noise Propulsion Noise Turbomachinery Noise	Unclassified - Unlimited

19. Security Classif. (of this report)	20. Security Classif. (of this page)	21. No. of Pages	22. Price*
Unclassified	Unclassified	116	$3.00

*For sale by the National Technical Information Service, Springfield, Virginia 22151

CONTENTS

CONTENTS (Cont.)

CONTENTS (Cont.)

Page

FIGURES

ANALYTICAL PARAMETRIC INVESTIGATION OF LOW PRESSURE RATIO FAN NOISE

BY F.B. METZGER, D.B. HANSON, R.W. MENTHE, G.B. TOWLE
HAMILTON STANDARD DIVISION OF UNITED AIRCRAFT CORPORATION

SUMMARY

A study has been conducted using a new calculation method developed to predict noise generated by subsonic tip speed, low pressure ratio fans. Estimates using this method are shown to correlate well with test data available for this new class of propulsive fans.

Source noise due to rotor and stator sources is included in the method. The calculation procedure assumes that rotor tone noise is due to inflow distortion present under even the most ideal test conditions. The rotor broadband noise calculation procedure is similar to that used to predict high frequency vortex noise in unshrouded propellers. The stator tone and broadband noise calculation procedure is based on a new theory which shows the result of interaction between rotor blade wakes and the stators. In this theory the effect on stator noise of unsteadiness in the blade wakes is considered.

It is concluded in this report that optimized low pressure ratio, low tip speed fans differ significantly from current generation supersonic tip speed turbofans and subsonic versions of these same turbofans. Reduction in tip speed and pressure ratio and increase in fan solidity were found to be the most significant factors in reducing noise for a given thrust. At pressure ratios from 1.1 to 1.25 the optimum blade count was found to be near 12 in contrast to the large number of blades used in conventional turbofans. At lower pressure ratios which are of interest for general aviation aircraft, tracked air cushion vehicles, and surface effect vehicles, the optimum number of blades was less than 12. Minimum stator vane count consistent with avoiding rotor excitation was found to produce minimum noise. A vane count of 7 appears to be the best choice. This small number of vanes is found optimum in contrast to the large vane counts of turbofans because acoustic cutoff of tone noise due to rotor stator interaction has little influence on the perceived noise level of these new low pressure ratio fans.

Duct lining to further reduce fan noise was also investigated. It was found that reductions in perceived noise level of 5 dB can be achieved with relatively simple duct wall treatment consisting of the perforated plate and honeycomb structures used in conventional turbofans. An attenuation of up to 11 dB appears feasible with additional treatment.

The results of the study indicate that large STOL aircraft in the 45,360 kg gross weight class can be designed using low pressure ratio propulsive fans to meet levels at or below 95 PNdB at 152 m. By use of lower pressure ratios and additional duct treatment, significantly lower levels can be achieved in tracked air cushion vehicles, surface effect vehicles and general aviation aircraft.

INTRODUCTION

For many years it has been recognized that increased bypass ratio can reduce turbofan noise. Recently, with the emphasis on further quieting of turbofans, reduction in tip speed as a further means of noise reduction is being explored in the NASA Quiet Engine program. Also a continuing program has been underway at NASA and in industry to improve fan duct acoustic treatment to reduce noise. With the developing interest in a STOL transport, an optimization of all operating and configuration parameters including increased bypass ratio (reduced pressure ratio), reduced tip speed, and application of duct lining appears necessary if stringent low noise objectives are to be met. The characteristics of this new class of low pressure ratio fans is defined in figure 1. It can be seen that they lie between unshrouded propellers and conventional supersonic tip speed turbofans in their characteristics. For propulsion of general aviation aircraft, surface effect vehicles, and tracked air cushion vehicles, pressure ratios as low as 1.05 are considered acceptable. However, as used in most transport aircraft applications these fans fall into the following category:

Fan Pressure Ratio	1.1 to 1.3
Bypass Ratio	30 to 10
Number of Blades	7 to 23
Tip Speed	183 to 274 m/s

Of course, the larger fan diameter that provides a good match between the takeoff and cruise requirements for a STOL transport requires a new technology to achieve a good performance-weight tradeoff. This must be achieved by use of a new lightweight blade technology and by use of variable pitch for reverse thrust to eliminate conventional thrust reversers. Further details on both of these subjects which are outside the scope of this study can be found in references 1 and 2.

Early in 1970 Hamilton Standard embarked on the development of a theoretical method for estimating low pressure ratio fan noise. Although little success had been achieved to date in estimating noise of conventional supersonic tip speed turbofans, it was believed that the simpler aerodynamics and more easily modeled acoustics of the subsonic tip speed low pressure ratio fans could be successfully evaluated by a theoretical method. A model test late in 1970 showed that these subsonic tip speed fans did in fact produce a more easily understood acoustic signature that could be evaluated by basic source theories. This method has been used in the study summarized in this report.

In conducting this study, initial work was done to (1) define the range of applicability of the noise theory, (2) define the parameters that affected noise, and (3) establish the range of the parameters which would show significant changes in noise. Also the potential of duct lining was explored in an initial study to determine the best location for treatment,

the most effective type of treatment, and the level of suppression on the various configurations studied. After this initial study the range of variables was established and detailed calculations were run to show trends and characteristics of the noise signature. Then the influence of duct treatment on the noise levels found in the study was calculated. As part of the detailed study the feasibility of model fan configurations found most promising was established.

The report is divided into two major sections: (1) Study Methodology and (2) Discussion and Results. The study methodology describes the methods used in source noise calculation, vane lean investigation, duct lining design, aerodynamic design, and mechanical design. Finally, a discussion of the correlation between the source noise theory and test results as well as a study of correlation between vane lean test and the theoretical calculation method used in this study is included in this section.

The discussion and results section presents the influence on noise of tip speed, pressure ratio, aerodynamic design, fan solidity, number of rotor blades, number of recovery vanes, distance between rotor blades and recovery vanes, thrust, vane lean, and duct acoustic treatment. Noise levels are calculated at 152 m distance in perceived noise decibels (PNdB) for the fan operating at 70 knots forward speed at sea level.

This condition was chosen as being most useful in assessing the levels of a STOL aircraft during takeoff or a surface effect vehicle or tracked air cushion vehicle at cruise speed.

In most cases several variables will be found in each curve. Every effort has been made to include the major parameters that influence noise. However, some second order effects do exist that cannot be adequately represented in a general study such as this.

SYMBOLS AND ABBREVIATIONS

AR	Exit area divided by rotor area	
A_w	Wetted perimeter of a duct	m
B	Number of rotor blades	
BVGAP	Axial distance from rotor blade trailing edge to stator vane leading edge normalized to blade chord	
b	Blade chord	m
C_f	Friction coefficient of a surface	
D_f	Duct internal friction drag	
D_L	Local shroud diameter	m
DIA	Rotor diameter	m
L	Length of surface used in duct treatment studies	m
M	Number of nodal circles	
P	Shaftpower	kw
PAM	Pulse amplitude modulation	
PNL	Perceived noise level	PNdB
PPM	Pulse position modulation	
PR	Total pressure ratio at fan duct exit	
PWL	Sound power level decibels re. 10^{-13} watts	
q_L	Local dynamic pressure	N/m^2
RN	Reynolds number	
SL	Sea level	
SPL	Overall sound pressure level in decibels re. .0002 microbar	

T	Period of repetition of a pulse	sec.
TS	Rotor tip speed	m/s
V	Number of stator vanes	
θ	Vane lean angle	degrees
$\theta_w(r)$	Orientation of rotor viscous wakes at interception by the stator	
ρ	Local air density	kg/m^3
μ	Number of nodal circles	

STUDY METHODOLOGY

Introduction

In this section the methodology used throughout the study is described. The major emphasis in the study was on the effect of various design and operating parameters on noise. Therefore the source noise methodology is discussed in some detail.

Since duct lining will play a significant role in achieving the low noise objectives for advanced surface vehicles or aircraft, its application to low pressure ratio fans has been studied. The methodology used is discussed below. Aerodynamic design methodology is also discussed as it plays an important part in defining the thrust that can be achieved in a fan and also provides the basic input parameters for the noise calculations. Finally, the study methodology employed in considering the mechanical design feasibility of the fan configurations found most promising is described.

Source Noise

Background.- The dominant sources of fan noise have been traced to unsteady flow and its interaction with solid boundaries. For low tip speed, low pressure ratio fans, the important noise components are broadband and harmonic rotor/stator interaction noise, rotor harmonic noise due to interaction with inflow distortion, and rotor broadband noise associated with vortex shedding. The methodology used in this study utilizes basic aerodynamic and acoustic theory with empirical coefficients derived from carefully controlled acoustic tests. The calculation procedures for the rotor noise components have been developed from previously existing theory; however, the stator noise components are calculated by use of a new unified theory which treats the interaction of the stator with the steady and turbulent components of the rotor viscous wakes.

The following subsections describe test data obtained from a model Q-FAN, the noise calculation methodology, and the correlation of the calculation results with the model test data. In addition, the method developed to study the effects of vane lean on low pressure ratio fan noise is discussed. This method is not part of the basic Q-FAN noise prediction computer program and has only been included to determine the potential of vane lean for noise reduction in selected cases in the parametric study summarized later in the report.

Model test results.-Late in 1970 a cooperative program between NASA Langley and Hamilton Standard was completed where the first noise measurements on the Q-FAN were obtained. These tests on an existing wind tunnel model of a Q-FAN were conducted under ideal conditions and produced data of unusually high quality. In this section the results of this program which are reported in detail in reference 3 are outlined.

The model fan tested in this program is shown in figures 2 and 3. Figure 2 shows the rotor and spinner with the front portion of the shroud removed. The low solidity of this fan relative to that normally seen in turbofans is evident in this photograph. The cross-section drawing of figure 3 shows the location of the swirl recovery vanes relative to the rotor blades. The spacing between the trailing edge of the rotor blades and the leading edge of the recovery vanes is equal to 1.9 blade chords at the mean radius. For the major portion of the program the bellmouth inlet shown in figure 3 was installed on the shroud to insure unseparated inflow similar to that expected at takeoff and landing speeds where transport aircraft noise is considered most critical.

Noise measurements were obtained using stationary and slowly sweeping microphones which can be seen in figure 4. The distance from the fan rotor center to the microphones was 3.05 m. This distance was more than five fan diameters and more than thirteen wave lengths of the lowest frequency of interest thus insuring that data was obtained in the far acoustic field. The axis of rotation was 3.5 m. above the ground to insure that ground reflection effects were essentially eliminated. Testing was done at night when the wind was less than three knots and in many cases the wind velocity was too low to register.

Tests were conducted at a range of tip speeds, thrusts, blade angles and shaftpowers. The tip speeds ranged from 152 m/s to 244 m/s. Thrust ranged from 979 N to 2869 N. Shaftpower ranged from 30 to 168 kw. Since the Q-FAN is a variable pitch device, the blade angle was varied from 35° to 50° to obtain the thrust and horsepower variation described above.

Acoustic data was recorded on a magnetic tape system whose frequency response was flat from 100 Hz to 40,000 Hz as described in Reference 3. Figure 5 is typical of the narrow band spectrum plots from that data. These plots show the details of the Q-FAN noise spectrum that are required to understand the mechanisms of noise generation. Note that the spectrum consists of tones at blade passage frequency and its harmonics superimposed on a broadband noise floor. Note also that in full scale, which would be about three times that of the model, the dominant tones would lie at relatively low frequencies where they would contribute little to perceived noise level, the measure of annoyance used in aircraft noise certification.

Separate 1/3 octave band analyses were also made from the tape recorded data. For comparison purposes a one third octave band plot and a narrow band plot for one test condition is compared in figure 5. It can be seen by comparing the 1/3 octave band and the narrow band plot that the tones are a dominant influence on 1/3 octave band levels up to four times blade passage frequency but broadband noise is dominant at the higher frequencies.

In addition to the stationary location plots such as those in figure 5, directivity plots such as those in figure 6 were made. These show the directional pattern of the blade passage harmonics. In the sample plot of figure 6 the typical directivity character of the Q-FAN can be observed. In this plot 0° is directly ahead of the fan, 90° is in the plane of rotation of the rotor, and 150° is close to the fan jet coming from the outlet of the shroud. It is shown that, at blade passage frequency, noise ahead of the plane of rotation is slightly higher than that behind the plane of rotation. The 1st overtone or twice blade passage frequency shows more pronounced lobes and again shows levels ahead of the plane of rotation which are slightly higher than those behind the plane of rotation. The 2nd overtone which is seen to be dominant in figure 5 is dominant behind the plane of rotation and thus the directivity shown in other plots of reference 3 show the Q-FAN to have a directivity peaking aft of the plane of rotation. The third and fourth overtones of figure 6 show the effect of the shroud on noise transmitted to the side of the fan (near the plane of rotation). The reduction in noise near 90° is not surprising since the wavelength of the third overtone is only 7% of the shroud length.

In addition to analysis of the data by conventional methods, the sound power levels of the tone and broadband components of the noise were obtained for use in a study of source noise by theoretical methods. Use of sound power level as a reference in theoretical studies eliminates effects such as reflection and diffraction of sound by rotor and duct, and refraction by velocity gradients. These affect directivity plots derived from stationary microphones but do not affect radiated sound power. In order to evaluate sound power level of the tone components, a 50 Hz bandwidth filter was tuned to the desired harmonic of blade passage frequency as the tape of a 5 minute microphone sweep from directly ahead of the fan to behind the fan was played back. A tracking filter using a fan speed signal as a reference was used to prevent small speed changes from shifting the harmonics out of the narrow filter pass band. In order to determine sound power level the rms value of the filter output was integrated digitally assuming symmetry around the fan axis of rotation.

In evaluating the sound power level of the broadband components of the fan noise, a 200 Hz bandwidth filter tracking at half harmonics, i.e. 1/2, 3/2, 5/2 etc. times blade passage frequency, was used in the manner described above. Results were bandwidth corrected to 50 Hz and used to correct for any broadband energy which entered the harmonic analysis.

A sample of the results of the tone (harmonic) and broadband sound power analysis is presented in figure 7. Similar results were found at powers ranging from 30 to 168 kw and tip speeds ranging from 152 to 244 m/s. The features of these figures used to develop the Q-FAN noise theory are described in the next section.

By use of the model data described above a theoretical method was developed to explain the features of the observed spectra. These spectra (see sample in figure 5) were found to differ from other fan spectra in that they included a multiplicity of blade passage frequency harmonics in the audible frequency range superimposed on a broadband noise floor that sharply decays in level as frequency increases. A detailed review of all the data from the test revealed that at moderate frequencies the differential between tone and broadband level tended to be constant but at higher frequencies the tones decayed in level till they were masked by broadband noise. The mathematical model described below has been developed to explain the observed features of low pressure ratio, low tip speed fan noise signatures.

Stator noise.-Stator noise is known to be the result of velocity perturbations in the stator inflow caused by the passing of upstream rotor blades. With the typical rotor/stator spacing of two or more blade chords in the low pressure ratio Q-FAN, only the viscous wakes of the rotor blades cause interaction noise. The theory of noise generation by these wakes which is utilized in this method represents a departure from the conventional wake defect model shown in figure 8. In stator noise theories described in the literature the wakes have a velocity profile as calculated from the Silverstein formulas of reference 4 which makes use of profile drag coefficients and mean flow parameters from fan aerodynamic performance calculations. Using this information a periodic train of pulses convected into the stator vanes can be predicted. Stator forces due to the inflow perturbations of the wake defects are calculated from Sears and Horlock theories of wing lift response described in references 5 and 6. The Sears theory treats the airfoil with a small sinusoidal upwash component superimposed on a steady inflow. The recent Horlock theory generalizes the Sears theory to include a chordwise component in the sinusoidal velocity disturbance.

The lift harmonics derived from the above theories are treated in the fan noise theory as acoustic dipoles. The stator is modeled as an array of dipoles phased according to the passing of the upstream rotor blades. The observer in the acoustic far-field receives the signals from each source and sums them to produce the resultant tone which is heard. In this model the sources are imperfectly phased as observed in the far-field so there is partial cancellation which may be interpreted as a reduction in the efficiency of the source. A model for the stator vane sources which includes enclosure by a duct could also be developed but would yield results with spectrum features not unlike those described below.

The model described above has treated the stator forces as perfectly harmonic; however, hot film anemometer surveys between the rotor and stator in subsonic tip speed fans have shown that the rms turbulence levels in the wakes can have the same order of magnitude as the mean velocity defect. Therefore the velocity distribution in the wake at any instant of time can be quite different from the mean distribution which would be shown by a long time constant velocity probe. Figure 9 illustrates the non-periodic nature of the wake velocity in a subsonic tip speed fan. For this photograph a hot film anemometer was installed at a mid span location in a fan operating at subsonic tip speed. To obtain the photograph shown, the hot film anemometer trace displayed on an oscilloscope was triggered once per revolution by a shaft angle reference signal. The camera shutter was left open for several rotor revolutions to show the modulation of the wake behind one blade. Note that in the photograph all of the superimposed pulses are made by the same blade during succeeding passes. Pulses from two adjacent blades are shown in the photograph. Although this data was obtained in a current generation high pressure ratio fan, the modulation effect is apparent. Changes in both amplitude and position can be seen in this photograph. Mugridge in reference 7 has also obtained similar photographs for more lightly loaded subsonic tip speed fans with results similar to those described above. In his work the wakes from each blade are distinct and amplitude modulation is quite pronounced. A review of the little data available (references 7 and 8) indicates that amplitude modulation may be as large as 100% while position modulation is present in a lesser degree.

The effect of pulse amplitude modulation (PAM) and pulse position modulation (PPM) on the spectrum character of a fan can be seen by first considering the work of MacFarlane (reference 9). Here the theory was developed for electrical signals from a single non-directional source where interference effects were not considered. In MacFarlane's work a

voltage pulse is considered which repeats indefinetely with period T with the result as shown in figure 10(a) being a periodic signal where power spectral density is a series of "spikes" at the fundamental pulsing frequency 1/T and its harmonics. The envelope of the power in this line spectrum is shown as dashed lines. The lines themselves have zero bandwidth.

If the pulses have random amplitudes but the same shape and periodic interval, broadband energy is added to the spectrum as shown in figure 10(b) and the line spectrum is unchanged. Thus a spectrum plot from a narrow band analyzer of a signal with PAM would show the harmonic spikes protruding from the broadband noise by a constant number of decibels over the entire frequency range. The amount of protrusion would depend on the amount of modulation and the bandwidth of the filter used in the analysis.

When the pulses are identical in shape and height but occur at random intervals in time, broadband energy due to PPM appears at the expense of harmonic energy as shown in figure 10(c). In this case the amount that the spikes protrude from the broadband noise decreases with increasing frequency.

In the stator noise method used for the parametric study summarized in this report the mathematics of MacFarlane's modulation theory have been applied to the Lowson (reference 10) free stator model with pulsed rather than harmonic dipoles representing the vanes. Both PAM and PPM are included. The statistics of the pulses are described in terms of their mean values and standard deviations. The mean pulse shapes and amplitudes are calculated from Silverstein wake formulas. The mean arrival time is compatible with the Tyler-Sofrin interaction theory (reference 11). The amounts of modulation (the standard deviations) are treated as empirical factors. Remarkably enough, the acoustic model can be solved exactly in the far-field. This represents a unified theory for stator harmonic and broadband noise which will be reported later in the literature. The results provide excellent agreement with test data as shown later.

Rotor tone noise.-Rotor tone noise is the result of unsteady loading on the rotor blades. Since the low pressure ratio fan operates in a duct at low tip speeds, the Gutin steady load tone can not propagate to the duct face. However, the experimental evidence from the Langley model test program shows a significant level of tone noise which could not originate from the stator since it is inefficient at the blade passage frequency. Therefore inflow distortion must be present even with an

ideal installation such as that for the Langley test. This would produce high levels at blade passage frequency and noticeable energy at high harmonics of blade passage frequency. The work of Lowson in reference 12 has been used along with the test data from the Langley program to develop a magnitude and slope for the rotor tone harmonics for the formulas used in the parametric study summarized in this report. It was found that one assumption for flow distortion gives good agreement with all test cases from the Langley program from 152 to 244 m/s and from 30 kw shaftpower to 168 kw shaftpower.

Rotor broadband noise.-For calculation of rotor broadband noise the work of F. W. Barry (see reference 13) developed over the past several years for free air (unshrouded) propellers has been adapted. The method of Barry includes a spectrum shape which has a broad peak at lower frequencies and after a break in the spectrum curve at some higher frequency rolls off at a constant slope. Evidence indicates that this curve which has been correlated with many propeller noise signatures includes effects from two regions: the blade tip and the airfoil trailing edge. The blade tip is believed, because of its larger scale, to be the cause of the low frequency peak. The high frequency noise is believed to be dominated by the vortex noise which is associated with the wake turbulence downstream of the propeller blade airfoil. Because of the presence of the shroud it is believed that the tip vortex effect is suppressed in low pressure ratio fan noise so the only noticeable contribution is from small scale high frequency vortex shedding from the airfoil. Therefore, only the high frequency portion of the Barry method is evident in the low pressure fan noise calculations made with the Q-Fan noise prediction procedure.

Q-FAN noise prediction computer program.-In this section the use and general input/output features of the Q-FAN Noise Prediction Computer Program are described. This program uses the source noise concepts described in in previous sections.

Because the fan source noise calculation procedure requires the steady flows and loads as input, the noise calculation has been set up as a subroutine to the Hamilton Standard Q-FAN Performance Program as shown in the flow chart in figure 11. The operation of the program is as follows.

Fan geometry is defined in terms of blade and vane section shape characteristics (solidity, camber, thickness ratio) and twist; duct area ratios; and hub to tip diameter ratio. Rotor tip speed, forward flight Mach number, and ambient temperature are specified. Then either the thrust or pressure ratio requirement is loaded and the performance program iterates automatically on rotor blade angle to meet this requirement.

When the performance requirements are met the program feeds the fan steady loads and flows and section operating conditions to the noise subroutine in a 10 radial station strip analysis. The noise program which is described in more detail later, computes: (1) a 1/3 OB power level (PWL) spectrum for each of four source components, (2) a spatially averaged 1/3 OB sound pressure level (SPL) spectrum, and (3) the maximum sideline perceived noise level (PNL) at the specified observer distance including effects of atmospheric absorption. For a given performance condition the program computes noise for any specified range of rotor/stator gap and blade and vane count, with fixed rotor and stator solidities.

For the stator noise calculation, the radial distributions of axial and swirl flow and blade profile drag coefficient are used with the Silverstein formulas (reference 4) to compute the blade viscous wake velocity defect. Then the Sears/Kemp/Horlock unsteady airfoil lift response theory is used to calculate the mean lift response pulse at each radial station. The stator harmonic radiation is calculated considering the harmonic component of the force on each vane to be concentrated at an effective radius as in the Lowson stator theory (reference 10). A major departure from the Lowson analysis, however, is that the wake turbulence though PPM removes considerable energy from the higher harmonics. The concentrated vane force is calculated as the integral of the magnitude of the fluctuating lift force per unit length over the span of vane. Thus radial phasing effects are neglected. The stator broadband is calculated considering the amplitude and frequency modulated pulses to be acting at 10 uncorrelated stations on each vane. The outputs of the stator noise subroutine are harmonic PWL's and 1/3 OB PWL's for the PAM and PPM broadband components.

The rotor harmonic noise is calculated assuming a steady inflow distortion which gives rise to blade loading harmonics. The load harmonic levels decrease exponentially with increasing harmonic order. The rotor radiation due to this kind of loading consists of harmonics which also decay exponentially. The "loading law" for loads normalized to the steady blade load was derived from the Langley Q-FAN model test and is constant over the wide range of pressure ratios and tip speeds tested. The output of the rotor harmonic routine is the harmonic PWL spectrum.

The rotor broadband radiation calculation requires the rotor tip speed, blade area, blade thickness, percent blade stall, and thrust for input. The output is the 1/3 OB PWL spectrum.

The output of the noise subroutine consists of: (1) the harmonic and 1/3 OB PWL's for each of the components described above, (2) the net 1/3 OB PWL spectrum, (3) the average SPL 1/3 OB spectrum derived from the PWL's using spherical spreading and atmospheric absorption for 25°C and 70% RH, and (4) the maximum sideline PNL calculated from the average SPL spectrum plus an experimentally derived PNL directivity index of 1.5 PNdB.

Correlation of calculations with experimental results.-The results of application of the method described above to the model Q-FAN measurements described in previous sections is discussed below.

Figure 12 shows a sample comparison of the blade passage frequency harmonic predictions with test data. In order to establish this correlation a small amount of PPM was used. This small amount of PPM has a small effect on lower harmonics but a large effect on the higher harmonics. Note that the change in slope of the harmonic envelope of the test data above the eighth harmonic does not fit the stator model. Since the stator fundamental is extremely inefficient and should be acoustically cut off by the duct, it is assumed that unsteady loading, as described in previous sections, is affecting the rotor. Using the Lowson (reference 12) formulas for rotor radiation due to non-uniform inflow, rotor harmonics of figure 11 can be calculated. It can be seen that the introduction of the rotor tone harmonics due to unsteady inflow significantly improves correlation between calculation and test at both the blade passage frequency and at high harmonics of blade passage frequency. It is apparent that the mid frequency harmonics are the result of stator radiation.

The broadband spectrum of figure 13 was calculated assuming a large amount PAM. The PPM used was the same as that used in calculating blade passage frequency harmonic information in figure 11. Again, at high frequencies a rotor broadband noise contribution is required to establish good correlation between theory and experiment. It can be seen in figure 13 that the correlation between theory and experiment using the Q-FAN noise prediction is quite good. It is interesting to note that the pulse amplitude modulation level required for good correlation is consistent with available test data.

In summary, the correlations described above show that the spectrum is divided between sources as shown in figure 14. The very low frequency broadband, not analyzed here, is attributed to jet noise and scrubbing of the fan exit flow on the test rig. The blade passing fundamental and harmonics above order 8 are shown to be due to non-uniform inflow to the rotor. The very high frequency broadband is rotor noise and the dominant intermediate frequency tone and broadband noise is shown to be

due to rotor/stator interaction.

In order to show the capability of this method it has been applied to all additional data from the Langley model test program. Figure 15 shows comparisons between measured and calculated 1/3 octave band spectra. It can be seen that agreement is excellent at all but the low frequencies where duct effects and scrubbing noise dominate. In addition perceived noise level calculations for sideline noise have been made for all available data from the Langley model test program. These along with the test data are shown in figure 16. It can be seen that correlation over the shaft-power range from 30 to 168 kw and 152 to 244 m/s tip speed is excellent. Differences between theory and experiment over the full range of shaft-power and tip speed is less $\pm$ 1.5 dB.

Vane Lean

In the present study, a simplified analysis is used which clearly shows how radial cutoff of the duct modes can be exploited for reduction of stator harmonic noise. This problem has also been studied in the past (reference 15 and 16) with different approaches.

In the classic Tyler-Sofin paper (reference 11), it was shown how a periodic acoustic disturbance in an annular pipe could be expressed in terms of spinning modes. Solving the wave equation for an infinite annular duct with hard wall boundary conditions, it was found that if the pressure fluctuation in a plane normal to the duct axis (say the stator disc) was specified, then the modal coefficients for each of the spinning modes could be calculated by a Fourier-Bessel analysis. The modes could then be considered separately by the principle of superposition.

This analysis also leads to a frequency condition for duct "cutoff" which depends on mode order, hub/tip diameter ratio, and rotor tip speed. Pressure disturbances in modes which are cut off decay exponentially along the duct axis. The propagating modes travel through the duct unattenuated and are partly radiated and partly reflected at the duct ends. For modes well above cutoff, the reflection coefficient is nearly zero. The mode order is given by the number of modal diameters, m, and the number of modal circles, μ. Thus, the higher the mode order, the more wavy the pressure distrubances in the stator disc. Stated non-mathematically, the cutoff condition requires a high driving frequency to propagate energy in a mode with high mode order.

For a given disturbance, in general, all the radial modes are generated. However, since the tip speed is finite, the higher radial mode orders are cut off. The intent of the method described below is to permit study of the coupling of rotor/stator interaction forces to the duct modes to determine the conditions where vane lean can be used to couple to higher order radial modes which cannot propagate energy in a duct.

In the method, the pressure disturbance at the stator disc is specified, a modal analysis of the disturbance is performed, and the cutoff condition is determined. The analysis is sensitive to blade count, vane count, hub/tip ratio, tip speed, blade vane gap, and pressure ratio.

The pressure disturbance at the stator is assumed to be generated at the vanes represented by lifting lines which can be radial or leaned with some angle $\theta\ell$ as shown in Figure 17. The disturbance is caused by interaction of the stator with the rotor viscous wake which in general has a non-radial orientation $\theta_W(r)$ by the time it reaches the stator as shown in Figure 18. For low pressure

ratio fans, a free vortex design is desirable and is assumed in this study although not always achieved in practice. With the free vortex design the "wake windup" $\theta_w(r)$ is determined by the pressure ratio, tip speed, and rotor/stator gap. Wake windup is increased by higher pressure ratio, lower tip speed, and increased gap. Figure 19 shows how a vane with negative lean, $\theta\ell < o$, tends to intercept more wakes at once than a radial vane and thus couples more strongly to the higher modes. For simplicity, phase effects associated with the lift response functions and the fact that the rotor trailing edge may not be radial are neglected. Also the reduction in lift response amplitude due to oblique inflow is neglected.

To assess the effect of lean, the modal amplitude coefficients are computed in normalized form. The normalization condition corresponds to the (fictitious) condition of radial wakes being intercepted by radial vanes. Thus 0 dB for the zeroth amplitude coefficient means that the stator forces are all in phase along a radius.

It is desirable to check any new theory against test results to assess its capabilities. However, there are little experimental data available in the literature which isolate the effect of vane lean on radiated noise. The major exception is the recent test report of a General Electric lift fan with and without lean (reference 17).

The pertinent design parameters for the General Electric lift fan are:

Pressure ratio	=	1.3
Number of blades	=	42
Number of vanes	=	90
100% tip speed	=	290 m/s
Hub/tip ratio	=	0.475
Lean at tip	=	-15° (30° at the hub)
Rotor/stator gap	=	2 rotor chords
Rotor solidity (assumed)	=	1.34

For the blade passing frequency fundamental, n=1, the large vane to blade ratio produces cutoff for all radial mode orders. The strong tone which appears at n=1 is probably rotor noise due to inflow distortion interaction. For the second harmonic, n=2, however, several radial mode orders for m=-6 propagate as shown in figure 20. The normalized amplitude coefficients are shown with and without lean and the radial mode order for cutoff is shown for 80% speed and 95% speed. A reduction in the normalized amplitude coefficient value would be associated with a reduction in sound pressure level. It can be seen that the lean produces a significant shift of coupling to the right in the figure to modes which are cut off.

Experimentally, as reported in reference 16, it was found that the lean reduced the sound power in the 1/3 octave band containing the second harmonic by 2.3 dB at both 80% and 95% speed. Since there is significant broadband energy in that band, the harmonic component was probably reduced more than 2.3 dB. Thus the results of the General Electric test are consistent with the calculated effects.

When the Hamilton Standard test fan (reference 3) is analyzed on a similar basis, it is found that lean could have reduced all harmonics.

Design parameters for that fan are:

Pressure ratio	=	1.09
Number of blades	=	12
Number of vanes	=	22
Design tip speed	=	213 m/s
Hub/tip ratio	=	0.43
Lean	=	0°
Rotor/stator gap	=	1.9 blade chords
Rotor solidity	=	0.72

With low pressure ratio, low tip speed fans the blade passing frequency can be very low so that many harmonics enter the PNL calculation. Therefore the effect of vane lean on several harmonic orders, n, is shown in figure 21. This figure shows that for the test fan at 1.09 pressure ratio the wake windup did not produce any significant cutoff.

However, if vane lean had been introduced in this fan figure 21 shows that a significant shift of coupling to the modes which are cut off would occur. This effect occurs at all harmonic orders and is more pronounced at the higher harmonics. Therefore, if leaned vanes were installed in this fan, the stator tone noise particularly at multiples of blade passage frequency would be reduced in level.

Duct Lining Design

Introduction.-The duct lining study was conducted using the procedures described below which have been evolved by Hamilton Standard from available test data and duct lining design experience. These procedures are based on theory extensively modified to reflect results of model duct lining tests, model fan tests, and full scale engine tests. Neither a theoretical or empirical approach alone has successfully predicted real life, full scale results where the effects of different noise sources; temperature, pressure and flow gradients; and influence of solid boundaries on modal distribution remain poorly defined. Thus the weighted empirical approach is considered most reliable as an indicator of full scale fan attenuation that may be expected.

Most of the noise of the Q-FAN originates with unsteady flows over the blades, vanes, and solid boundaries of the duct. Fluctuating forces caused by the unsteady flow, radiate noise which couples into the inlet or outlet duct modes. The acoustic energy propagates within the duct to the duct ends where sound is radiated to the observer. Experiments and analyses indicate that considerable noise reduction can be achieved by optimization of performance and configuration parameters. However, when the remaining noise is still objectionable, additional reduction can be obtained by acoustic treatment in the duct transmission path.

Theoretical analysis by solution of the wave equation within the duct shows that the efficiency of propagation of the sound through the duct depends basically on source mode distribution, duct geometry, and the complex wall impedance. Extensive modifications of the wave equation solutions have been necessary to explain observed duct lining test results in test facilities, real fans, and real engines. These studies have shown the importance of flow, flow gradients, boundary layer and temperature.

These duct lining theories indicate that considerable attenuation can be obtained with optimum duct linings consisting of tuned resistive resonators. These theories can be used to predict the complex impedances required of the lining configurations. Furthermore, tuning and attenuation trends can be predicted with variation in acoustic parameters. The prediction of the complex impedances of practical linings in real conditions, however, generally remains inaccurate, though semi-emperical mathematical models have been devised which permit accurate calculation of tuning characteristics and attenuation characteristics under moderately severe conditions. In the full scale fan and engine tests, however, the theoretical predictions are seldom matched.

The Hamilton Standard duct lining procedure is based on theory which incorporates empirical modifications to establish correlation with numerous published and in-house measurements of attenuation achieved with single degree of freedom resonator linings consisting of perforated

plate over a honeycomb-filled backing space. Extensive data has been recorded with this type of lining permitting parametric design procedures. Furthermore, observed trends have been verified by theory to permit broader application with increased confidence.

Duct lining design method.-The treatment analysis begins with the calculated description of the maximum perceived noise level (PNL) heard during an aircraft flyover.

Figure 22 shows schematically the procedures used in calculating the sideline noise, attainable reduction, noise attenuation spectra and required lining characteristics for selected areas of the Q-FAN inlet and exhaust.

The previously described theoretical analysis which has been correlated with Q-FAN tests provides the input description of the candidate fan configuration. The parameters calculated include fan geometry, operating conditions, duct velocities and noise power levels generated by each of the major sources within the duct. From the estimated power spectra of each source within the Q-FAN (rotor tone, rotor broadband, stator tone, and stator broadband) together with directivity from model tests, the noise spectra heard at the observed location is computed.

The spectra at the point of max PNL is reduced to noy values in each third octave to demonstrate graphically the most effective suppression characteristics for minimizing PNL. Figure 23 shows a typical observed noy spectra with a selected suppression level which is essentially determined by the peak attenuation achievable within the duct geometry constraints. The attenuation spectra (tuning of the lining) required for minimum PNL, however, is determined primarily by backing depth behind the acoustic lining.

PWL calculations made with the Q-FAN noise calculation program indicate the rotor tone and broadband noise dominate the spectrum up to the third octave above blade passing frequency. Above this frequency, stator sources dominate. Moreover, results of model tests show that noise in the acoustic field ahead of the fan is dominated by noise transmitted forward within the duct while noise in the aft field is dominated by rearward transmission within the duct. It is readily apparent that the lining characteristics must differ in each section of the Q-FAN duct to suppress the different source spectra traveling different transmission paths. Separate sections selected for individual treatment are: (1) the inlet duct to the Q-FAN rotor, (2) the duct between rotor and midchord of the stator and (3) the exhaust duct from midchord of the stator to shroud exit.

The peak attenuation is determined by duct length, duct height, duct velocity and to a lesser extent backing depth. An estimated peak attenuation is calculated first with an assumed depth and is revised by iteration as required. This maximum value of attenuation together with the untreated noy spectra determines an optimum attenuation spectra. An optimum attenuation spectrum is shown in figure 24 together with a typical attenuation characteristic determined by test. Clearly some portions of the lining attenuation are partially ineffective for the Q-FAN spectra. This lining attenuation together with emperical attenuation directivity is entered in the program with source power levels to calculate new levels of side line PNL. The procedure is repeated separately or in combination with other treated sections of the duct as shown in figure 22 to arrive at the optimum treatment for a particular Q-FAN design.

Aerodynamic Performance Losses Due to Duct Lining

The loss in performance of a propulsive fan when acoustic duct lining is installed is of great concern in design of an aircraft. With the increased emphasis on noise reduction in new aircraft, performance penalties not considered acceptable in the past may be required to meet noise goals. While the use of low pressure ratio, low tip speed fans show great promise for meeting stringent noise goals, it is possible that acoustic duct lining may be required. Therefore, in assessing the noise reduction potential of duct linings for low pressure ratio fans as described in the previous section, a parallel study has been conducted to show the performance losses imposed by these linings.

The method used for calculating losses is semi-empirical in nature. For a given condition and configuration, the internal flow characteristics along the entire duct length are calculated.

The friction coefficient C_f can be calculated in a smooth surface duct in turbulent flow as:

$$C_f = 0.074/(RN)^{1/5}$$

where RN is Reynolds Number.

For an acoustically lined duct consisting of either a smooth perforated plate with about 10% of the area perforated or a porous-polyimide impregnated woven fiberglass surface, the frictional drag coefficients have been estimated using information from Reference 17. For cruise flow in the duct, C_f is about 0.004 for the perforated surface and 0.0047 for the woven surface while C_f for a smooth surface as calculated by the above equation is about 0.003.

In assessing the influence of extending the duct and treating the extended surfaces the friction drags are calculated information from the fan performance calculation method. Then by knowing the net performance, changes in internal friction due to the acoustic lining can be estimated by choosing the proper empirical friction coefficient. Briefly, the method is described below.

The internal friction drag, D_f, is defined as

$$D_f = 0.1124\ \rho\ V_L^2 A_w C_f$$

where ρ = local density, kg/m^3

V_L - local velocity m/s

A_W = wetted area, m^2

C_f = friction coefficient

The wetted area, A_W is calculated as

$$A_W = \pi D_L L$$

where D_L = local diameter, m

L = length over which friction is computed in m

Three sources of increased losses were assumed:

1. Added friction due to the liner without the extension;
2. Total internal friction of the liner extension
3. Smooth external friction of the extension.

For the liner which included a splitter ring, the drag of a thin annular airfoil at zero angle of attack was added to the drag for wall treatment on the shroud and center body alone. The annular airfoil drag, D, is

$$D = 0.2248\ C_D q_L \pi D_L L$$

where C_D = drag coefficient which includes the profile drag of the airfoil.
q_L = local dynamic pressure N/m^2

For the calculation done on the parametric study C_D was assumed to be 0.01 for the woven lining material and 0.009 for the perforated lining.

Aerodynamic Design

The aerodynamic method of analysis used for design of the Q-Fan rotors and stators for this study is a proven computerized method which can be used to perform design calculations for axial-flow fans and compressors. The program input is in the form of gap/chord, thickness distributions, flow, RPM, inlet conditions and a desired stagnation pressure distribution at the exit from the last blade row. From this the camber and metal angle distribution are determined for both the rotor and stator.

The program includes cascade data for a variety of airfoil shapes which are included in the turning and loss data portion of the design and performance analysis. Losses in addition to the cascade loss system are input and included in the design analysis and in the evaluation of the blade loading parameters. An experimental endwall, or secondary loss generalization is included as input. Calculations using this method have shown good performance correlations with Hamilton Standard's 1969 low pressure ratio (1.05-1.15) Model test and other tests of higher pressure ratio fans conducted at United Aircraft Corporation. The program is a compressible flow analysis utilizing radial equilibrium after each blade row. Continuity, of course, is satisfied between each blade row with stream quantities computed in the presence of the endwall and the cascade system losses.

Aerodynamic performance, including duct drag, is predicted for the Q-Fan hardware utilizing a second method which takes the mass averaged quantities from the rotor-stator analysis and relates the fan-duct exit conditions to the free stream operating conditions. In this method, the duct nozzle area is sized to maintain the rotor inlet flow at the desired design level, with the assumption that the flow exhausts to ambient static pressure. This analysis yields the quantities: net thrust, rotor thrust, stator thrust, exit velocity and rotor absorbed shaft power for any flight condition. In addition, the flow parameters required by the noise program are generated. The program is written so that Q-FAN performance results can be iterated upon for net thrust or shaft power at a given rpm, flight operating condition, and nozzle area with a given Q-Fan geometry. The performance program is coupled to the noise program, so that performance and noise can be obtained in a single computation on the computer.

Mechanical Design Methodology

The general shape of a fan blade is determined by aerodynamic requirements. This shape may be modified during mechanical design in order to alter critical speeds or to reduce stresses. The resulting structure may be described as a non-uniform, twisted, cantilever beam. In order to describe the blade for analysis, it is broken up into convenient segments at a number of stations along the radius. For each of these segments, the mass and stiffness properties are determined.

With a definition of the mass and stiffness distributions, the steady loads and stresses generated by the whirling blade itself are calculated. With the necessary aerodynamic information, the dynamic and steady response of the blade to its environment is calculated. The distribution of these forces within the blade can then be established and the resulting stresses calculated. It is also possible to define the loads exerted by the blade on its retention system and hub.

The primary forces exerted by the blade are centrifugal force resulting from its rotation, a net twisting action around its radial axis resulting from aerodynamic and body forces, and steady and cyclic bending moments resulting from the aerodynamic environment. These forces are properly summed to establish a retention and hub sizing criterion. The net twisting moment is used to determine the capacity of the blade pitch changing mechanism.

The steady and cyclic calculated stresses are compared with established material allowables as appropriate for each component and different areas of the component. For example, the airfoil portion of the blade is subjected to an environment that includes sharp objects and corrosive elements while the retention portion is not. Proper allowances are made for nicks and gouges as well as modest corrosion for the case of the airfoil.

RESULTS AND DISCUSSION

Introduction

The purpose of the study summarized in this report was first to evaluate by use of analytical procedures, the influence of various operating and design parameters on noise produced by low pressure ratio subsonic tip speed fans, second to determine the influence of acoustic duct lining on noise produced by these various fan configurations and third to evaluate the practicality of the most promising configurations from a mechanical design standpoint. In the first area of study, the following parameters were varied:

Aerodynamic design
Rotor Solidity
Tip speed
Distance between rotor blades and stator vanes
Diameter
Pressure ratio
Thrust
Number of stator vanes
Number of rotor blades
Shroud exit area
Stator vane configuration (vane lean)

In the duct lining study, the most promising fan configurations were studied to determine the influence of duct lining on the noise level variations seen in the basic parametric study described above. Performance losses were also considered in this portion of the study as the duct lining increases nacelle drag.

In the third area of the study, the feasibility of the most promising configurations from a mechanical design standpoint was considered. Centrifugal twisting moment and centrifugal load on the hub were considered as well as the potential problems in blade and blade retention design.

Basic Parametric Study

Introduction - The study was conducted using four analytical procedures, a fan design method, a fan performance prediction method, a basic computerized noise prediction method, and a special vane lean analytical method. All of these are described in an earlier section of this report titled Source Noise Methodology. The parametric study had two major phases. In the first phase, an existing fan aerodynamic design was used to determine parameters that most influence noise. In the second phase, the areas of investigation were expanded in the directions found most fruitful in the first phase and fan aerodynamic designs were tailored to suit the new operating conditions. The results of the phase two study are summarized in this section as they incorporate all the results of phase one.

In the first phase, it was found that the most promising fan configuration had few vanes (7), few blades (12), had a gap between the trailing edge of the rotor blades and leading edge of the stator vanes equal to two blade chords, and operated at some optimum tip speed which was a function of pressure ratio, shroud exit area, and fan rotor solidity.

In the second phase, primary emphasis was placed on detailed study of a 1.0 solidity rotor as that appeared compatible with (1) the desire to provide reverse thrust by rotating the blades through the flat pitch setting like those of a propeller blade (of course reverse thrust by moving the blades through the feather position is also possible with this solidity), (2) the indication that increasing solidity reduces noise, and (3) the indication that the 1.0 solidity design was structurally adequate for model tests. In this phase of the study the influence of vane lean was also studied. Significant changes in vane tone noise were shown to result from leaning the vanes. However, an assessment of the importance of lean in the total fan noise signature will require further experimental work. Fan solidity effects were studied in this phase of the study using a 0.79 and a 1.6 solidity design.

In order to assess the magnitude of this multi-dimensional study, the range of variables studied in this phase of the study is summarized in Table I. It can be seen in this table that the study was conducted assuming an aircraft speed of 70 knots at sea level. This condition was chosen as it represents the lift off velocity for most STOL aircraft where the most stringent sideline noise limitations are generally imposed. For tracked air cushion vehicle and surface effect vehicle noise levels, this condition provides a good indication of the low noise potential of low pressure ratio fans.

Number of vanes effect - For low pressure, low tip speed fans with small number of blades (< 20), the blade passing frequency is so low that the noise in the 1/3 octave bands near blade passing frequency are not important from a PNL standpoint. Thus as shown in Figure 25, the trend in Perceived Noise Level (PNL) versus number of vanes, V, is controlled by the stator broadband noise and higher harmonics of blade passage frequency. This portion of the stator spectrum is nearly independent of number of vanes if stator solidity is preserved. As shown in Figure 26, the acoustic cutoff of the blade passage frequency by use of many vanes, which is considered important in suppressing turbofan noise is found to have a negligible effect on PNL of vane tone noise.

If swirl recovery is held constant as V is decreased, the vane chord increases to the point where eventually the steady flow field around the vanes causes unsteady loads on the rotor. This effect has been checked with a separate calculation and has been found to become noticeable at around V=7. Thus, below V=7, it is expected that the PNL will tend to increase.

Figure 27 shows the trend of PNL as a function of V if thrust is held constant at 27,800 N. The difference between 55 vanes and 7 vanes is seen to be about 1 dB regardless of fan pressure ratio, PR. Figures 28, 29, and 30 show the effect of varying V at different levels of thrust from 13,900 to 222,411 N. Figure 28 shows the effect at 1.05 PR. Figure 29 shows the effect at 1.15 PR. Figure 30 shows the effect at 1.25 PR. The difference between 55 vanes and 7 vanes remains about 1 dB regardless of thrust and pressure ratio variation.

Numbers of blades effect - Figure 31 shows the variation of PNL with variation in number of blades, B, from 7 to 29. A minimum is seen at about 12 B for PR from 1.10 to 1.25. Figure 32 shows that this is due to the dominance of rotor tone noise at low B and the dominance of rotor broadband, stator broadband, and stator tone noise components at high B. At the 1.05 PR condition, figure 32 shows that B for minimum noise has not been reached even at as few as 7B. Thus it appears that very low pressure ratio fans such as those used on TACV's and SEV's will produce minimum noise with less than 7B. Figure 31 demonstrates the importance of selecting the proper number of blades for minimum noise particularly at 1.25 PR where very few blades produce a dominance of rotor tone noise which can be seen on the right in figure 32.

Figure 33 shows the effect of changing B on spectrum character. This figure shows the typical low pressure ratio noise character with dominant tone components appearing at frequencies below 2000 Hz and a fairly rapid rolloff of higher frequency

noise. In addition, it can be seen that the rotor blade passage frequency at 288Hz is dominant in the 7 B spectrum while increasing B first reduces the blade passage tone at 492Hz for 12 B and then completely suppresses its presence at 863Hz with 21 B. In minimizing PNL, the strength of the strong blade passage frequency tone at low B must be balanced against the higher levels of broadband noise at higher frequencies found with higher B.

The increasing stator noise is linked to three competing effects: (1) The stator unsteady forces decrease with increasing B because the stator lift is reduced through the Sears function; (2) for a given force, radiated power is proportional to frequency so that power increases with B; and (3) noise at higher frequencies is penalized through the PNL calculation.

The drop in rotor tone with increasing B is predicted by the Lowson (ref 11) formulas assuming a given inflow distortion. Finally, the slight rise in rotor broadband is due to the increased frequency associated with the reduced blade thickness at larger B. The radiated power is preserved for constant rotor solidity but the higher center frequency again incurrs a PNL penalty.

Figures 34, 35, and 36 show the effect of thrust and PR. It is seen that PR is the dominant effect. Also, except for the 1.05 PR cases, the minimum noise occurs for 11 to 13 B with variation in PNL at the 1.25 PR being less than 1.5 dB at higher thrust levels as B is varied from 12 to 29.

Blade vane gap effect.-With a short distance between the trailing edge of the rotor blades and the leading edge of the stator vanes (BVGAP), the intensity of stator broadband noise as shown in figure 37 dominates the noise generated by the fan particularly at low pressure ratios (1.05) where rotor tone and broadband noise are less significant. As the stator vanes are moved downstream, the total noise is reduced due to reduction in stator generated noise until the rotor broadband floor becomes dominant. At higher pressure ratios the rotor broadband and tone noise is more significant. Therefore increasing BVGAP at higher pressure ratios is not as rewarding as a means of reducing total fan noise.

Figure 38 shows the influence of PR and BVGAP on total noise. At the 1.05 PR worthwhile reductions are achieved with BVGAP's as great as 4 but at 1.1 PR and higher the stronger influence of rotor noise prevents worthwhile reductions at BVGAP's greater than 2. Therefore the fan configurations studied in this program have included BVGAP of 2 as a standard distance between rotor and stator. It should be noted that this assumption might lead to longer ducts when higher solidities (wider blades) are included in the configurations since the BVGAP is in terms of number of blade chords.

Figures 39, 40, and 41 show the influence of thrust and BVGAP for PR's of 1.05, 1.15, and 1.25 respectively. The PR effect as shown in figure 38 is seen to be more significant than the thrust effect shown in figures 39, 40 and 41. However a comparison of the BVGAP effect at 13,900 N thrust with that at 222,400 N thrust shows that the high thrust configurations are generally less influenced by BVGAP than the low thrust cases. This is due to the shift of stator tone and broadband components to very low frequencies where their contribution to PNL is minimized as thrust (and therefore size) is increased. It is the contribution of these components that cause the BVGAP effect.

Exit area ratio effect.-Figure 42 shows the variation in level of the source noise components of a fan as exit area ratio, AR, is varied. For a small exit area (low AR) the rotor broadband noise is seen to dominate over all other components. This is due to the loading on the rotor which is highest (for a given thrust) when exit area is lowest. As AR is increased the rotor is unloaded and rotor broadband noise decreases. However the angles of attack along the rotor blade radius decrease below those for minimum drag as the rotor unloads resulting in increased drag coefficients. Since the rotor blade wake defects are a function of drag coefficient the increase causes an increase in stator tone and broadband noise. The minimum

noise point is a compromise between rotor unloading and increasing rotor drag coefficient.

Figures 43 and 44 show the AR effect for various PR's and solidity of 1.0 and .79. While the influence of AR on noise does not appear large in these figures, noise levels could be increased by 3 dB if AR is not correctly chosen.

Tip speed effect.-The study summarized in this report is multi-dimensional in nature in that many parameters must be optimized to minimize noise produced. In early work in the program it was found that reduction in tip speed was a significant factor in minimizing noise for a given thrust. Subsequently in attempting to reduce the tip speed while maintaining good fan performance it was found that an increase in solidity was beneficial. Therefore both tip speed and solidity variations are included in the study results.

The major emphasis throughout the study has been on the characteristics of a 1.0 solidity fan. This design permits rotation of the blades through feather or flat pitch to produce reverse thrust while catering to the desire for maximum solidity. In addition a 0.79 solidity design, which is an optimized version of the 0.72 solidity fan tested at NASA Langley in 1970, has been included as well as a 1.6 solidity fan which must be reversed by rotation through the feather position. Each of these three designs was operated over the full PR range at minimum performance loss by proper selection of AR. The basic design point for the 0.79 solidity fan was 247 m/s tip speed, 1.18 PR, and 1.669 corrected flow per unit area ($kg/s/m^2$). The design point for the 1.0 solidity fan was 213 m/s tip speed and 1.20 PR. The design point for the 1.6 solidity fan was the same as the 1.0 solidity design. In the study summarized in this section very low tip speed cases have been included. It is not clear at this time that operation at these low tip speeds would be satisfactory due to limited surge margin. While limited experience with Q-FAN's and other low tip speed turbofans has not shown surge to be a problem, more testing will be required to establish that operation at very low tip speeds is completely acceptable from a surge standpoint.

Figure 45 shows the typical characteristic of the tip speed variation curves for a constant thrust of 27,800 N at 70 knots and for the 1.0 solidity design. A minimum noise point is seen to occur for each PR studied. Also as PR is reduced, the tip speed of the minimum noise point is reduced. It appears that the optimum tip speed for the 1.05 PR fan lies below 122 m/s tip speed. Figure 46 shows the source noise components that define the shape of the noise versus tip speed curves.

In the 1.25 PR case shown at the right it can be seen that rotor tone and broadband noise are the dominant factor and reduction in tip speed would cause further increases in noise. This increase due to stator noise with reduction in tip speed is caused by increases in rotor drag coefficient particularly near the tip. At the design tip speed, drag coefficients are minimized and equal across the span of the blade. At higher tip speeds the increase in noise is due to rotor tone noise, which is related to rotor thrust. Although the rotor total pressure rise remains constant the static pressure rise has to increase to overcome falling rotor efficiency.

In the curves to the left in figure 46 the variation in source noise components for the 1.0 solidity rotor operating at 1.05 PR is shown. Here the rotor is lightly loaded so the dominant noise is the result of the stator. Of course, as described elsewhere in this report an increase in BVGAP for the 1.05 PR case could further reduce the stator contribution.

The trend studies summarized in this report have been based primarily on constant thrust levels. For example, figure 45 presents trends for a constant 27,800 N thrust with AR and fan diameter allowed to vary. In figures 47 and 48 the conditions actually encountered in an installation are shown. In figure 47 fan diameter and AR is held constant as PR is varied. This curve shows the reduction in thrust and variation in noise level that results. If a given fan is available and it is possible to introduce optimum exit area ratios then the noise level and thrust variation in figure 48 results. Little difference in noise level is shown between these two figures. However thrust is generally enhanced by use of the correct AR.

Figures 49 and 50 show the tip speed variation for the .79 and 1.6 solidity fans similar to that shown for the 1.0 solidity fan in figure 45. Close inspection of these curves does not show striking differences in the shape of each pressure ratio curve except that the minimum noise occurs at a lower tip speed as solidity is increased. Characteristics from these curves are discussed further in the solidity effect section of this report.

Fan solidity effect.-The influence of fan solidity on noise at various PR's can be seen by replotting some of the information presented in earlier sections. Figure 51 shows a replot of the minimum noise as a function of tip speed presented earlier in figures 45, 49, and 50. It can be seen that PNL increases rapidly from 1.05 to 1.15 PR in the .79 solidity fan. This increase is more gradual in the higher solidity fan design. Above 1.15 PR the increase in noise is not as marked as that seen at the lower PR's. It appears that the greatest reductions in PNL

are achieved with reductions in PR while increases in solidity have less effect.

Figures 52 and 53 show the components of the noise at various AR's studied for 1.1 and 1.2 PR respectively. In figure 52 the noise of the .72 solidity model Q-FAN design tested at NASA Langley in 1970 is included. Also noise of a .79 improved low solidity rotor and a 1.0 higher solidity rotor is shown. It can be seen that the dominant noise source is stator broadband in the .72 solidity fan since the drag coefficients were abnormally high due to off design operation. In the improved low solidity design (.79 solidity) the stator broadband noise is suppressed and rotor broadband becomes important. In the 1.0 solidity design rotor broadband noise is dominant but further suppressed by the increased rotor solidity.

Figure 53 shows that for 1.2 PR, rotor broadband is dominant at the optimum tip speed for the .79 solidity design. However increases in solidity reduce the level of broadband noise to the point where the 1.6 solidity fan is rotor tone dominated.

Figure 54 shows the effects of rotor solidity and pressure ratio for all of the fans studied. The noise of the .72 solidity fan (acoustically tested in model form at NASA Langley) is plotted at the upper left. The minimum noise occurs at 198 m/s tip speed. By increasing the solidity of the fan to .79 and improving the aerodynamic design the curve at the left of figure 54 shows the PNL can be reduced by 9.3 dB. This reduction is found at a lower tip speed. A further increase in solidity to 1.0 gives a further reduction of 5.4 dB at a further slight reduction in tip speed. The same effects are apparent at 1.2 PR as shown in the curves at the right of figure 54. Here by increasing solidity from .79 to 1.6 a reduction of 8.7 dB is found. It is interesting to note that a .79 solidity fan 1.69 m in diameter is only .9 dB less noisy at 1.1 PR than a 1.0 solidity fan 1.25 m in diameter operating at 1.2 PR. It appears that the need for low noise levels with small diameter fans may be satisfied by properly designed higher solidity rotors.

Thrust effect.-Figure 55 shows a typical variation of PNL with thrust and PR. The PNL increase is very close to 2.5 dB per doubling of thrust regardless of PR. On a sound power basis an increase of 3 dB per doubling of thrust might be expected but as thrust increases the size of the fan increases and frequency of dominant noise shifts lower in frequency as shown in figure 56. When this shift is evaluated on a PNL basis the low frequency contribution is not weighted as heavily as the noise at frequencies above 1000 Hz. Therefore the increase is found to be 2.5 dB per doubling of thrust rather than 3 dB per doubling.

Pressure ratio effect.-The influence of pressure ratio, PR, on noise has been of great interest in design of quiet STOL aircraft as it was known that reducing PR should reduce noise. However, the increase in fan diameter accompanying the reduced PR was found to result in aircraft designs with difficult control problems and limited cruise speeds. Figure 57 shows the influence of PR on PNL. Reducing PR does reduce PNL particularly below 1.10 PR. Rotor broadband noise is seen to be the dominant component of fan noise. Below 1.1 PR stator broadband noise is more of a factor in the total fan noise.

Because of the aircraft design constraints, it is interesting to consider the shaftpower and fan diameter required for the PR variation shown in figure 57. Figure 58 shows that shaftpower increases substantially from 1.05 to 1.25 PR for a constant thrust. The shaftpower required at 1.25 PR is seen to be 1.7 times that at 1.05 PR. Also the major reduction in diameter occurs in shifting from 1.05 to 1.10 PR. The fan diameter is seen to be reduced by half in shifting from 1.05 to 1.2 PR. With further increases in PR further reductions in diameter will be small. Thus higher pressure ratios would be expected to yield further increases in noise without significant reduction in fan diameter.

Figure 59 shows how the spectrum character of the fan noise varies with PR. At low PR the major noise is found below 1000 Hz where it contributes little to PNL. As PR increases the higher tip speed of operation and smaller diameter at a given thrust raise the frequency of major noise contributions. Also the rotor noise contribution at blade passage frequency is seen to become more pronounced. This increase, however, is not a major factor in PNL as the blade passage frequency is usually less than 1000 Hz.

As an indication of the results of the study the information in figure 60 is instructive. Here the PNL's derived from this study for a four engine STOL aircraft are plotted as a function of PR. These trends are compared with those presented in the NASA Propulsion conference in 1970. It is encouraging to see that the trends are similar in shape to the NASA projections and that the levels estimated in this study are equal to or less than those in the reference. It should be noted that figure 60 does not include the results of the duct lining study which are discussed in a later section of this report.

Vane Lean Effect

Introduction.-The simplified duct mode analysis described in the methodology section was employed to study acoustic effects associated with shearing the rotor wakes at the stator rather than chopping them in phase from hub to tip. This effect is always present to a certain

extent because of the wake distortion which results from the rotor swirl distribution. Leaning the vane tips in the direction of rotor rotation can accentuate the effect. Trend studies were performed using plots of amplitude coefficients for the spinning modes versus radial mode orders and relating these coupling curves to the radial cutoff condition. It is found that low tip speed fans are in a different class with respect to radial phase effects than are the higher tip speed turbofans. In particular a low pressure ratio fan whose stator tone cannot be suppressed adequately by reduced profile drag on the rotor and large rotor/stator gap could benefit from lean. However the optimized fan designs discussed in other sections of this report would probably not benefit from lean because wake distortion will produce adequate radial cutoff with no performance penalty.

Vane lean trends with tip speed and pressure ratio.-For this study a fan with 12 blades, 1.0 solidity, a BVGAP of 2, and a 0.5 hub/tip ratio has been used. Modal amplitude coefficients (analogous to sound pressure level) vs radial mode order are plotted in figures 61, 62, and 63 with and without lean for tip speeds of 152, 213, and 279 m/s and pressure ratios of 1.05, 1.10, and 1.15. The cutoff correlation shown is for no nodal diameters which is pessimistic for the first harmonic but irrelevant at higher harmonics as shown by a study of the cutoff correlation equations. Thus for the higher harmonics the number of vanes is unimportant with respect to the cutoff arguments. Also the cutoff becomes sharper for large harmonic order.

Figure 61 shows the trends with tip speed at 1.10 PR. At low tip speed the wake windup alone produces considerable radial cutoff for all harmonics which is lost at around 274 m/s tip speed. The lean pushes the response further into cutoff and would be a benefit for tip speeds greater than 274 m/s

Figures 62 shows the trends with pressure ratio at a tip speed of 213 m/s. At a 1.05 pressure ratio the peaks of the modal amplitude curves are on the propagating side of the cutoff line without lean but are strongly cutoff with lean. At higher pressure ratios the wake windup probably produces adequate cutoff.

Figure 63 summarizes the tip speed and pressure ratio study by showing only the peak of the modal amplitude curve and how it moves with lean. Clearly, the trend is to increased radial cutoff (reduced noise level) with reduced tip speed, increased pressure ratio, and increased lean.

DUCT LINING STUDY

Initial Study

Using the method described in an earlier section of this report, a general study was conducted using an actual Q-FAN configuration which included the correct duct lengths, centerbody size and engine inlet splitter. For this study a 0.79 solidity fan operating at 1.15 PR was used. The objective in this study was the development of a treatment location philosophy that would give maximum attenuation with minimum treatment. A careful review of the Q-FAN model test results showed that both stator and rotor contribution existed in the directivity patterns of fan noise. Therefore, inlet treatment was primarily tuned to minimize rotor noise while aft treatment was usually optimized to minimize stator noise.

Figure 64 shows the results of the initial study. The sketch at the top of the page shows the configuration studied as well as the location of the various treatment modules referred to in the table below. Treatment is broken into three modules, inlet treatment ahead of the rotor, mid treatment extending from aft of the rotor to the stator quarter chord point, and exhaust treatment aft of the stator quarter chord point. The exhaust treatment was found most effective with an attenuation of 4.5 dB for optimized treatment. Installation of mid treatment to suppress stator noise passing upstream through the inlet was found to be more effective than extension of the exhaust treatment. Also a splitter in the exhaust is considered equal in effectiveness to extending the wall treatment. As shown later, the splitter appears to be a better choice from a cruise thrust loss as well. After the initial reduction in noise due to aft wall treatment further increases appear more difficult. For example, to double the 4.5 dB attenuation of aft wall treatment; wall treatment in inlet, mid section, and in a significantly extended aft section (or two splitters) is required. Inlet treatment with a splitter is shown in figure 64 to be required only after splitters in the exhaust plus treatment in the mid section is installed.

Detailed Study

From the above study, three basic treatment systems were selected which appeared to have the greatest noise reduction potential with minimum cruise thrust loss. These are shown in the sketches of figure 65. The first system, the minimum treatment configuration, offers the greatest reduction in noise for the least treatment installed. The second system is either the mid section treatment with extended aft treatment or a splitter in the aft section. This system, in the initial study, showed a worthwhile gain in attenuation over the minimum treatment. The third system was similar to the second system, but included inlet wall treatment in addition to the mid section and aft treatment. More extensive treatment systems were not considered in the detailed study because of the significant performance losses at high cruise speeds (Mach. 0.75 at 6096 m). Of course, more

extensive treatment is feasible for tracked air cushion vehicles or surface effect vehicles which operate at lower cruise speeds and are less sensitive to the increased weight of additional treatment.

The performance losses of the systems selected were evaluated as described in an earlier section of this report. Due to a lack of experimental data on losses of acoustic duct lining, the analytical semi empirical approach described in the earlier section was used to estimate the performance losses. Calculations were done for a typical aircraft cruise speed of Mach 0.75 to 6096 m to indicate the losses that might result from the installation of the duct linings selected. Initially, both perforated plate over honeycomb and woven fiberglas impregnated with resin were considered as compared with smooth aircraft skin. The skin friction coefficient as calculated for the cruise case was found to be 0.0040 for the perforate, 0.0047 for the woven material and 0.0030 for the smooth aircraft skin. Since the penalty for the woven material was significant, it was decided that it would not be considered further in the study.

Calculations were done by summing frictional drags from four sources:

1. The added friction due to the liner without any extension.

2. The total internal friction of any liner extension.

3. The external friction (smooth surface) of any liner extension.

4. The added internal drag of a thin annular airfoil (if present) at zero angle of attack where the drag assumed includes friction and profile drag.

The results of these calculations are summarized in figure 66. It is shown that the losses for the splitter ring systems is less than that for the extended treatment. Also the losses are significant for any but the minimum treatment. Increases in PR reduce losses but any treatment other than the minimum shows significant loss in cruise thrust. Of course, a reduction in cruise speed would reduce these losses.

The percentage loss in net thrust drops considerably at lower forward speeds. For example, at the 70 knot takeoff condition, the internal mach numbers are lower yielding, lower incremental frictional drags but more important the net thrust at the lower speed is as much as 5 times larger than that at mach 0.75. Thus the percentage losses shown in figure 66 can be divided by at least 5 at the 70 knot takeoff case and thus become insignificant. Therefore, in considering the losses in cruise thrust, the potential reduction in these losses as cruise speed is reduced should be considered.

It should be noted that this study was conducted primarily to put the performance losses for duct lining in perspective when considering the noise reduction potential for the liners which is described below. Of course optimization of materials and their application could modify the above results. Also test data on losses is needed to fully assess cruise thrust degradation.

Figure 67 shows the reduction estimated for the configuration shown in Figure 65. Attenuation for both the 0.79 and 1.0 solidity fan are shown. Better attenuation is achieved at higher PR's because the duct height is more satisfactory for the frequencies found dominant. It is interesting to compare fans on an equal noise basis. For example, an untreated 0.79 solidity fan operating at 1.08 PR produces the same PNL as a 0.79 solidity fan at 1.25 PR with treatment consisting of extended wall treatment or wall treatment plus aft splitter. The 1.25 PR fan will also be penalized with an 8% loss of cruise thrust according to Figure 66. Moving to the 1.0 solidity design, a 1.15 PR untreated fan could be used to produce the same 95.6 PNdB level.

Figure 68 shows the influence of tip speed on attenuation of the three systems of Figure 65. No substantial shift in performance of the liners can be seen in this figure indicating that for the optimum fan design, a shift in tip speed provides little benefit in further noise reduction.

Figure 69 shows the effect of number of blades on treatment performance. The shift in frequency achieved again has little influence on treatment performance.

MECHANICAL DESIGN STUDY

The feasibility of manufacture and test of scale models of the various fan designs used in the study was assessed in a mechanical design study. For this study major emphasis was on manufacture and test of a 0.457 m diameter fan with ground adjustable pitch capability. No limitations were found in the manufacture or test of the twelve blade 0.79 or 1.0 solidity designs.

In the case of the 1.6 solidity design it was found that an eighteen blade variable pitch 1.6 solidity fan would be acceptable. This model would produce essentially the same noise as the twelve bladed 1.6 solidity design. Also a twelve blade 1.6 solidity fan could be built with dovetail retention. Several hubs with different slots would be used in testing this configuration. In assessing the feasibility of fabrication and test of the twelve blade 1.6 solidity fan design, slight reductions in solidity or increases in model size could be considered to eliminate any mechanical design or test restrictions.

CONCLUSIONS

In a multi dimensional analytical study such as summarized in this report, many conclusions can be drawn. However, only those considered most important will be presented here. It is emphasized that the conclusions are based on analytical study correlated wherever possible with existing test data. Much experimental work is required in this new low pressure ratio operating regime to refine the existing methods and establish the ultimate minimum noise fan system that can satisfy stated performance objectives.

From the work in this study, the following conclusions have been drawn.

1. Both rotor blades and stator vanes contribute to the noise signature of low pressure ratio fans. Tone noise at blade passage frequency and at the higher harmonics of blade passage frequency are the result of non-steady inflow to the fan. Tone noise at twice blade passage frequency and several higher harmonics result from interception of rotor blade wakes by the stators. The mid-frequency broadband noise also results from interception of wakes by the stators. However it is the randomness in amplitude and arrival time that generate the broadband stator noise. Rotor broadband noise is a contribution only at high frequencies where the level of stator broadband decays.

2. At pressure ratios from 1.1 to 1.25, optimum low pressure ratio fans have been found to have few blades (11 to 13) and few stators (as few as 7). In contrast past and current turbofans have many blades and generally a stator number more than twice the number of blades. At pressure ratios lower than 1.1, fewer than 11 blades appear to produce minimum noise. A blade-vane gap of 2 blade chords is found to provide the major reduction in rotor stator interaction noise in fans operating at 1.1 pressure ratio or higher. At lower pressure ratios, additional worthwhile reductions are achieved at a blade-vane gap of 4 blade chords. Optimization of fan aerodynamics at the lowest operating tip speed possible has been found to be the most powerful means to reduce fan noise at a given pressure ratio. Also high solidity has been found to reduce noise at a given tip speed. Of course reduction in pressure ratio reduces noise.

3. If stator tone noise is a significant source relative to stator broadband and rotor tone and broadband noise, then vane lean can be a useful noise suppression technique. The calculations in this study show that, for low

tip speed, very low pressure ratio fan (<1.1) vane lean can reduce the stator harmonic radiation. However, for low tip speed low pressure ratio fans (1.15 to 1.25) with reasonable blade-vane gap, the benefits of radial cutoff are already achieved by wake windup. If, at these intermediate low pressure ratios, a fan design is required with a small blade-vane gap so that little wake windup develops then lean could be a significant advantage.

4. Duct lining can be very effective in reducing noise of low pressure ratio fans. Reductions of 5 dB in perceived noise level have been calculated for simple aft shroud treatment that produces less than 1% loss in high speed cruise thrust. With greater cruise thrust penalties, attenuations of 11 dB in perceived noise levels have been calculated. Better attenuations for a given treatment system were achieved at higher pressure ratios. However, these higher pressure ratio fans produced significantly more noise which must be suppressed at some performance loss.

5. With minimum treatment, 1.0 solidity fans operating at 1.15 pressure ratio can be designed to meet an objective of 95 PNdB at 152 m for a 45,360 kg 4 engine STOL aircraft. With slightly more treatment or increased fan solidity, this objective can be met with 1.25 pressure ratio fans.

REFERENCES

1. Rosen, G., "PROP-FAN - A High Thrust Low Noise Propulsor," SAE Paper 710470 presented at the National Air Transportation Meeting, May 1971.
2. Rosen, G., "Trends in Aircraft Propulsion" Canadian Aeronautics and Space Institute, paper presented at the 12th Anglo-American Aeronautical Conference, July 1971.
3. Metzger, F. B. and Ganger, T. G., - Results of Initial Prop-Fan Model Acoustic Testing," NASA CR111842, (Also Hamilton Standard Engineering Report HSER 5787, Windsor Locks, Connecticut, Dec. 4, 1970).
4. Silverstein, A. Katzoff, S. and Bullivant, W. K., "Downwash and Wake Behind Plain and Flapped Airfoils," NACA Report 651, 1939.
5. Sears, W. R., "Some Aspects of Non-stationary Airfoil Theory and Its Practical Application," Journal of the Aeronautical Sciences, Volume 8, 1941.
6. Horlock, J. H., "Fluctuating Lift Forces on Aerofoils Moving Through Transverse and Chordwise Gusts," Transactions of the ASME - Journal of Basic Engineering, December 1968.
7. Mugridge, B. D., The Generation and Radiation of Acoustic Energy by the Blades of a Sub-Sonic Axial Flow Fan Due to Unsteady Flow Interaction, Phd Thesis, University of Southampton, Southampton, England, January 1970.
8. Clark, L. T., "The Radiation of Sound from an Airfoil Immersed in a Laminar Flow." ASME Paper No. 71-GT-4, ASME 16th Annual Gas Turbine Conference. March 28 - April 1, 1971.
9. MacFarlane, "On the Energy Spectrum of an Almost Periodic Succession of Pulses Proceeding of the IRE," 1949 (37) 1139.

10. Lowson, M. V., "Theoretical Studies of Compressor Noise, "National Aeronautics and Space Administration, Washington, D. C., NASA CR-1519, April 1970.
11. Tyler, J. M. and Sofrin, T. G., "Axial Flow Compressor Noise Studies," Transaction of the Society of Automotive Engineers, 1961, pp. 309-332.
12. Lowson, M. V., "Rotor Noise Radiation in Non-Uniform Flow, "Paper presented at the Symposium on Aerodynamic Noise, Loughborough University of Technology, Loughborough, England, September 1970.
13. Barry, F. W. and Magliozzi, B., "Noise Detectability Prediction Method for Low Tip Speed Propellers, "Technical Report AFAPL TR71-37, June 1971.
14. J. Nemec, "Noise of Axial Fans and Compressors: Study of its Radiation and Reduction, "J. Sound and Vibration, 6, (2), 1967.
15. G. V. R. Rao, "Study of Non-Radial Stators for Noise Reduction, "NASA CR-1882, National Aeronautics and Space Administration, Washington, D. C.
16. "LF 336/6 Modification and Acoustic Test Program", General Electric Compnay, Cincinnati, Ohio, September 1970.
17. Hoerner, S. F., "Fluid Dynamic Drug, publisher by the author, 1958.

Table I

Range of Study Parameters

Tip Speed 122 to 244 m/s

Pressure Ratio 1.05 to 1.25

Fan Rotor Solidity 0.79 to 1.6

Number of Blades 7 to 29

Number of Vanes 3 to 55

Exit Area Ratio 0.75 to 1.25

Fan System Thrust at 70 Knots 13,900 to 222,400 N

Blade Vane Gap 1 to 6 rotor blade chords

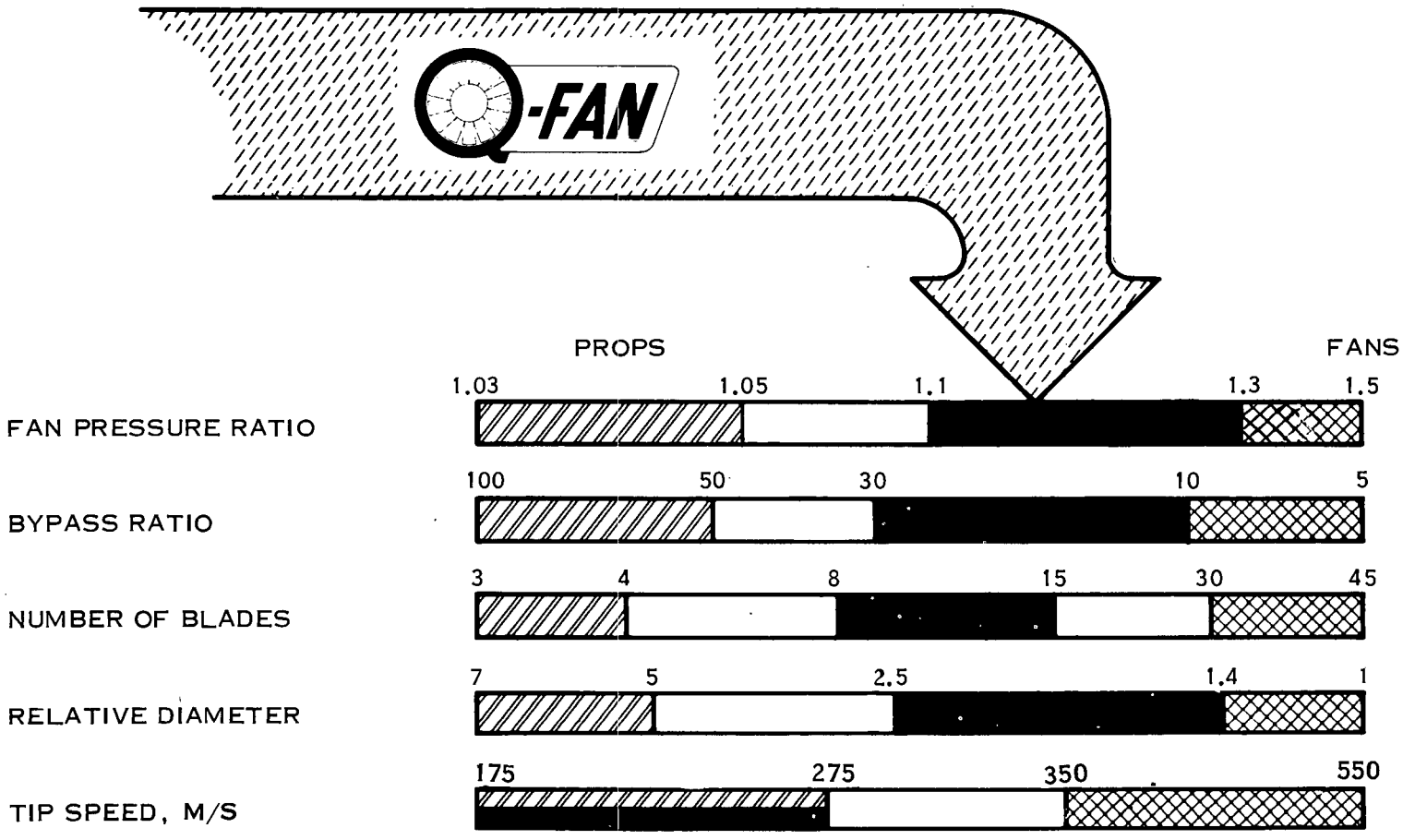

FIGURE 1. Q-FAN CHARACTERISTICS

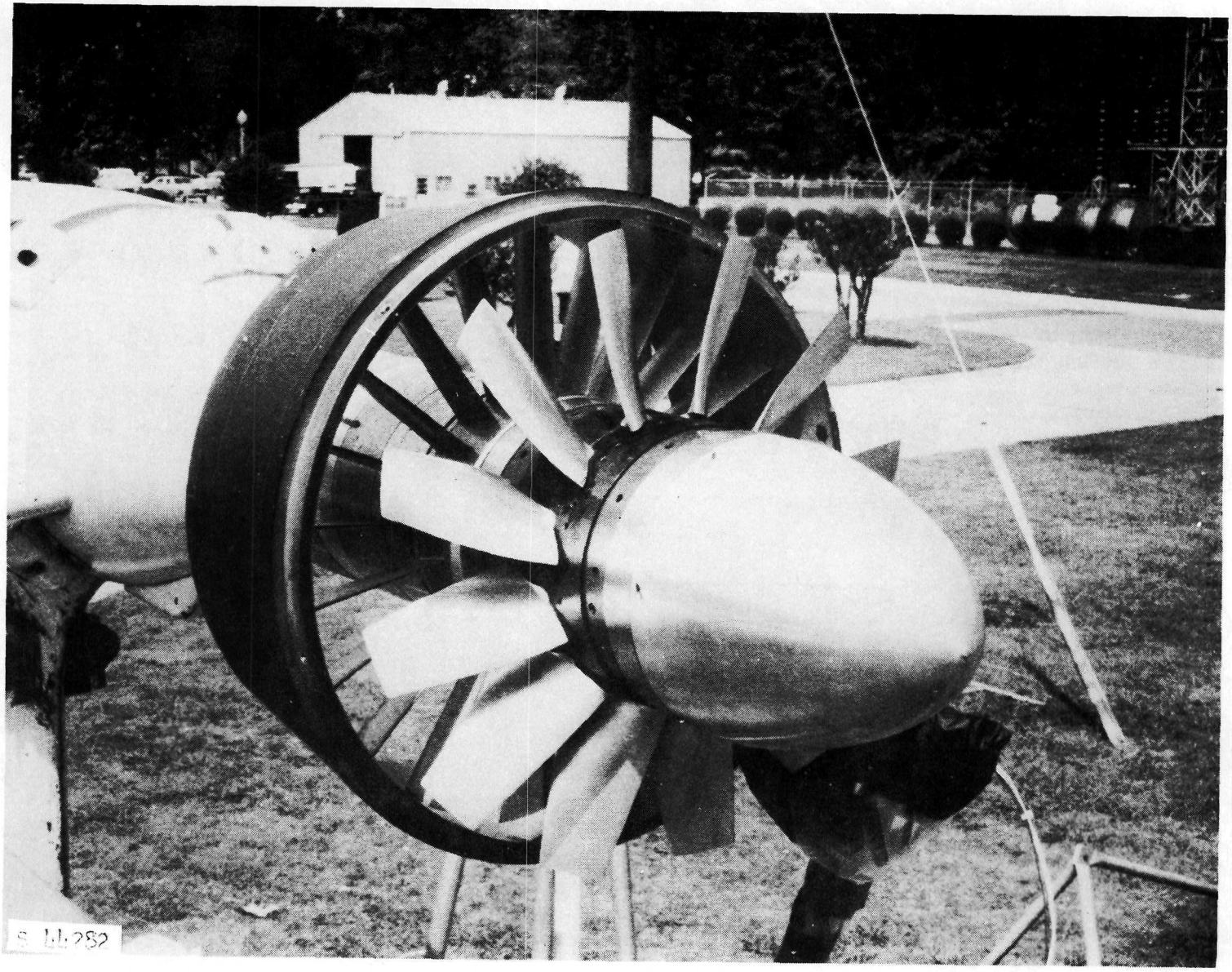

FIGURE 2. Q-FAN MODEL

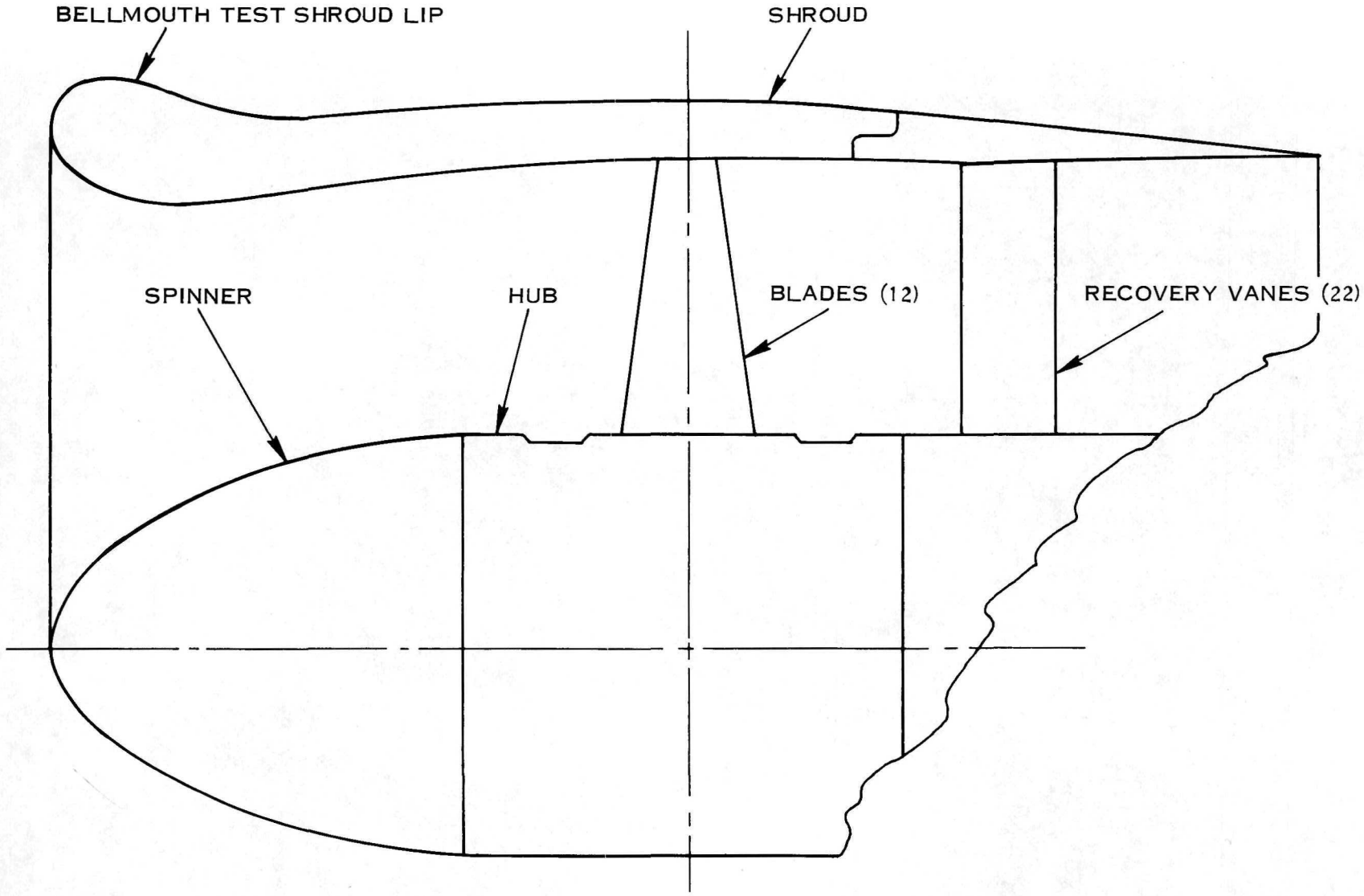

FIGURE 3. Q—FAN MODEL

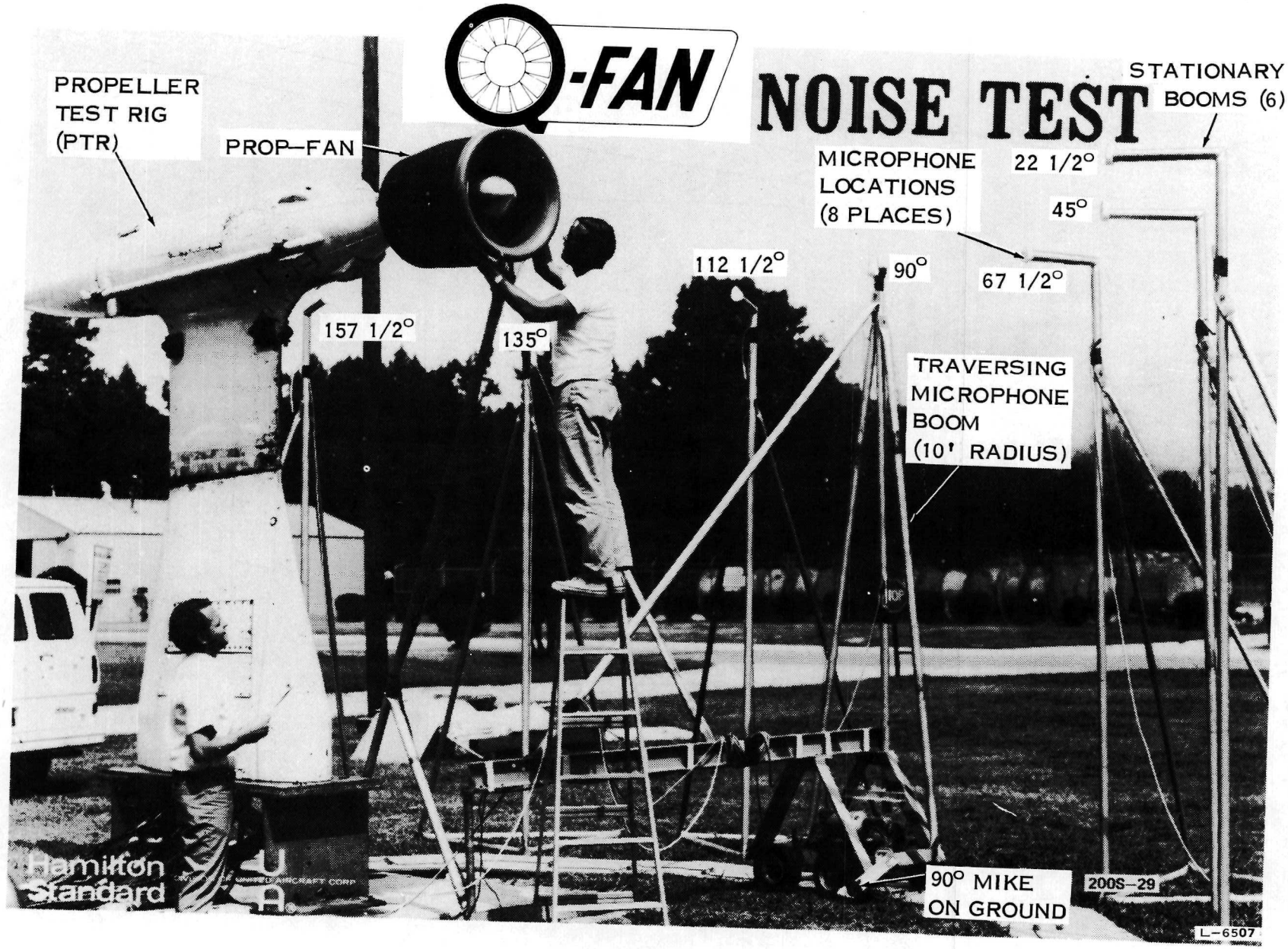
Q-FAN
NOISE TEST
PROPELLER TEST RIG (PTR)
PROP-FAN
STATIONARY BOOMS (6)
MICROPHONE LOCATIONS (8 PLACES)
22 1/2°
45°
67 1/2°
90°
112 1/2°
135°
157 1/2°
TRAVERSING MICROPHONE BOOM (10' RADIUS)
90° MIKE ON GROUND
200S-29
L-6507
Hamilton Standard

FIGURE 4.

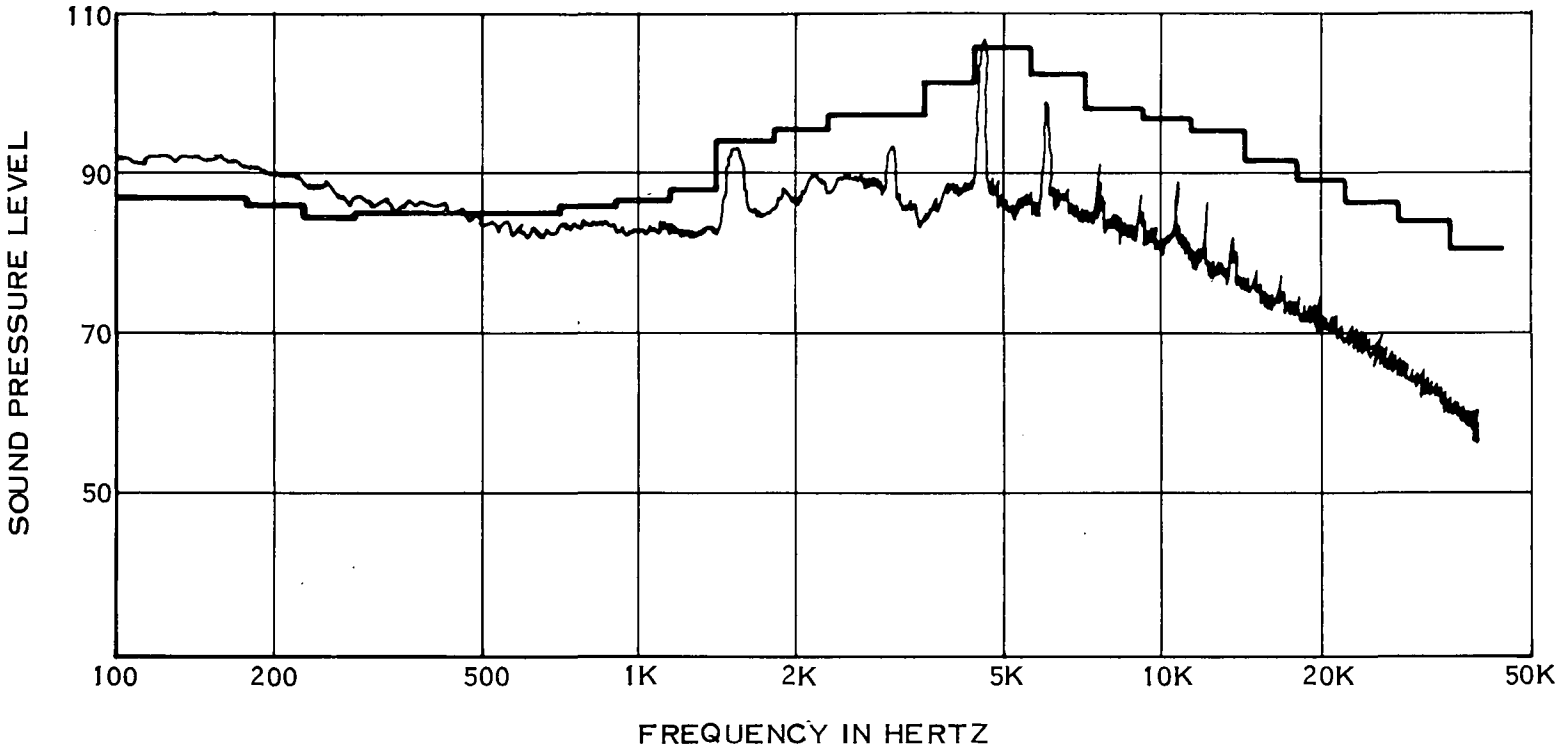

100 Hz FILTER	STATIC SHROUD (BELLMOUTH) BLADE ANGLE 45° TIP SPEED 213 M/S MICROPHONE LOCATION 3.05 M, 112-1/2°

FIGURE 5. Q-FAN MODEL NOISE

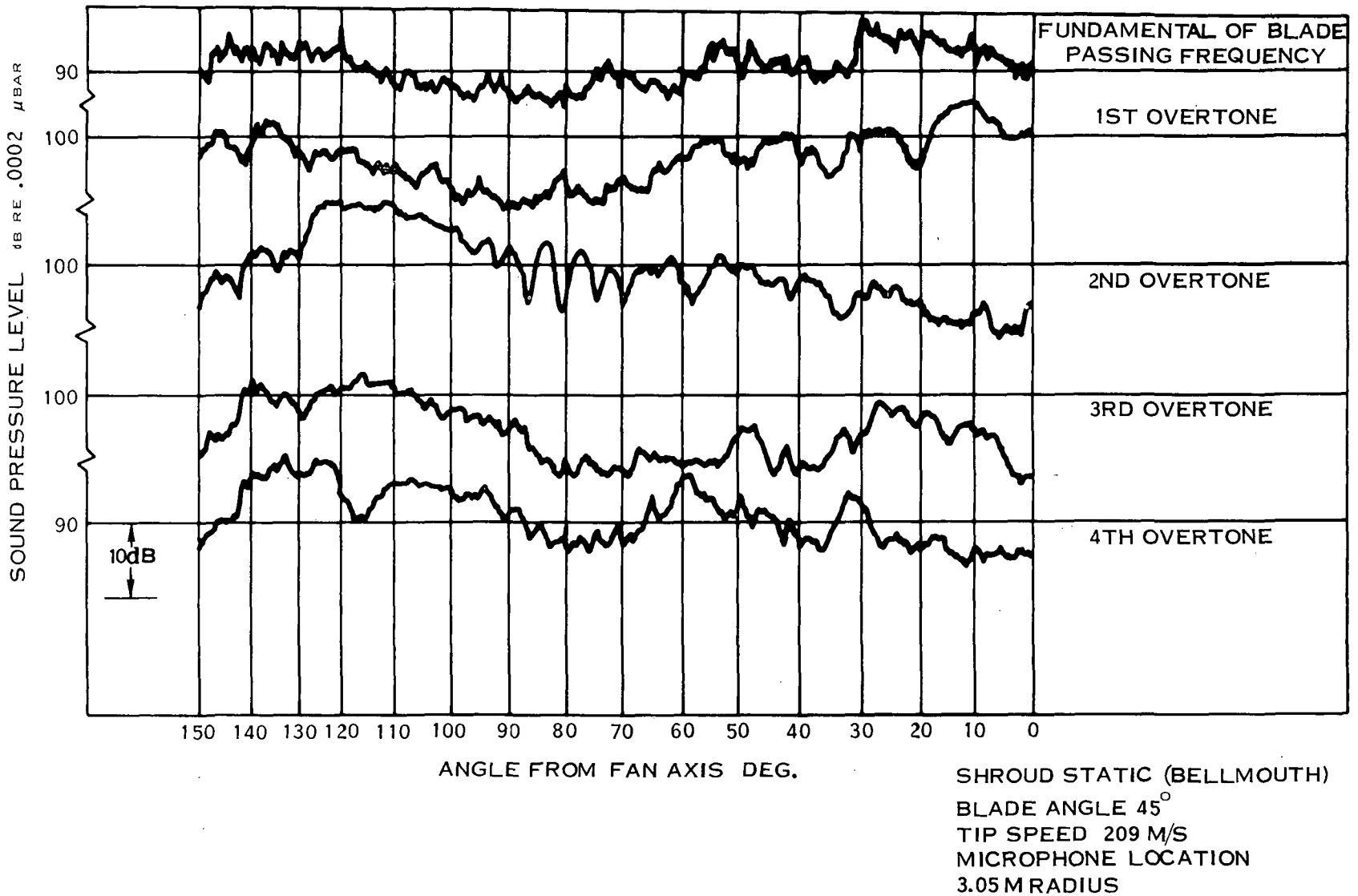

FIGURE 6. Q-FAN MODEL NOISE

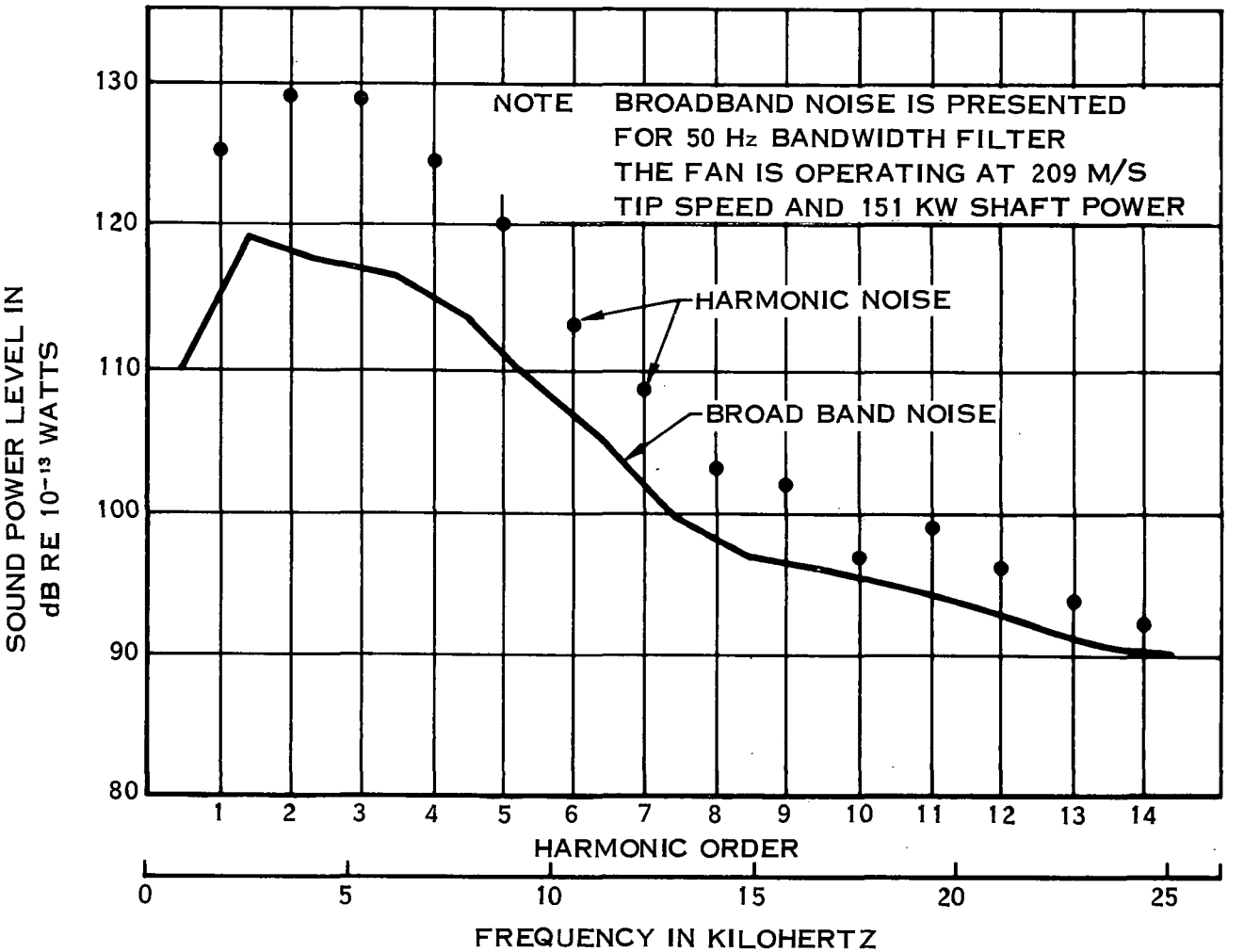

FIGURE 7. SAMPLE SOUND POWER LEVEL ANALYSIS

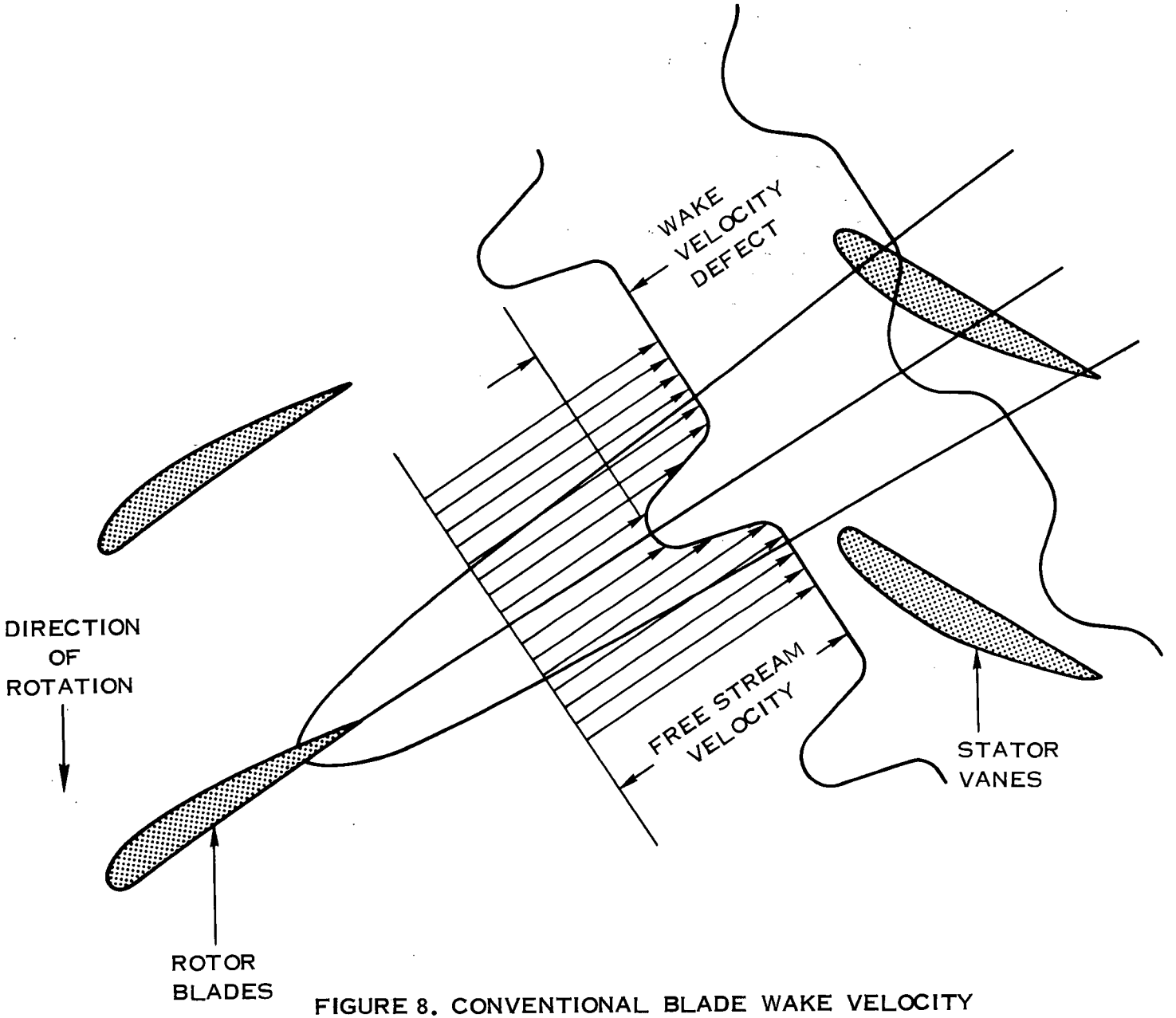

FIGURE 8. CONVENTIONAL BLADE WAKE VELOCITY DEFECT MODEL

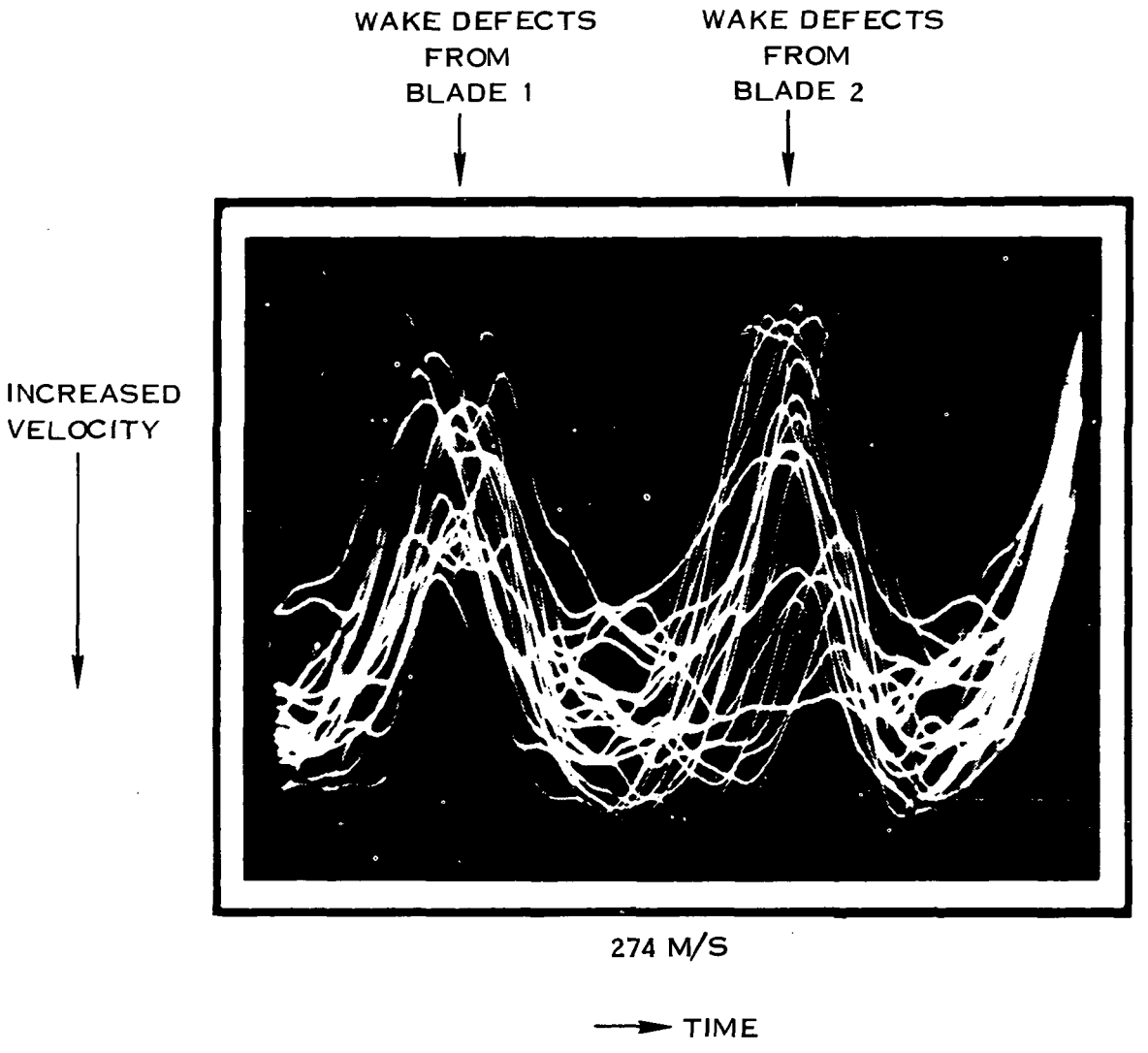

FIGURE 9. SUBSONIC TIP SPEED TURBOFAN BLADE WAKE TRACES

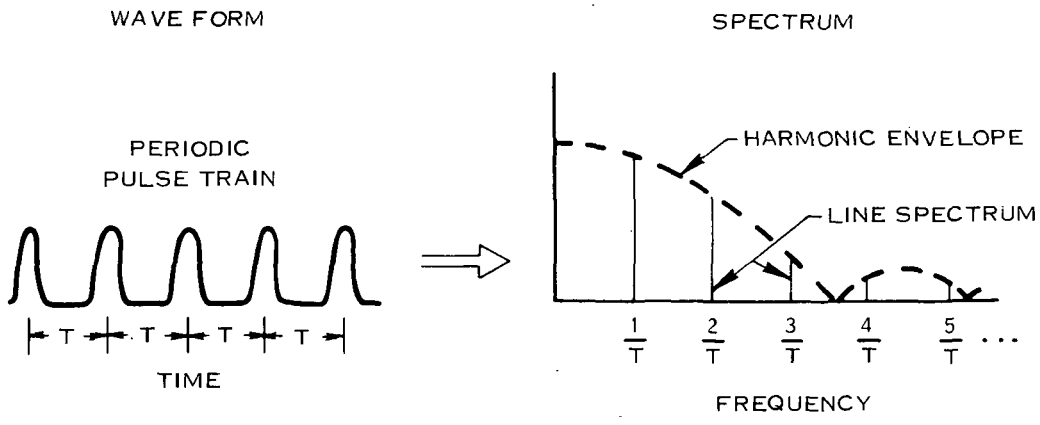

A. PERIODIC SIGNAL

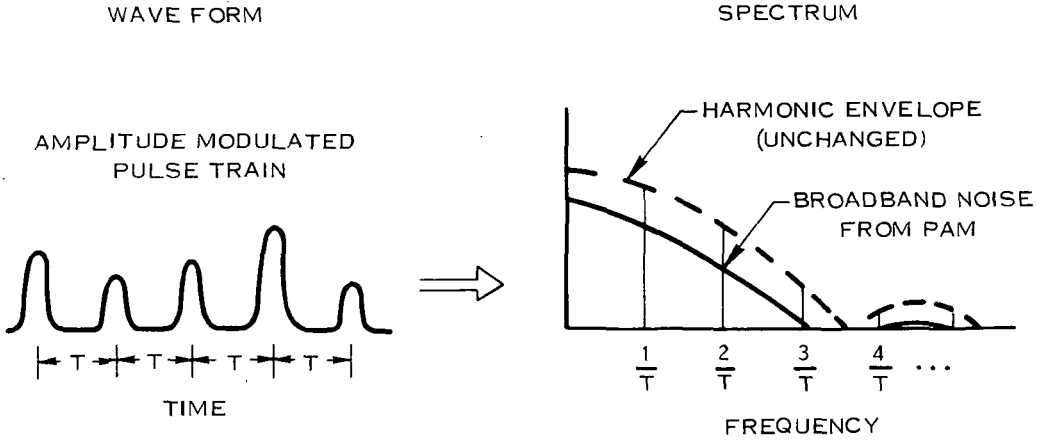

B. AMPLITUDE MODULATED SIGNAL

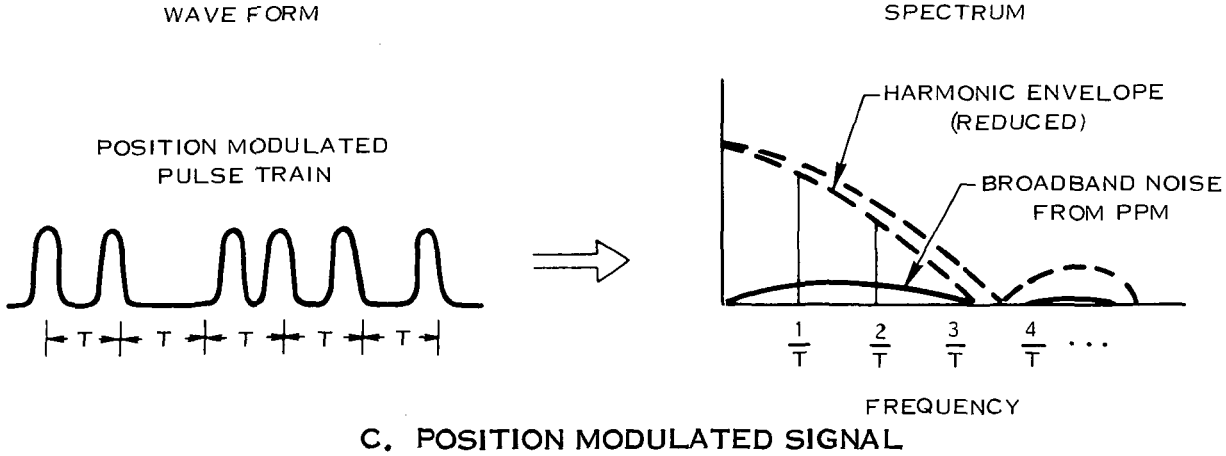

C. POSITION MODULATED SIGNAL

FIGURE 10. EFFECTS OF MODULATION ON SPECTRUM

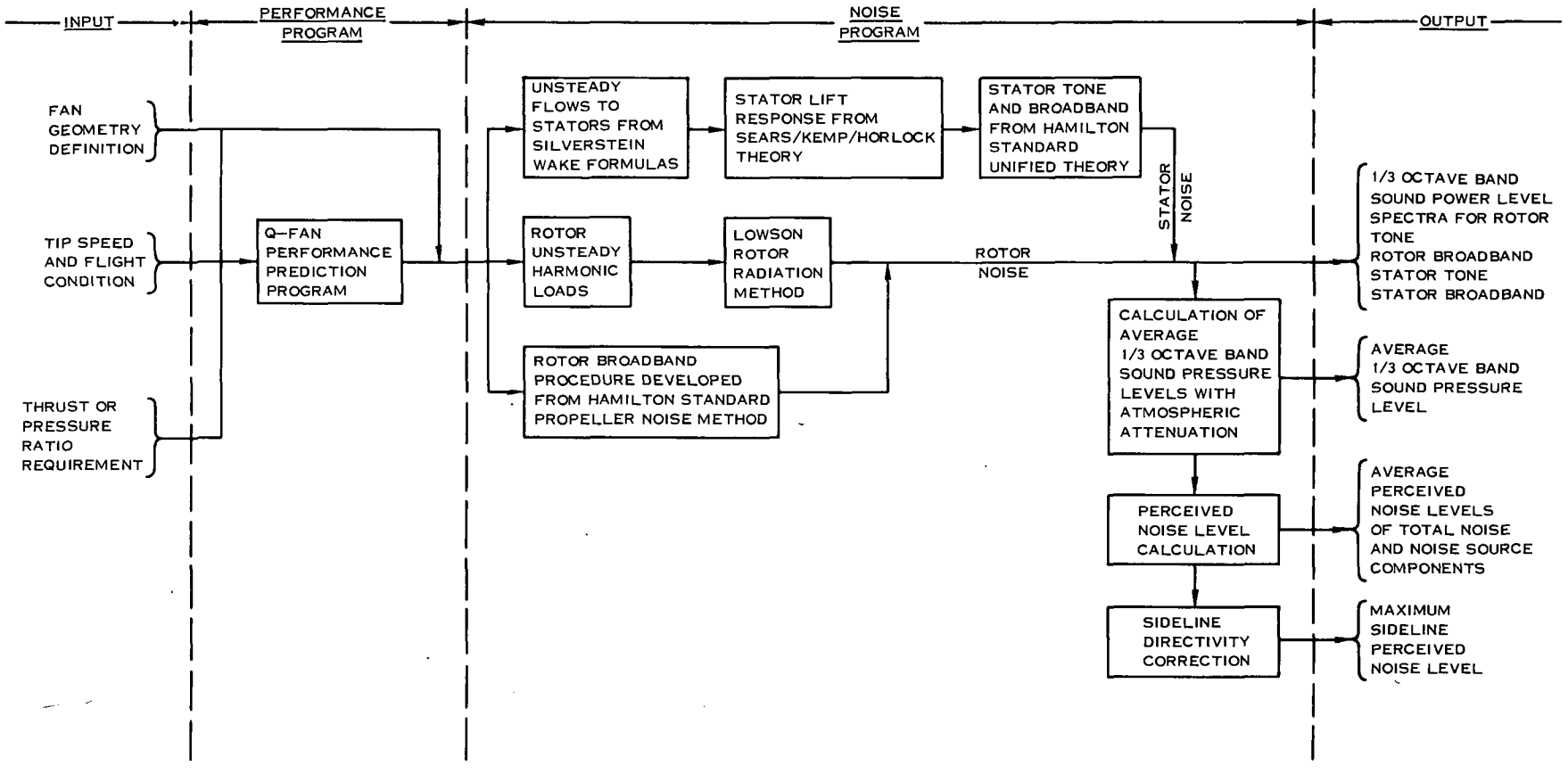

FIGURE 11. HAMILTON STANDARD Q-FAN NOISE PREDICTION COMPUTER PROGRAM FLOW CHART

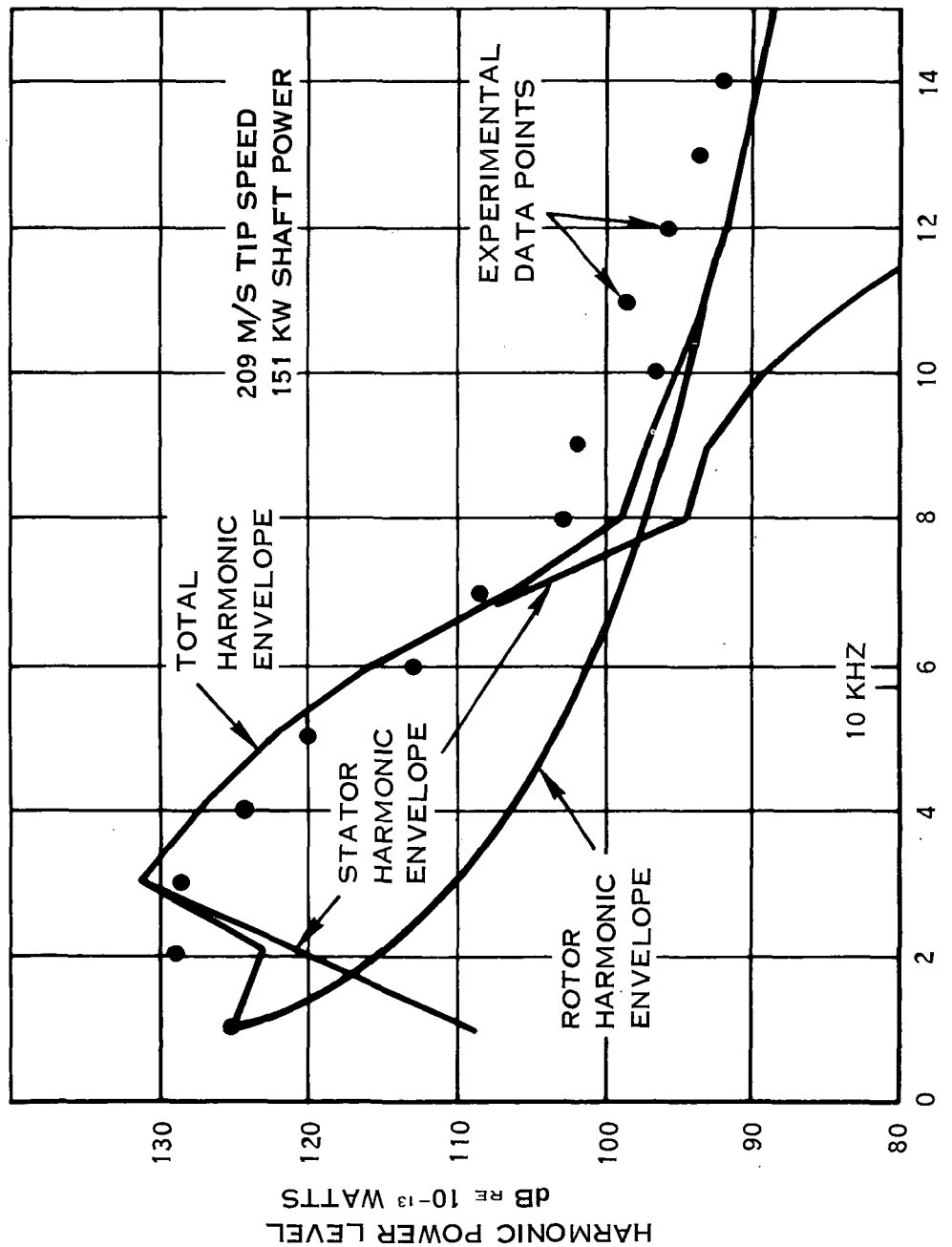

FIGURE 12. TONE NOISE EXPERIMENT & THEORY

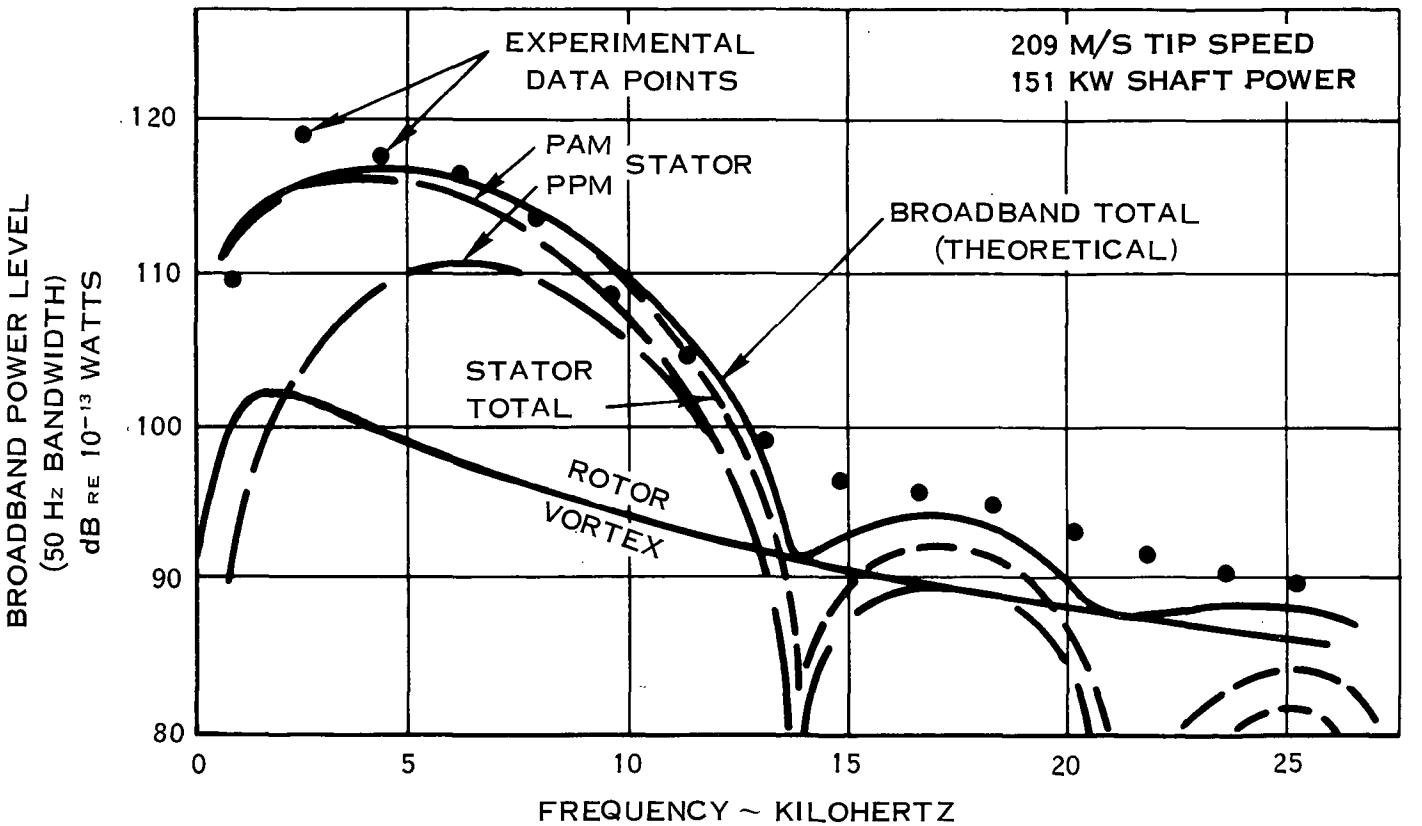

FIGURE 13. BROADBAND NOISE EXPERIMENT & THEORY

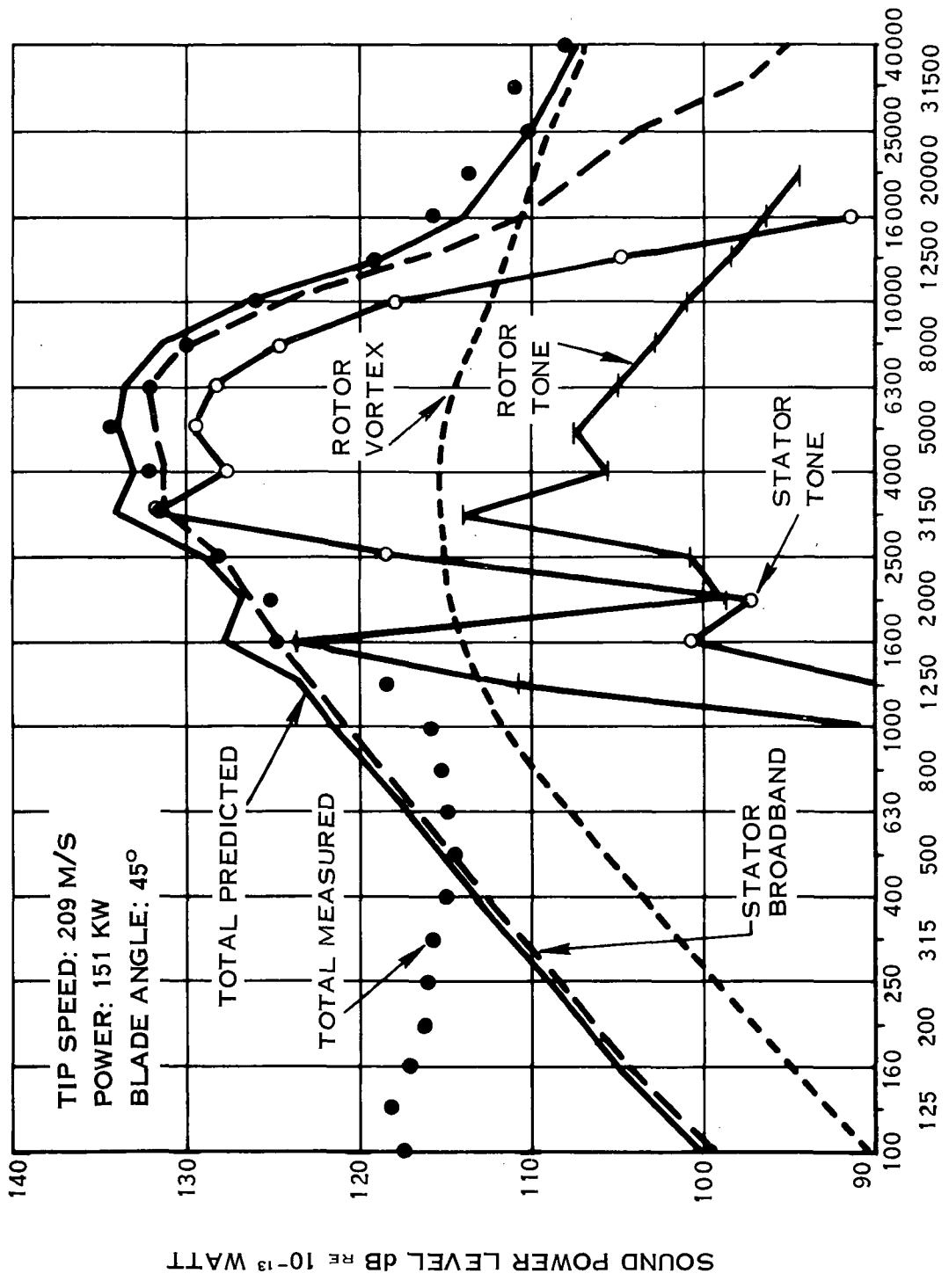

FIGURE 14. ONE-THIRD OCTAVE BAND COMPARISON OF EXPERIMENT AND THEORY-NOISE COMPONENTS

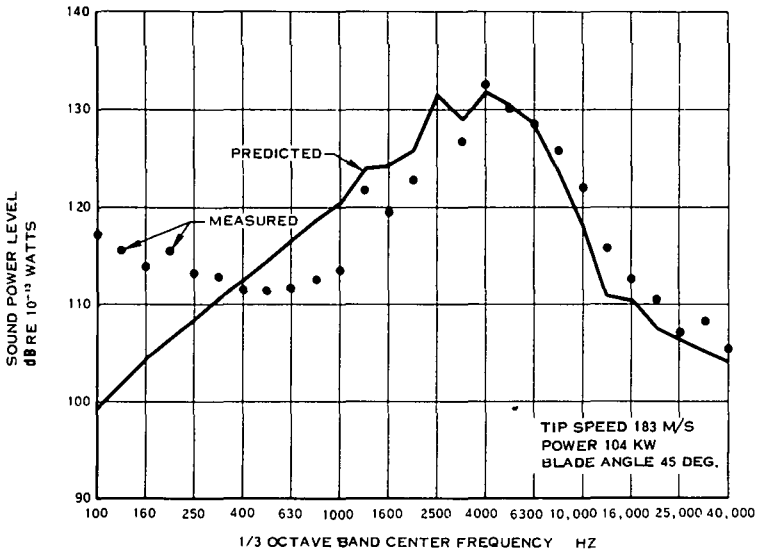

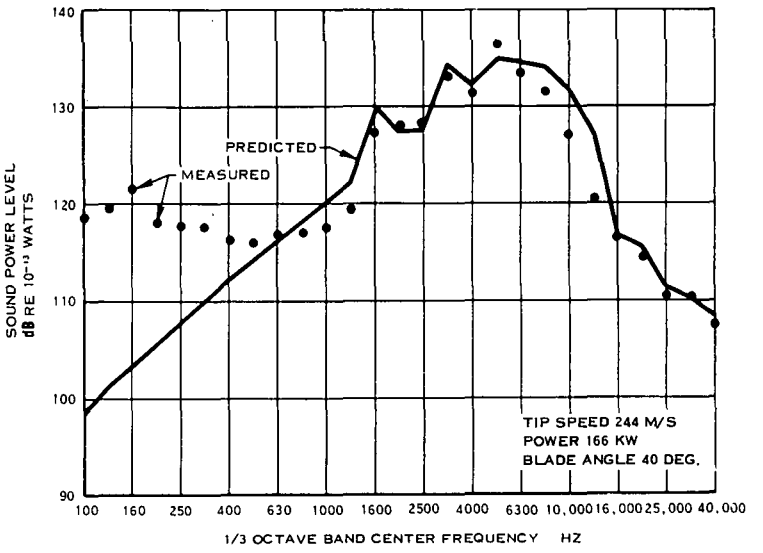

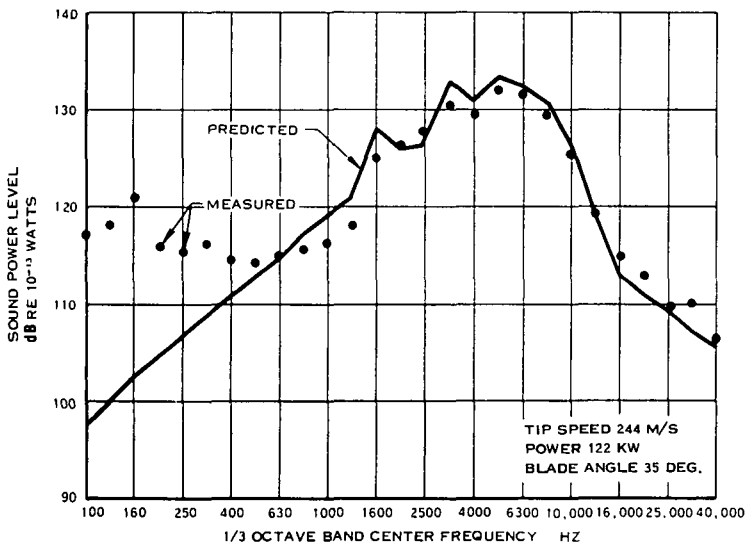

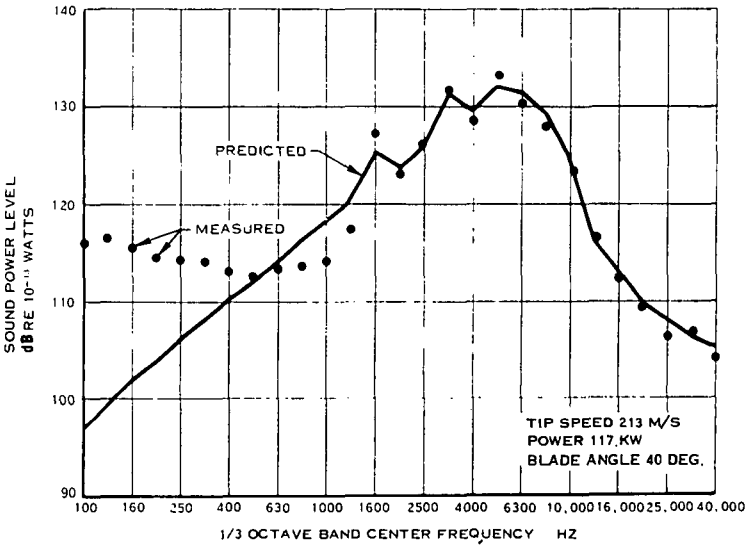

FIGURE 15. ONE—THIRD OCTAVE BAND COMPARISON OF EXPERIMENT AND THEORY

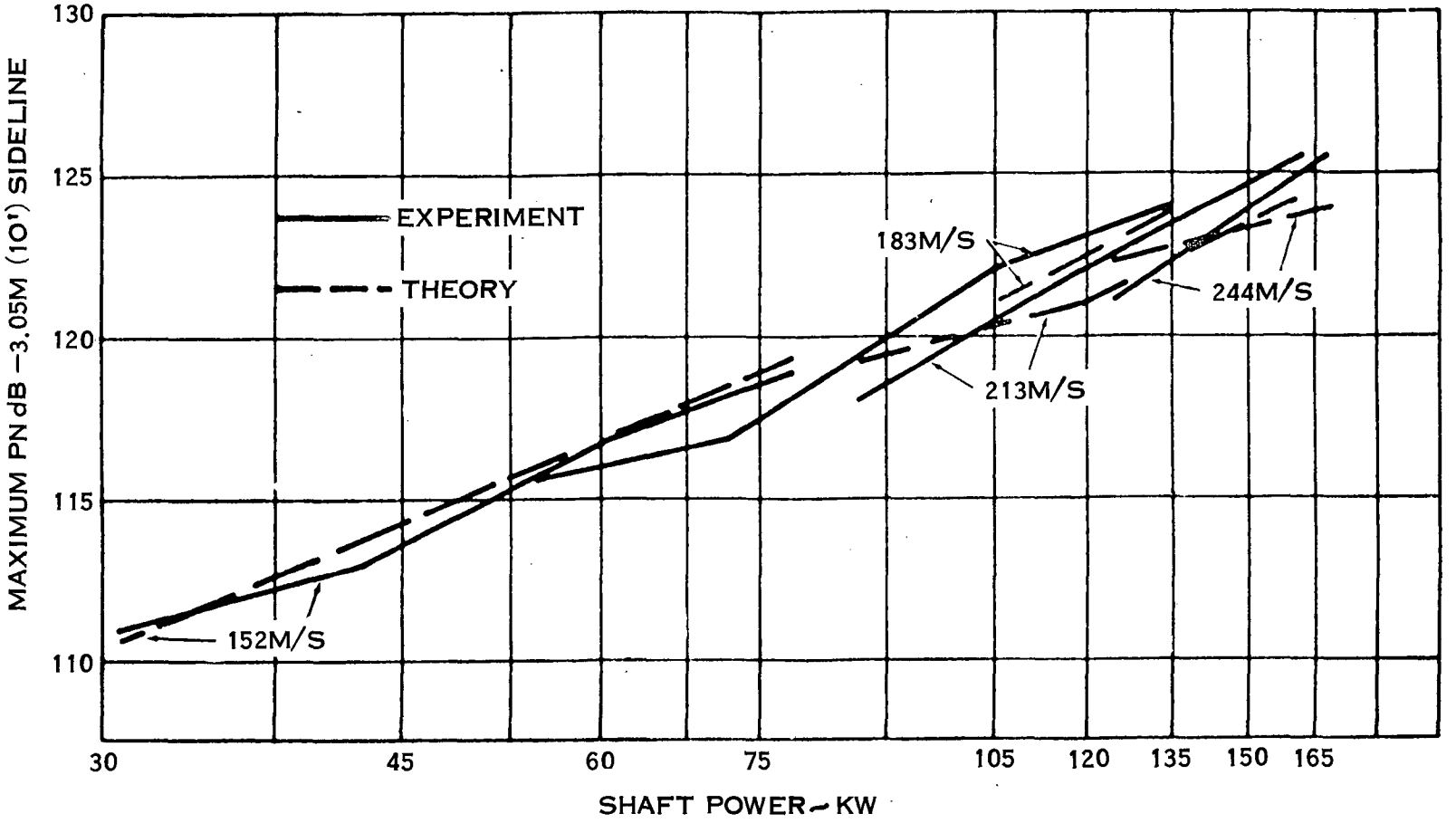

FIGURE 16. CORRELATION OF PERCEIVED NOISE LEVEL EXPERIMENT AND THEORY

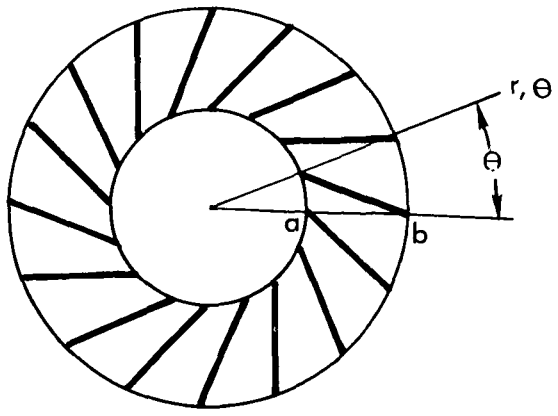

FIGURE 17. STATOR WITH LEANED VANES

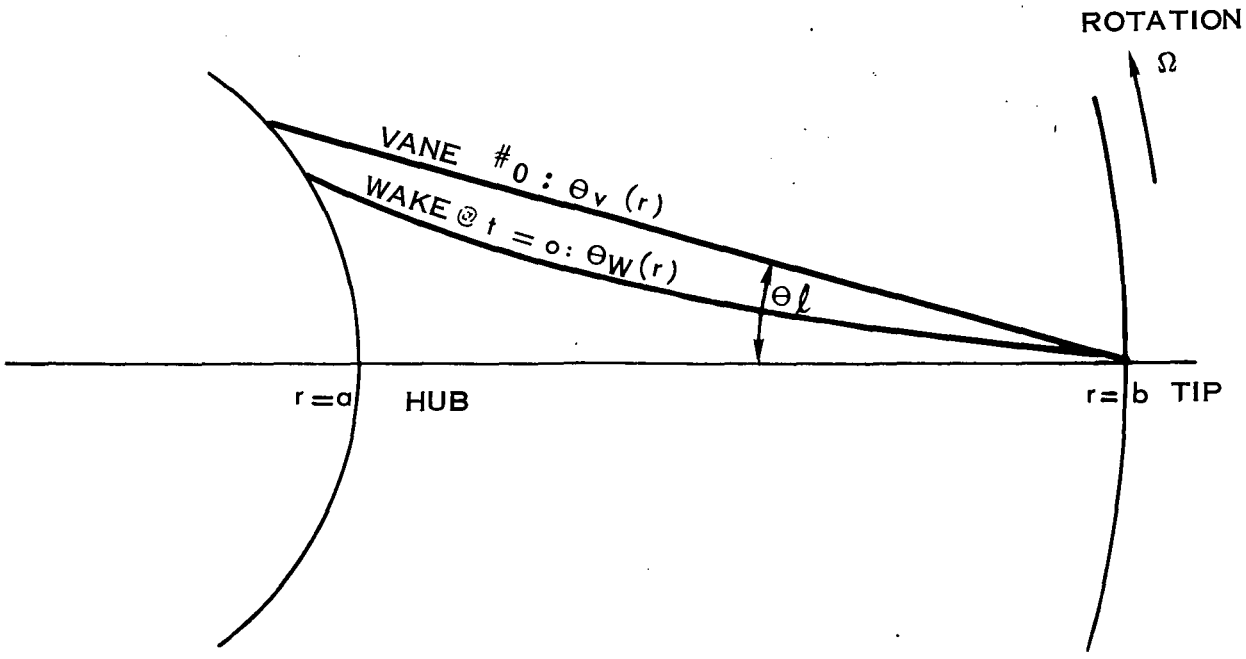

FIGURE 18. WAKE AND VANE GEOMETRY

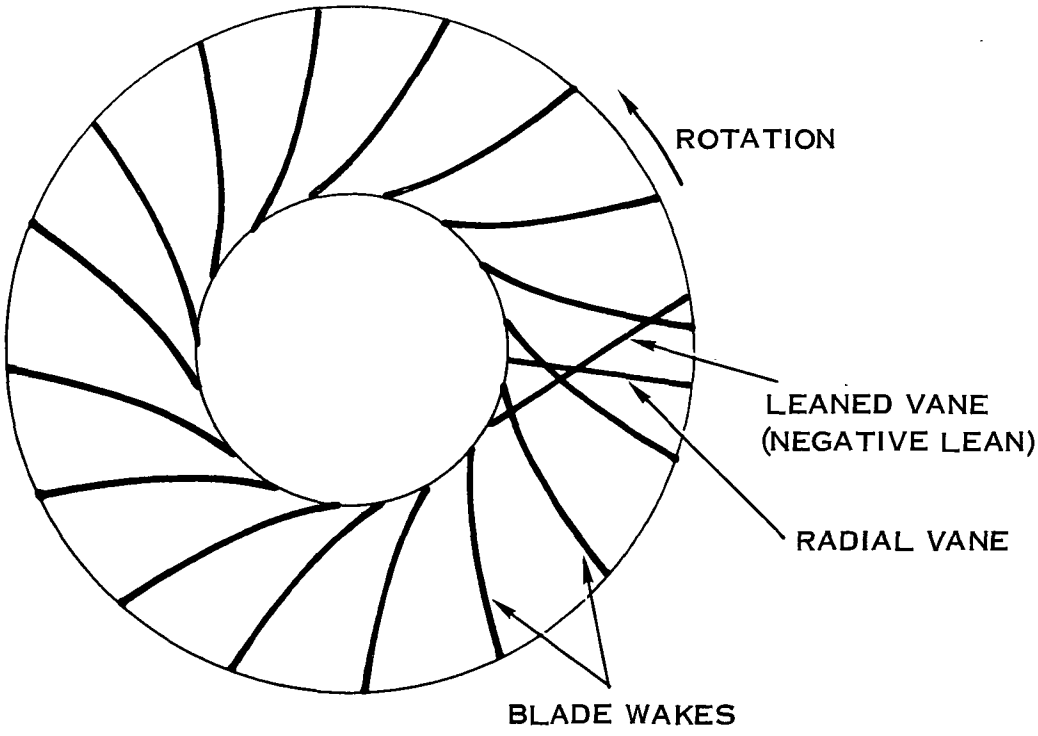

FIGURE 19. INTERACTION OF BLADE WAKES AND VANES

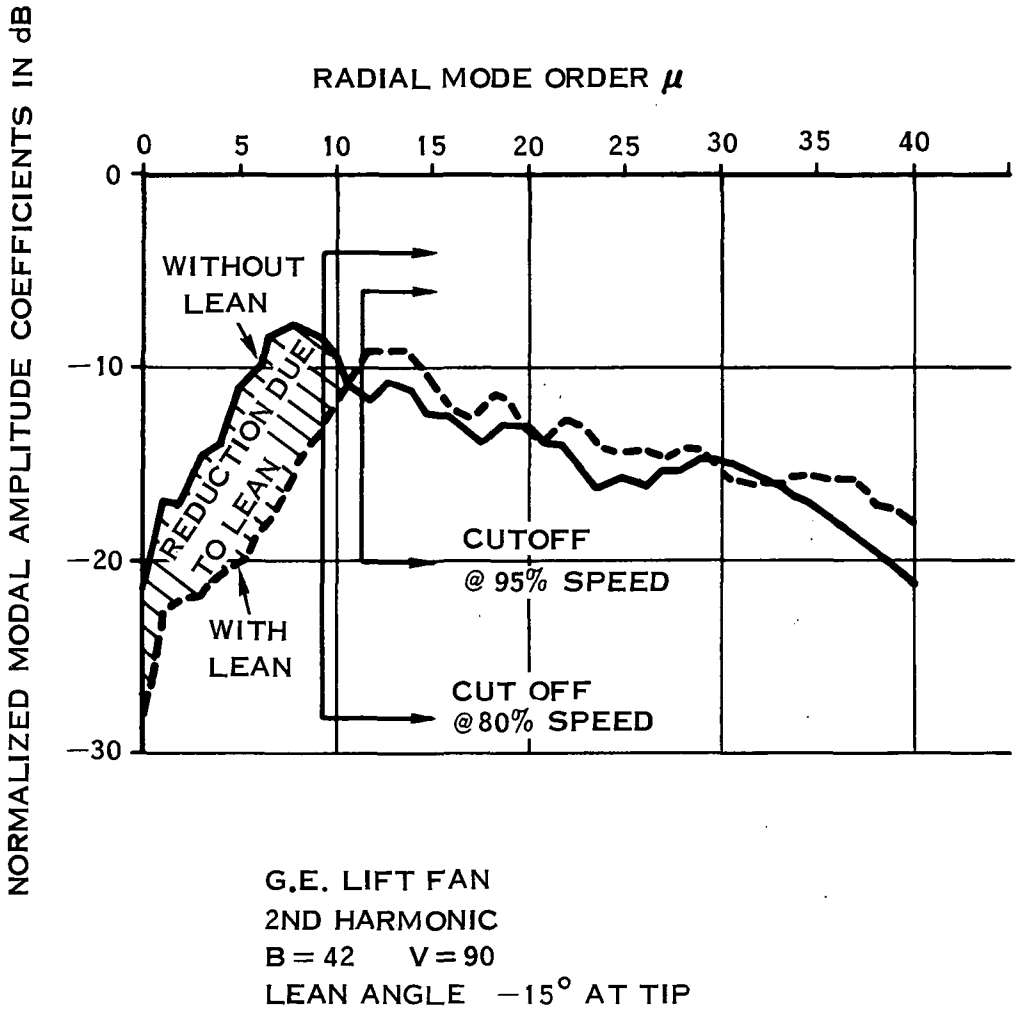

FIGURE 20. MODAL AMPLITUDE COEFFICIENTS FOR G.E. LIFT FAN

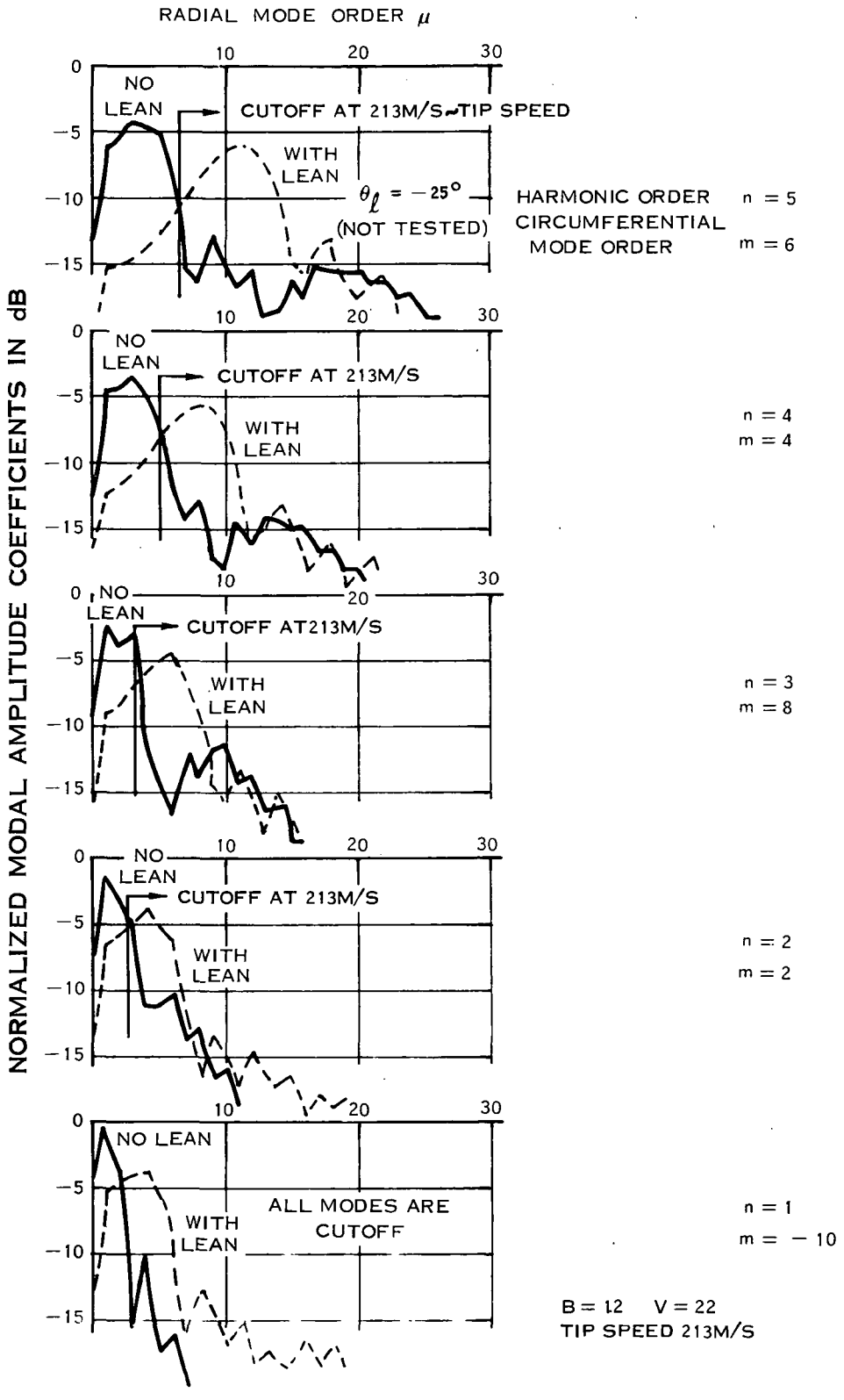

FIGURE 21. MODAL AMPLITUDE COEFFICIENTS FOR HS TEST FAN

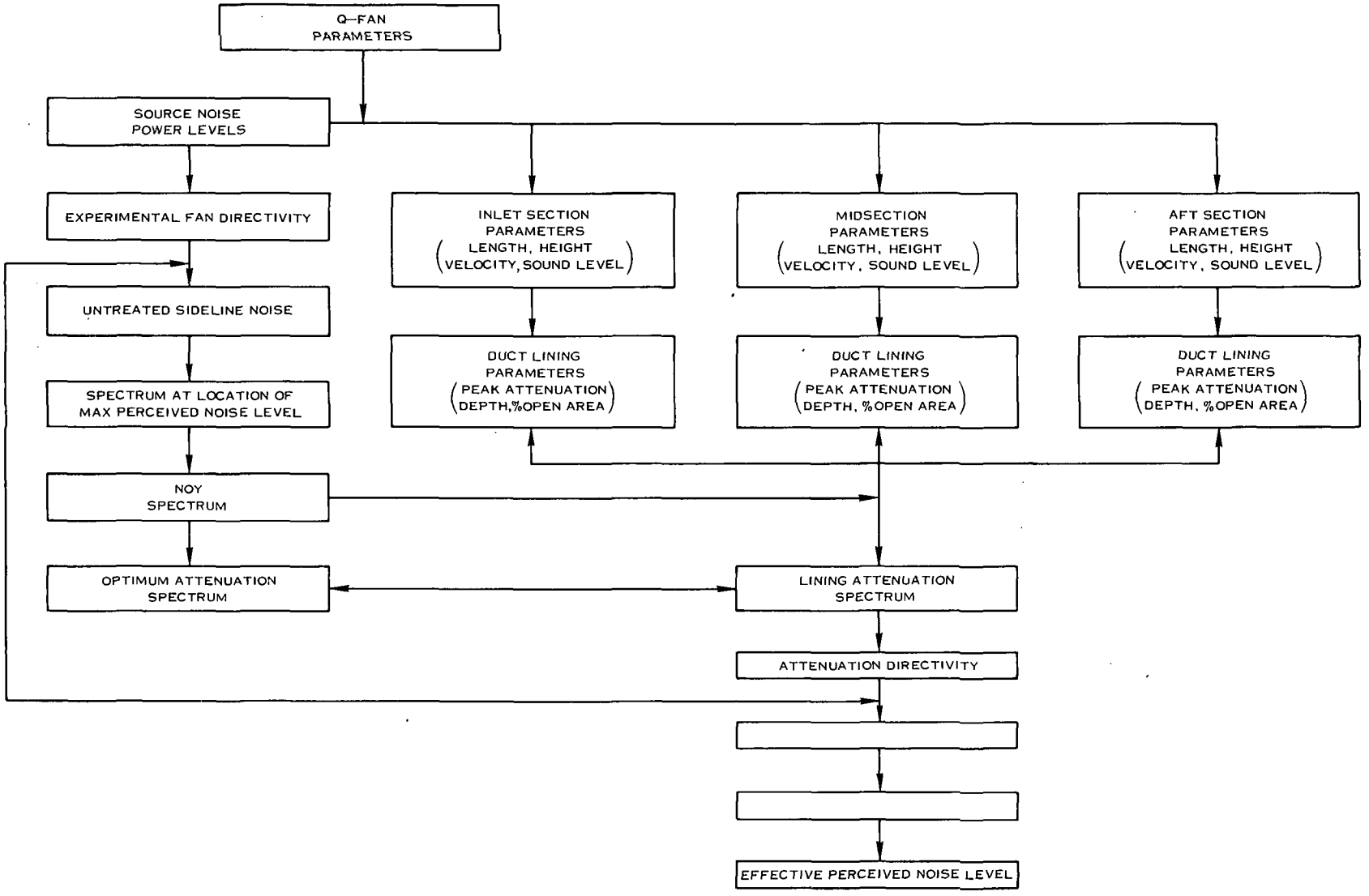

FIGURE 22. Q-FAN DUCT LINING DESIGN METHOD

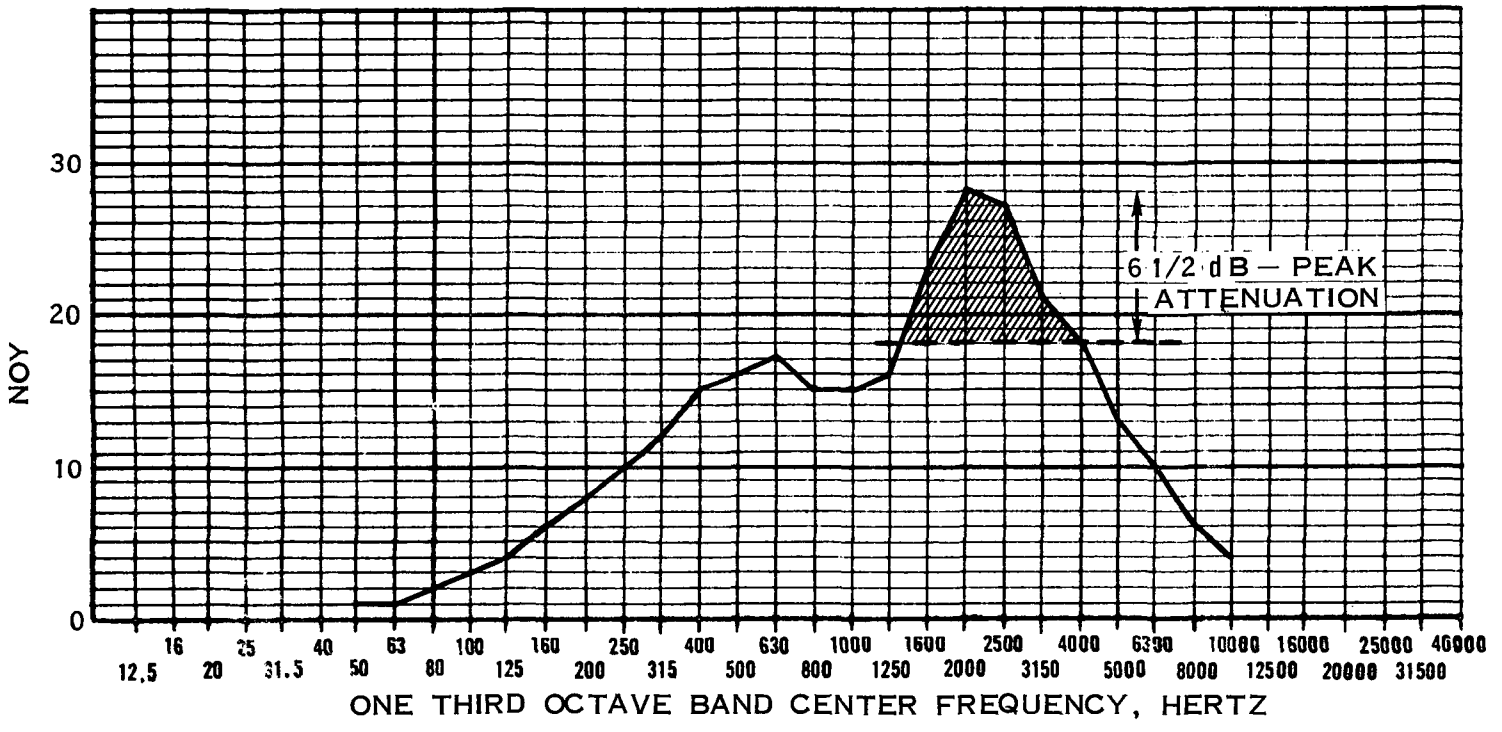

FIGURE 23. TYPICAL OBSERVED NOY SPECTRUM

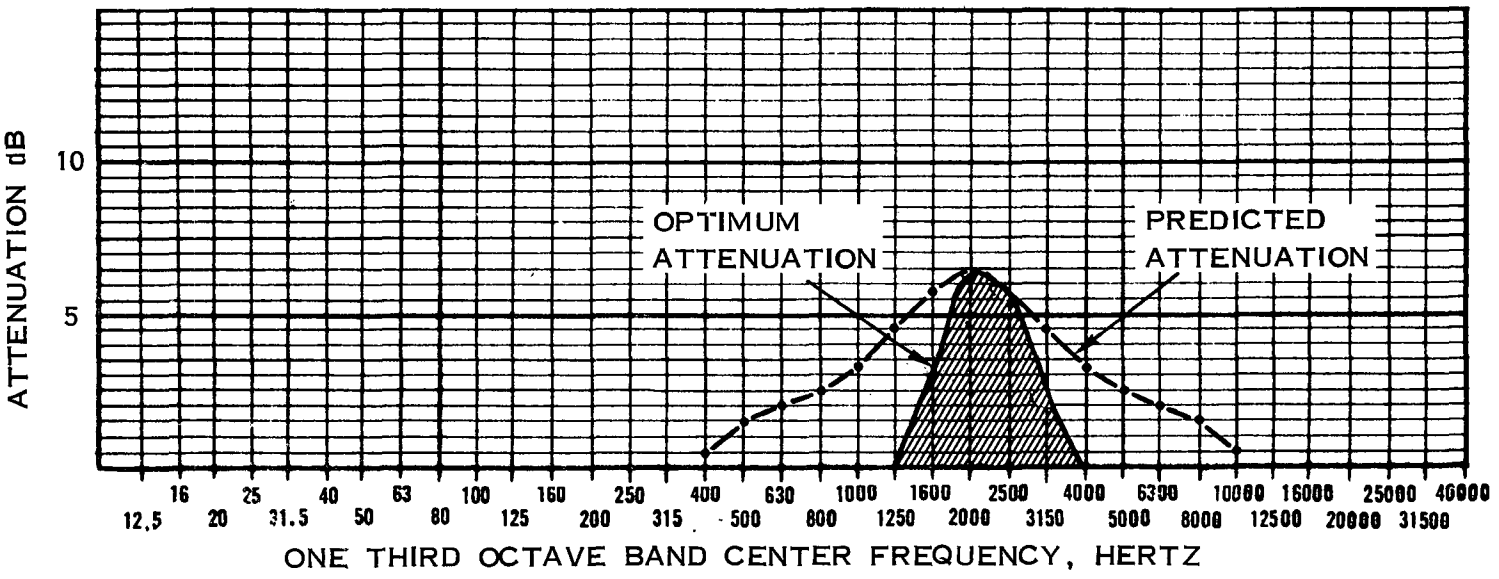

FIGURE 24. COMPARISON OF OPTIMUM AND PREDICTED ATTENUATION SPECTRUM

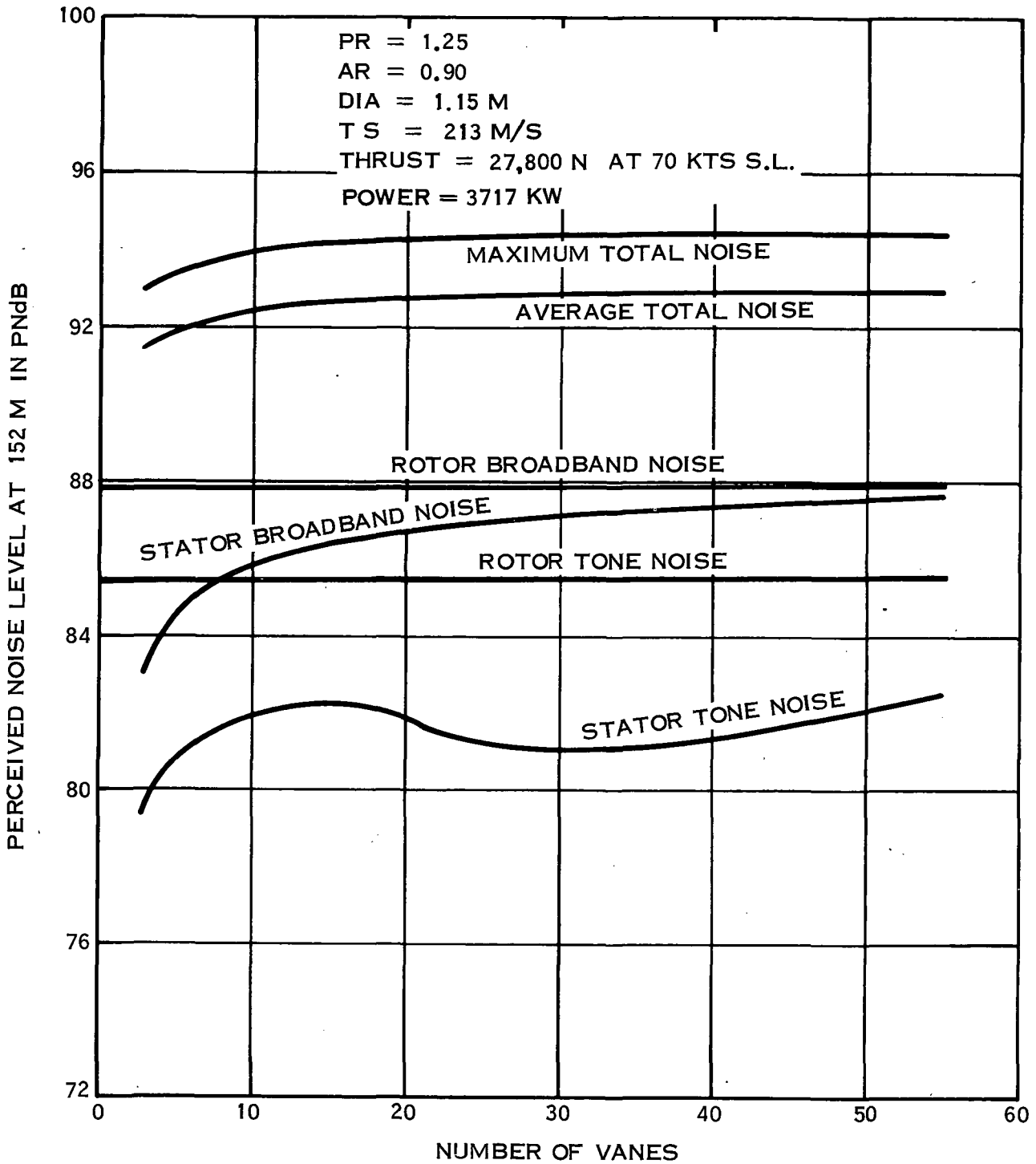

FIGURE 25. EFFECT OF VANE NUMBER ON COMPONENT NOISE OF 1.0 SOLIDITY ROTOR

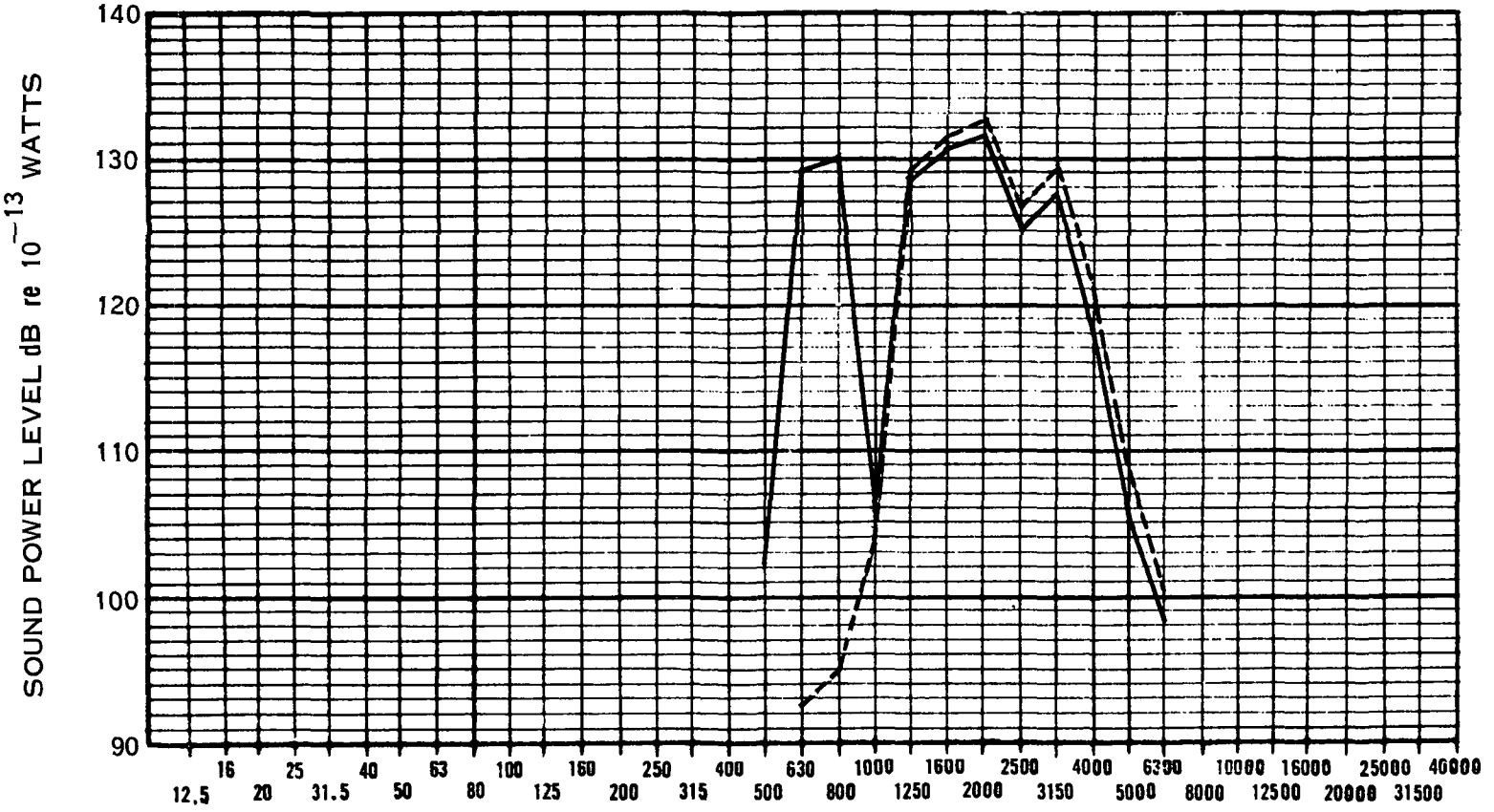

FIGURE 26. EFFECT OF VANE NUMBER ON VANE TONE NOISE SPECTRUM

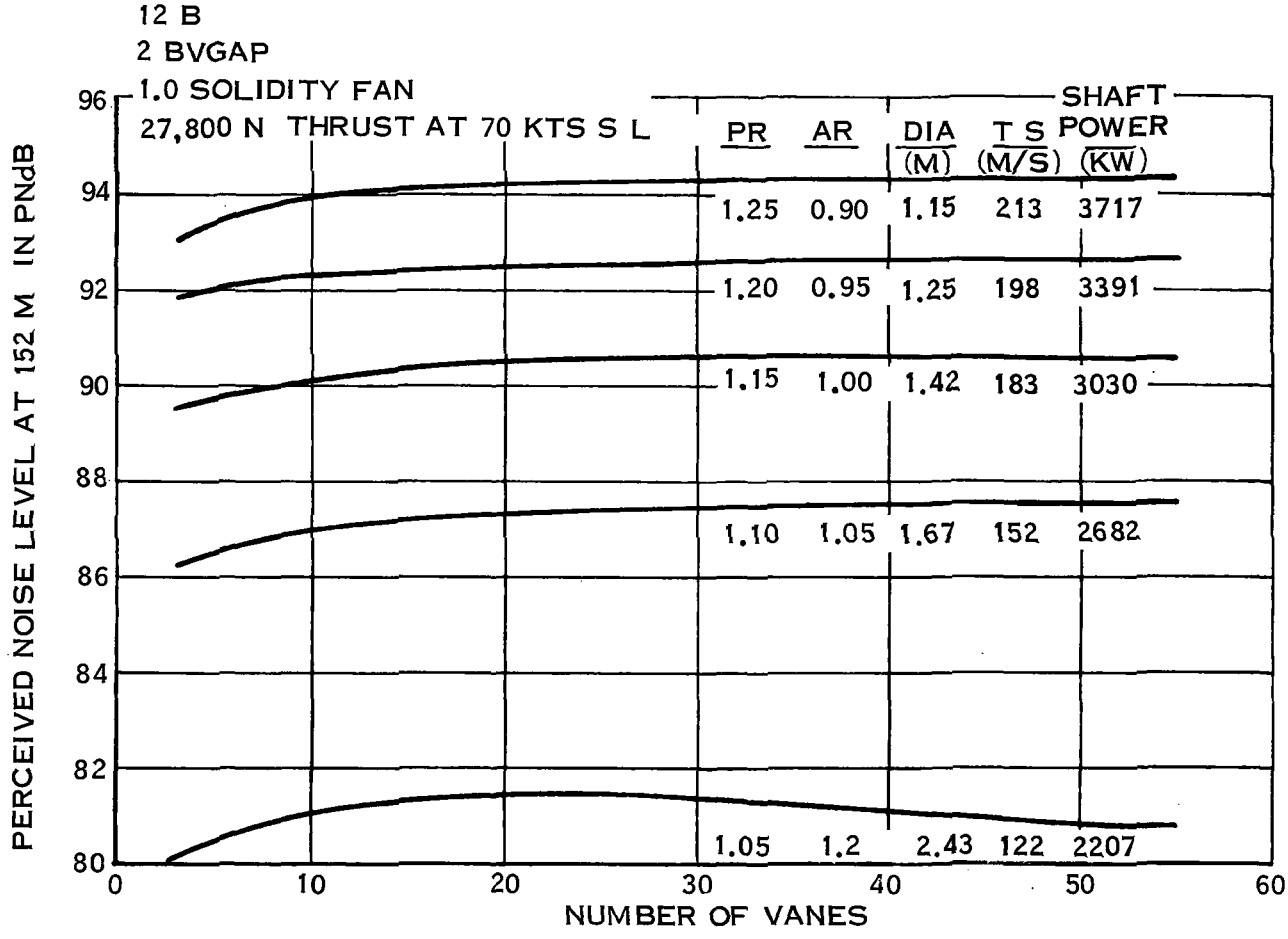

FIGURE 27. EFFECT OF VANE NUMBER AND PRESSURE RATIO ON NOISE AT 27,800 N THRUST

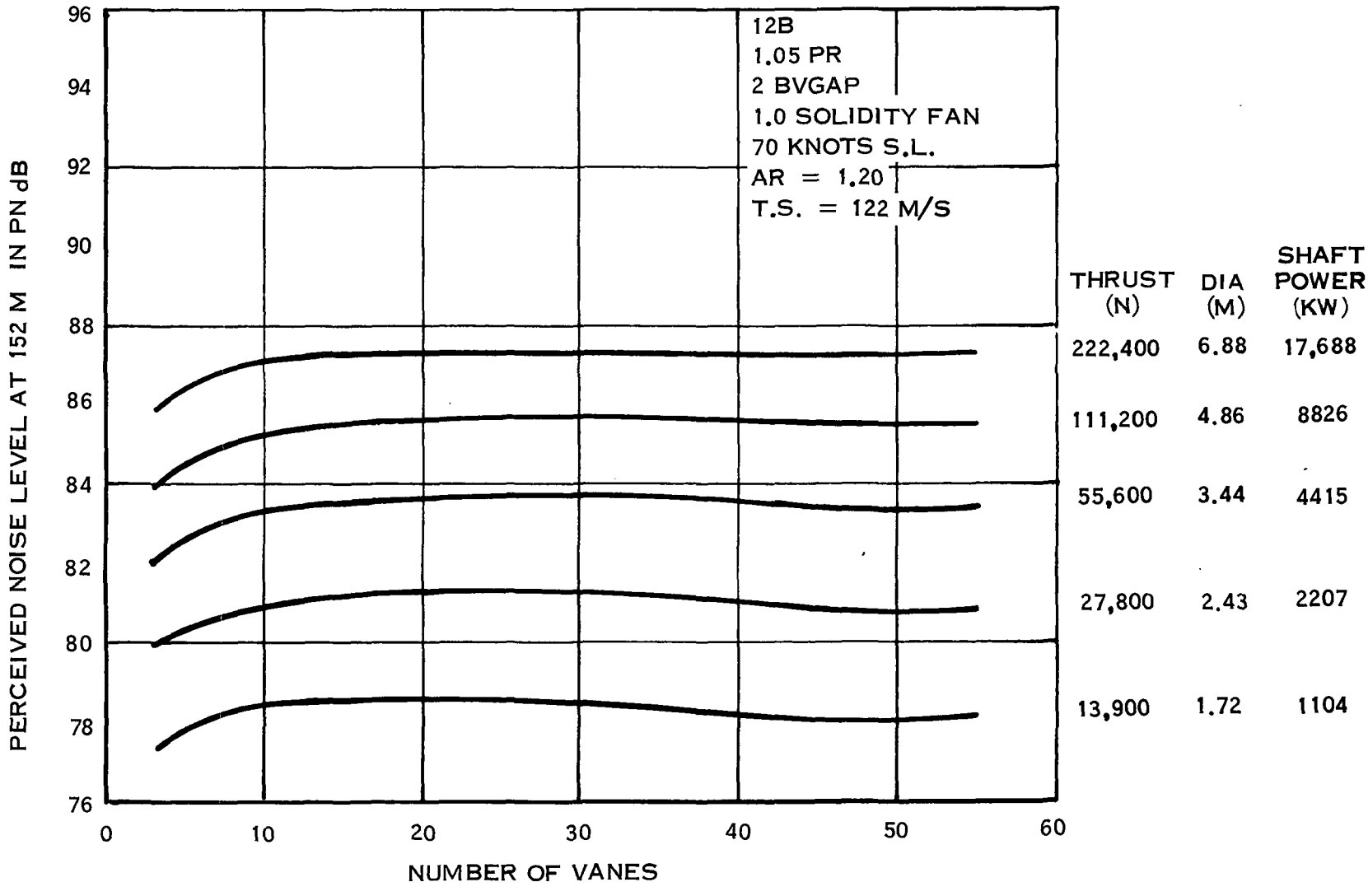

FIGURE 28. EFFECT OF VANE NUMBER AND THRUST ON NOISE AT 1.05 PRESSURE RATIO

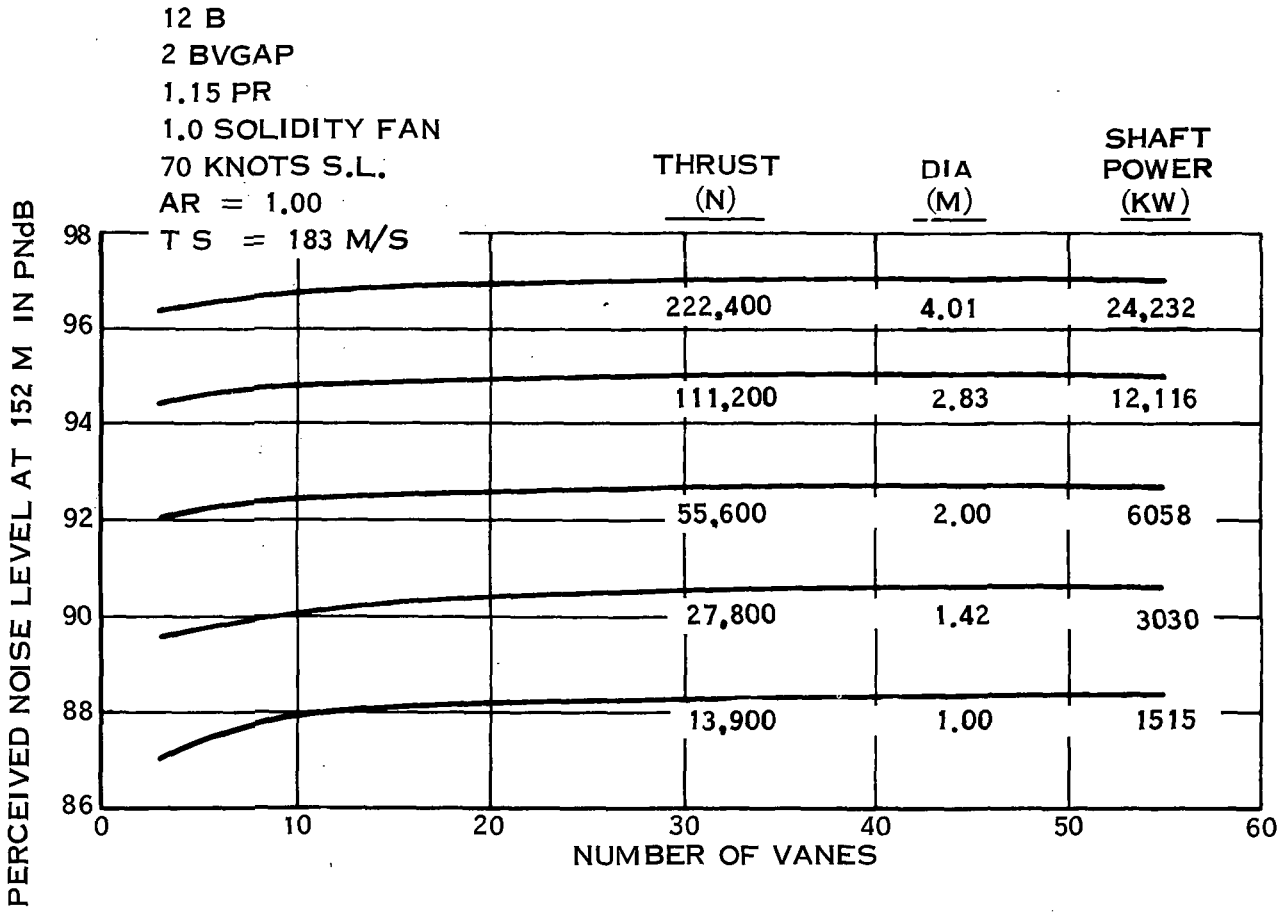

FIGURE 29. EFFECT OF VANE NUMBER AND THRUST ON NOISE AT 1.15 PRESSURE RATIO

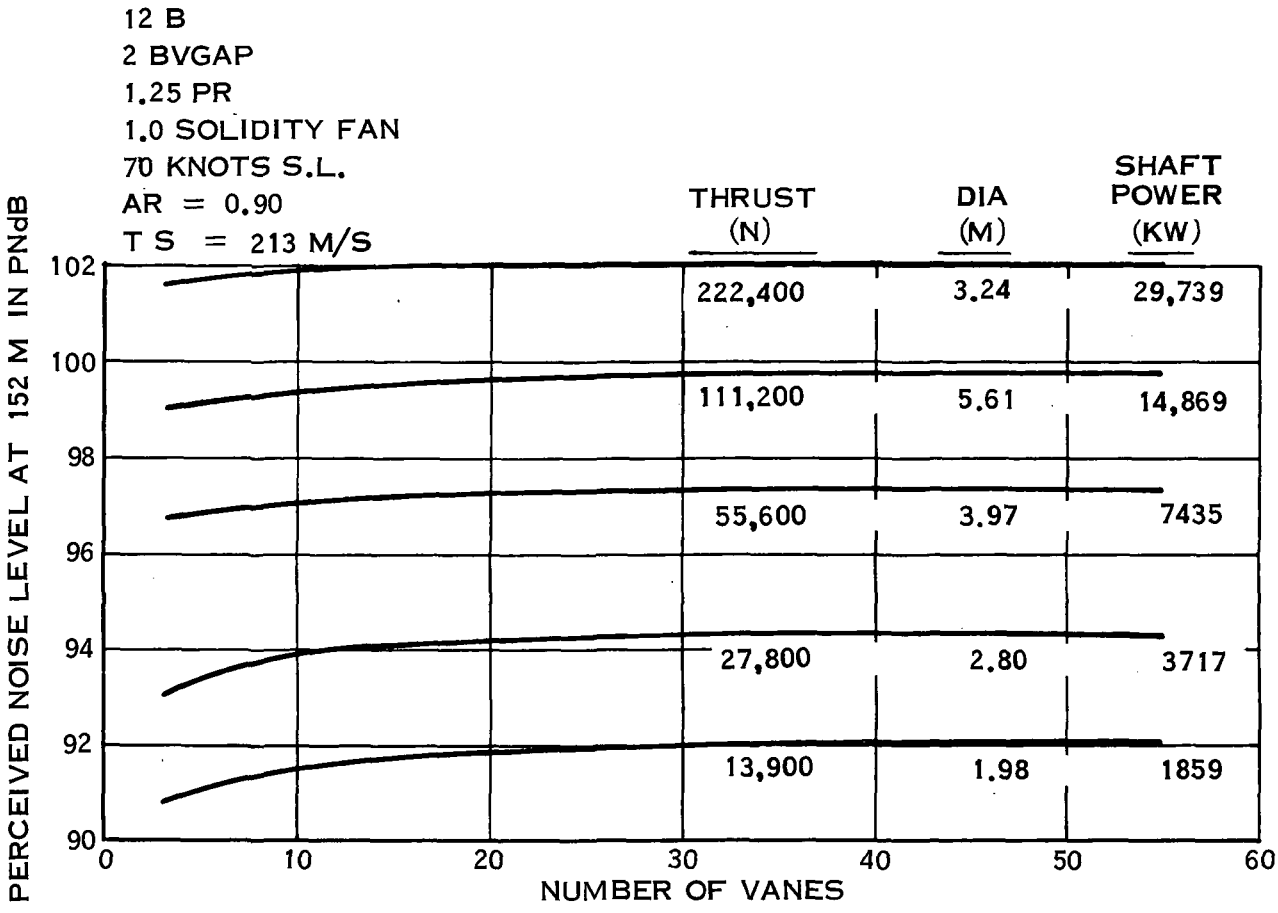

FIGURE 30. EFFECT OF VANE NUMBER AND THRUST ON NOISE AT 1.25 PRESSURE RATIO

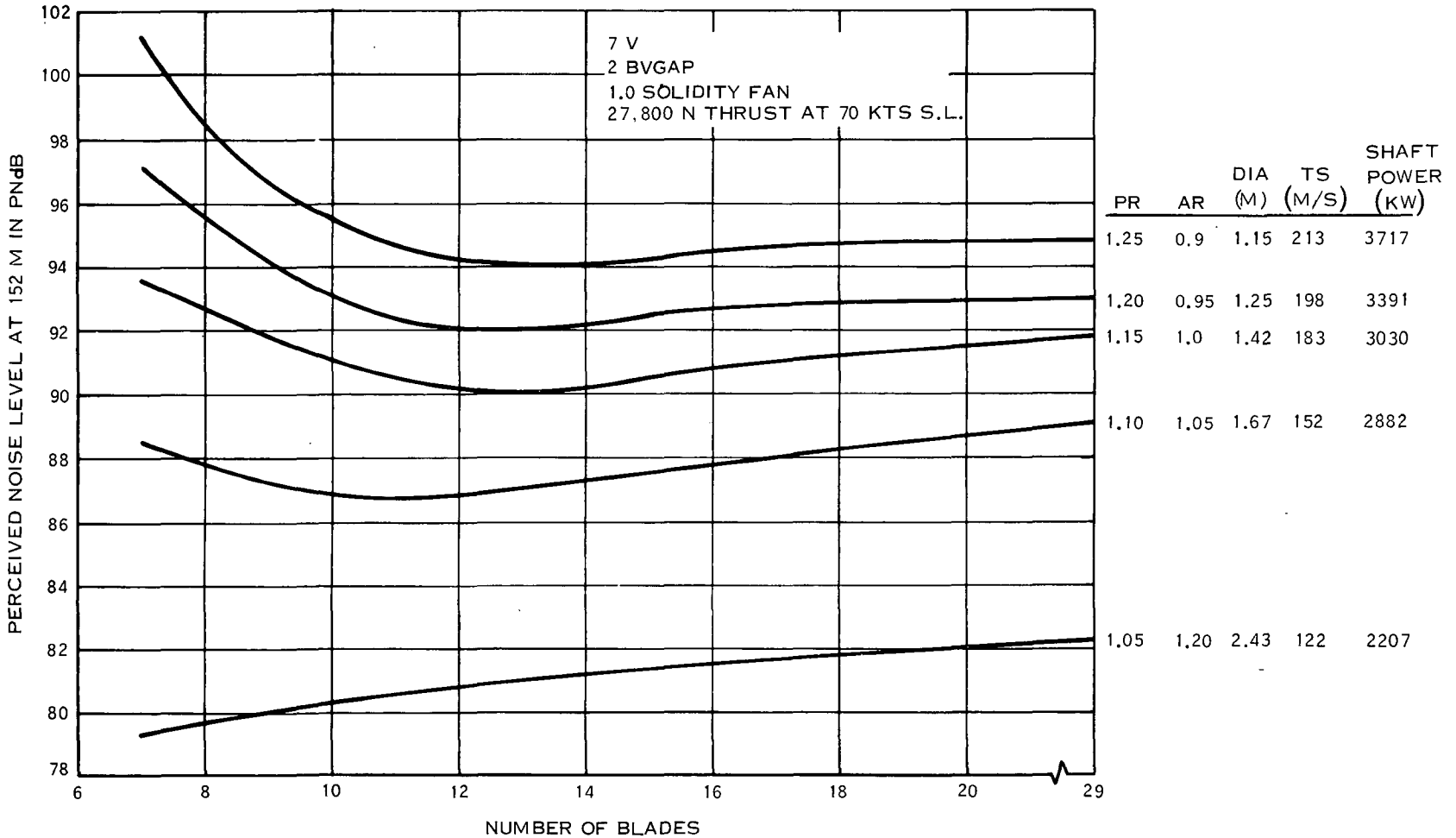

FIGURE 31. EFFECT OF BLADE NUMBER AND PRESSURE RATIO ON NOISE AT 27,800 N THRUST

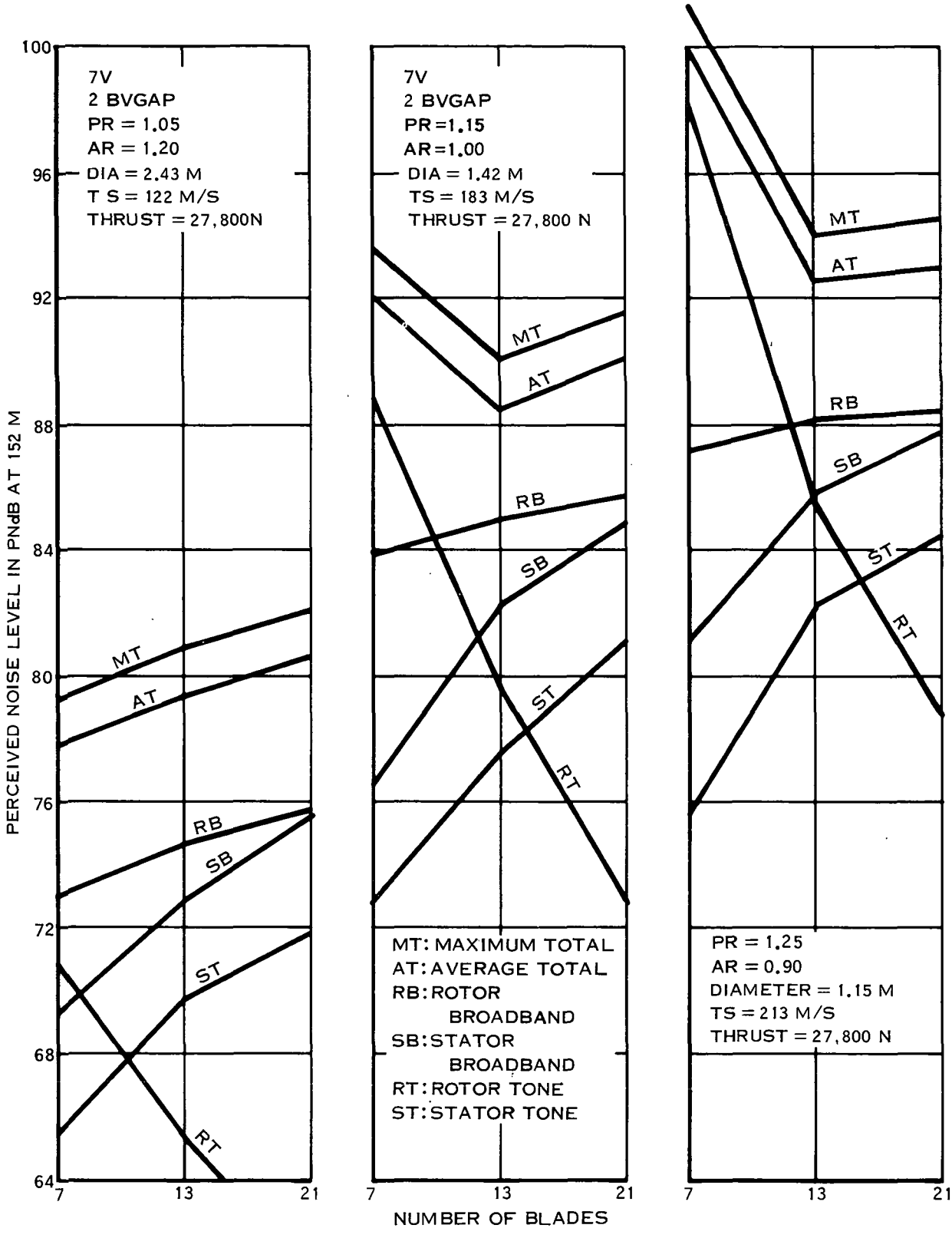

FIGURE 32. EFFECT OF BLADE NUMBER ON COMPONENT NOISE OF 1.0 SOLIDITY ROTOR

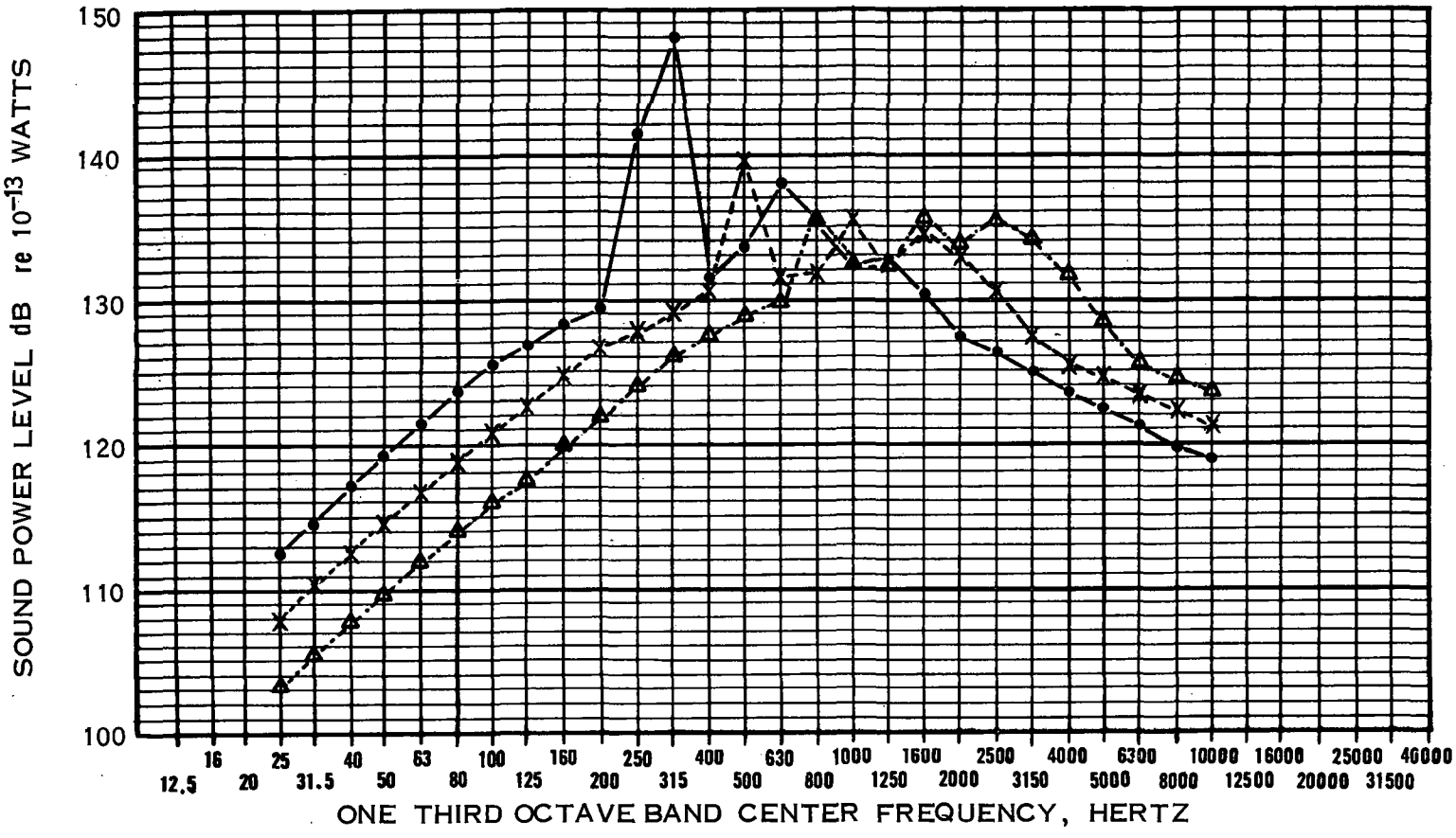

FIGURE 33. EFFECT OF BLADE NUMBER ON SPECTRUM

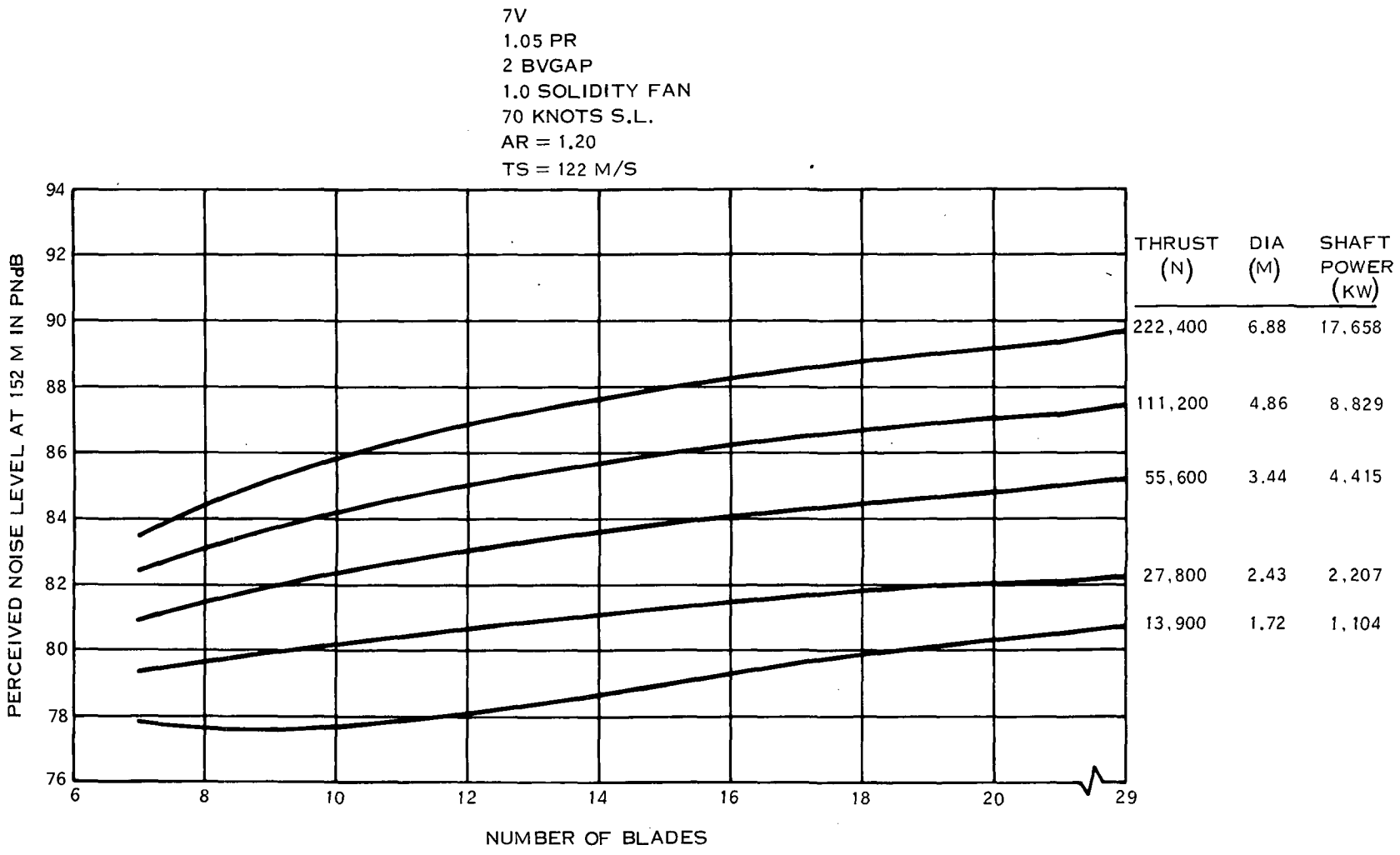

FIGURE 34. EFFECT OF BLADE NUMBER AND THRUST ON NOISE AT 1.05 PRESSURE RATIO

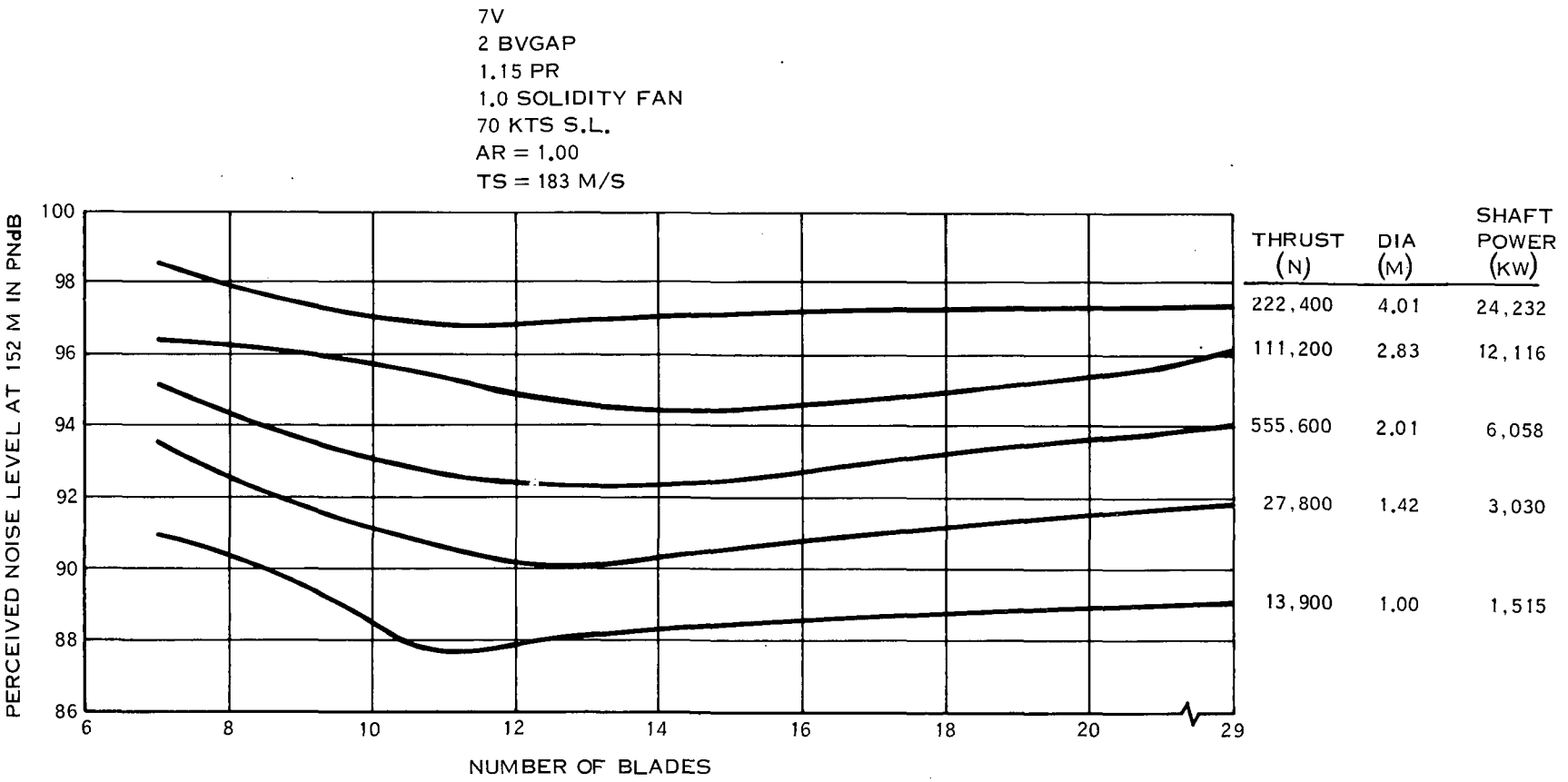

FIGURE 35. EFFECT OF BLADE NUMBER AND THRUST ON NOISE AT 1.15 PRESSURE RATIO

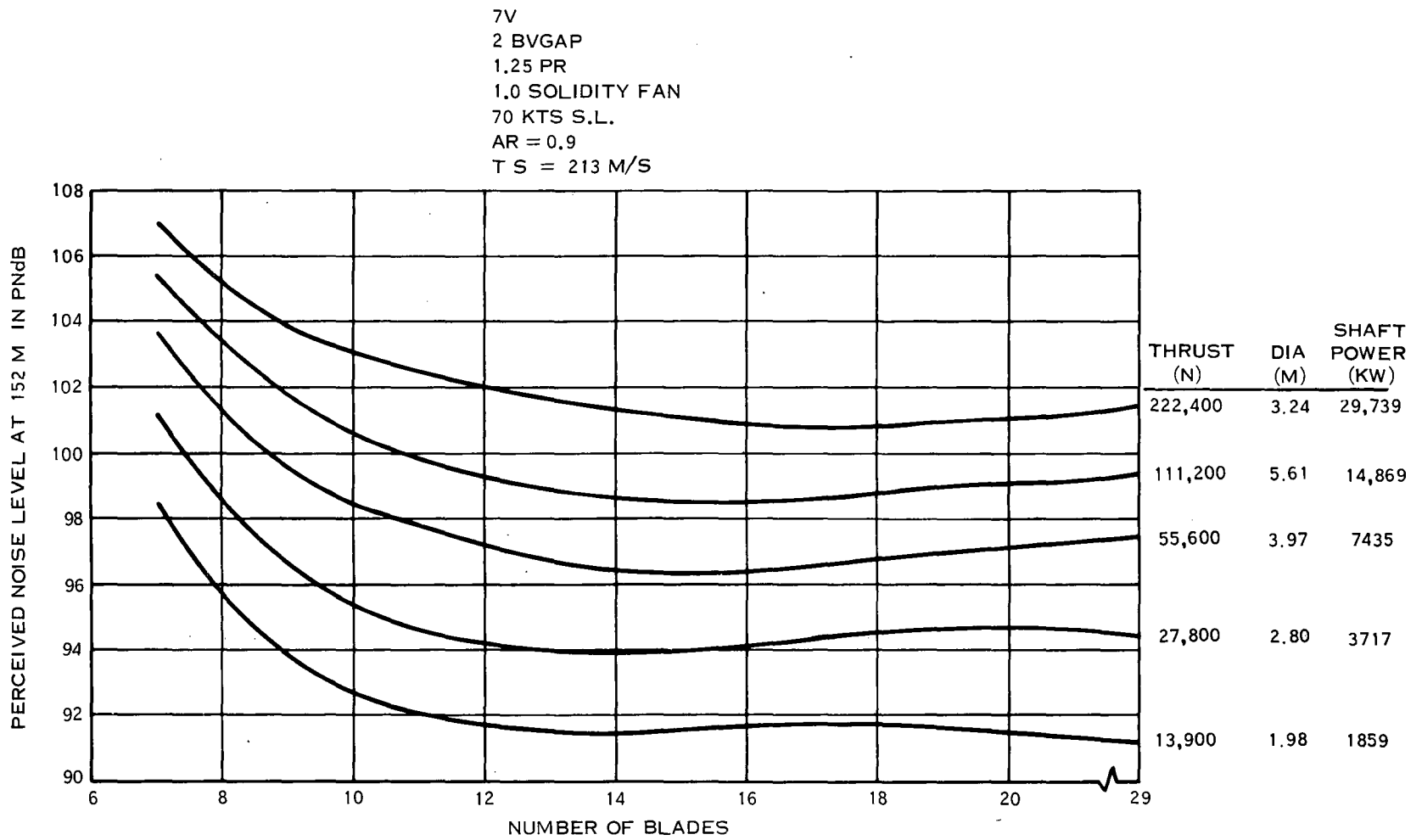

FIGURE 36. EFFECT OF BLADE NUMBER AND THRUST ON NOISE AT 1.25 PRESSURE RATIO

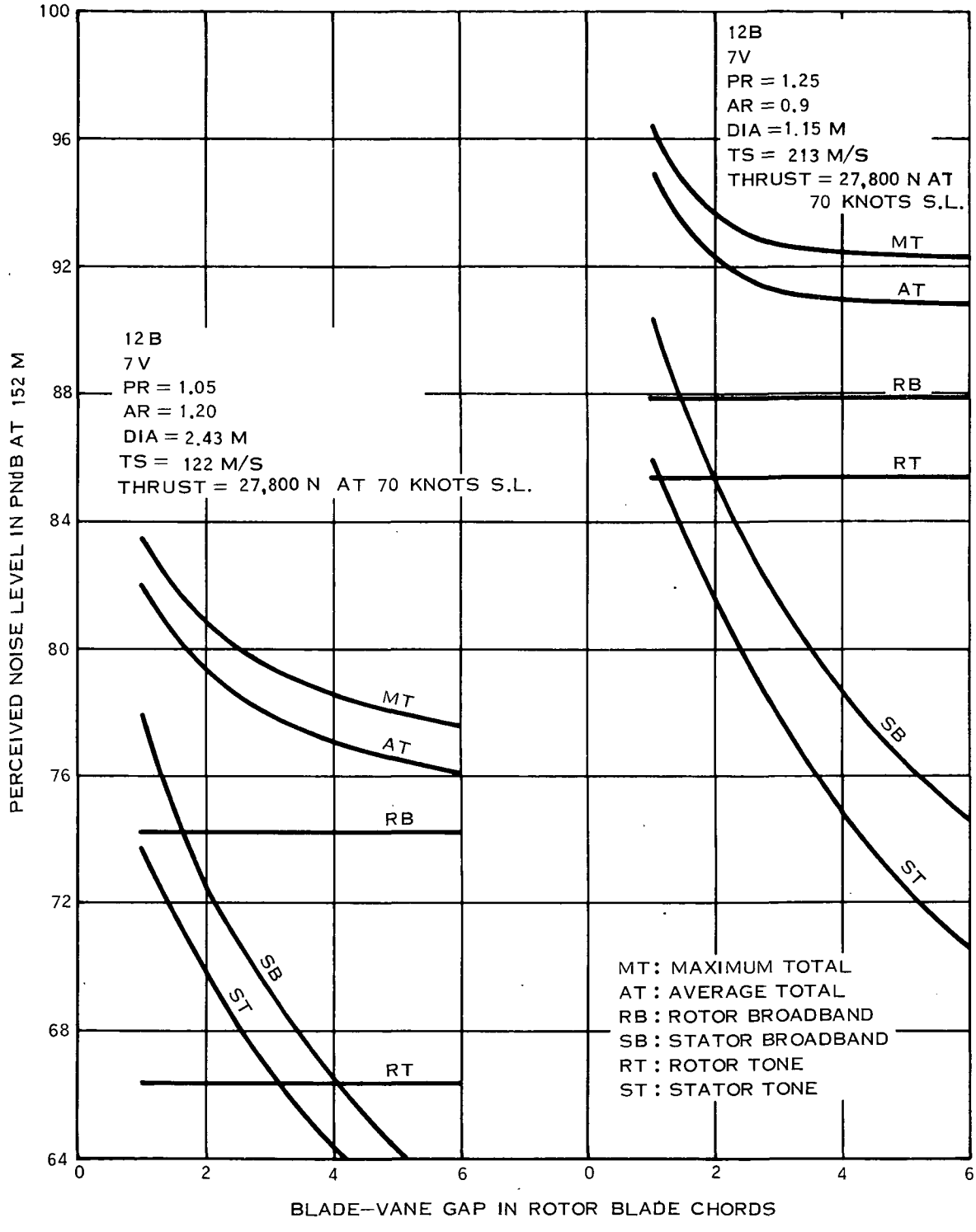

FIGURE 37. EFFECT OF BLADE–VANE GAP ON COMPONENT NOISE OF 1.0 SOLIDITY ROTOR

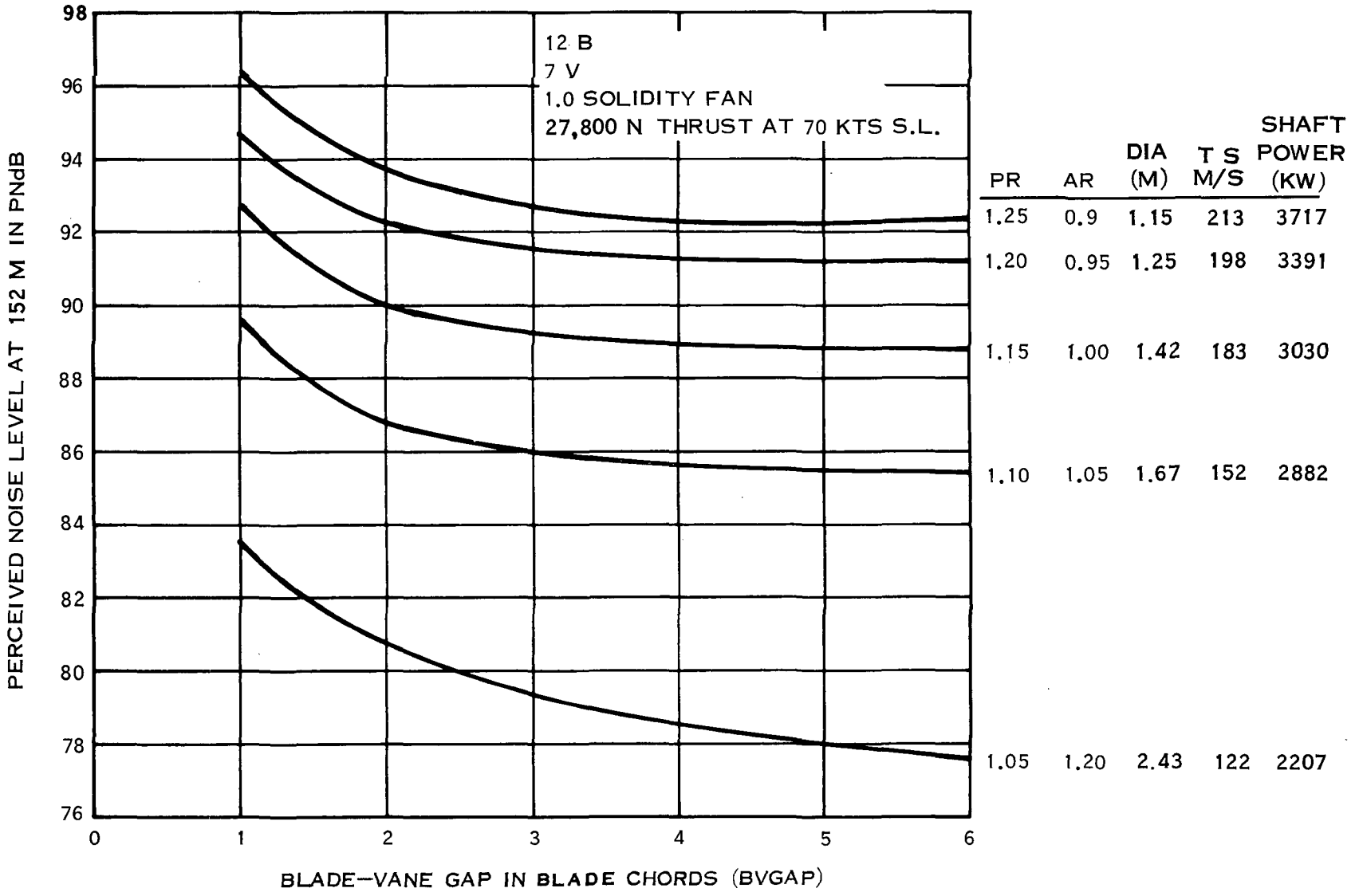

FIGURE 38. EFFECT OF BLADE–VANE GAP AND PRESSURE RATIO ON NOISE AT 27,800 N THRUST

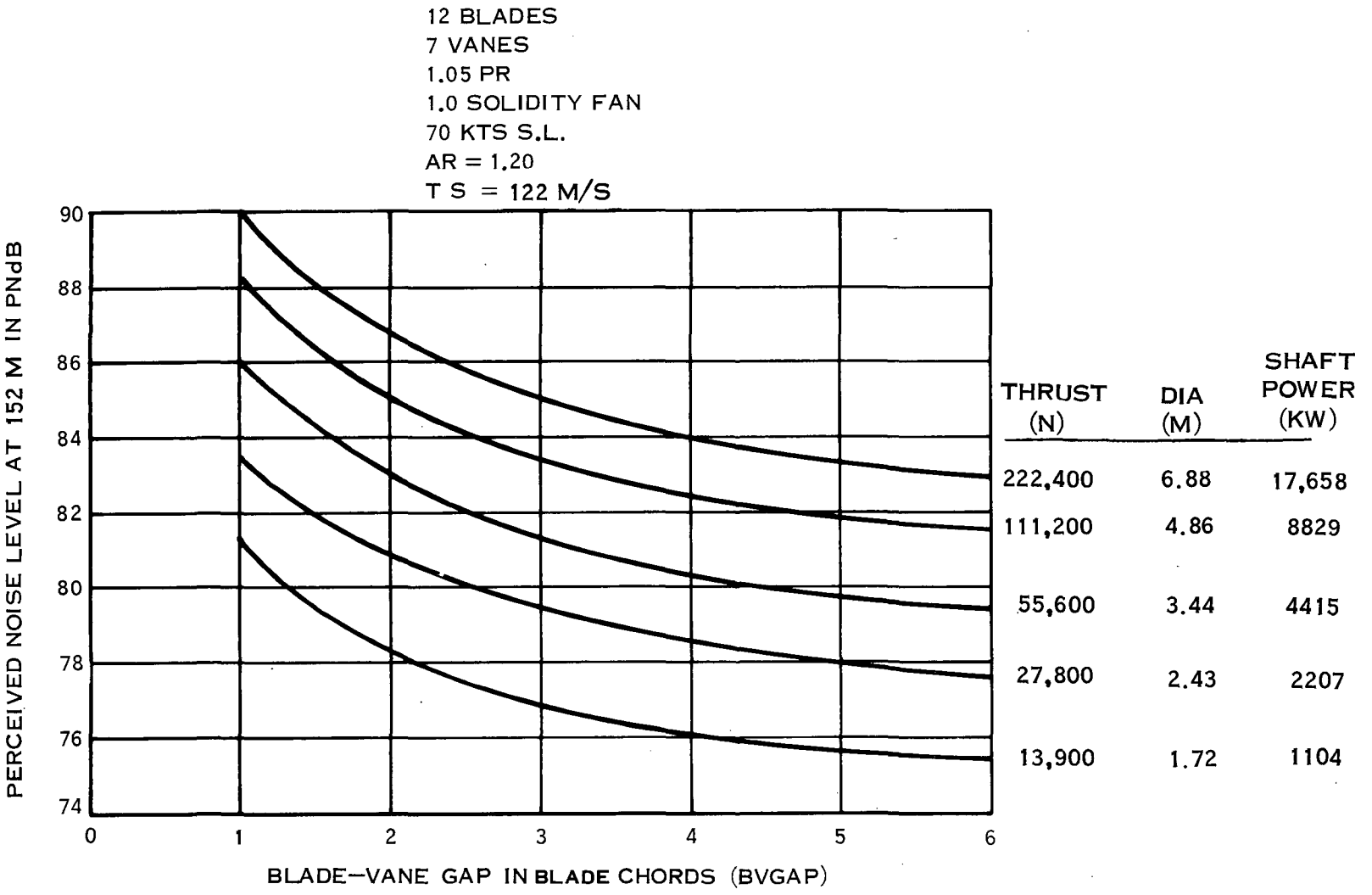

FIGURE 39. EFFECT OF BLADE–VANE GAP AND THRUST ON NOISE AT 1.05 PRESSURE RATIO

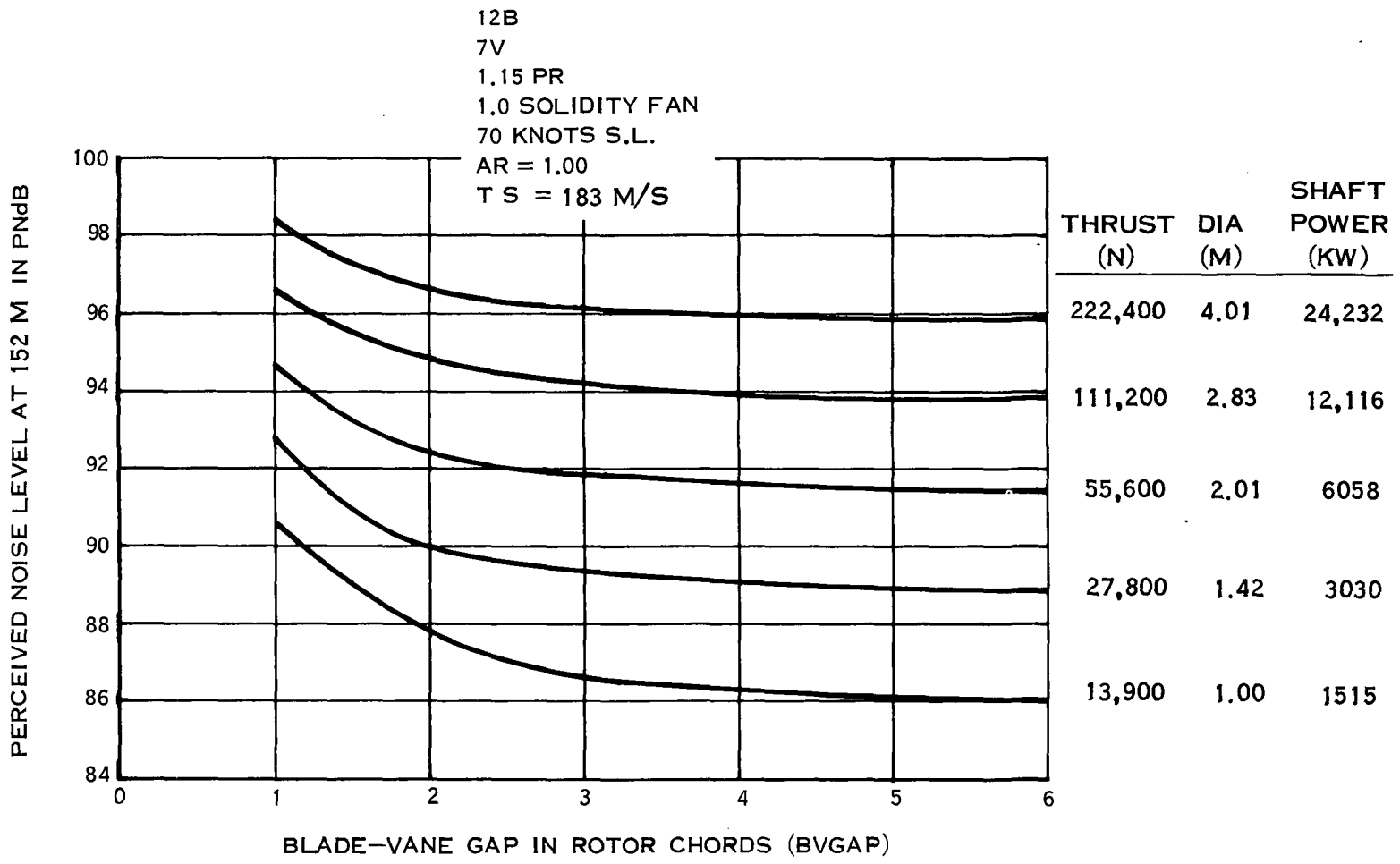

FIGURE 40. EFFECT OF BLADE–VANE GAP AND THRUST ON NOISE AT 1.15 PRESSURE RATIO

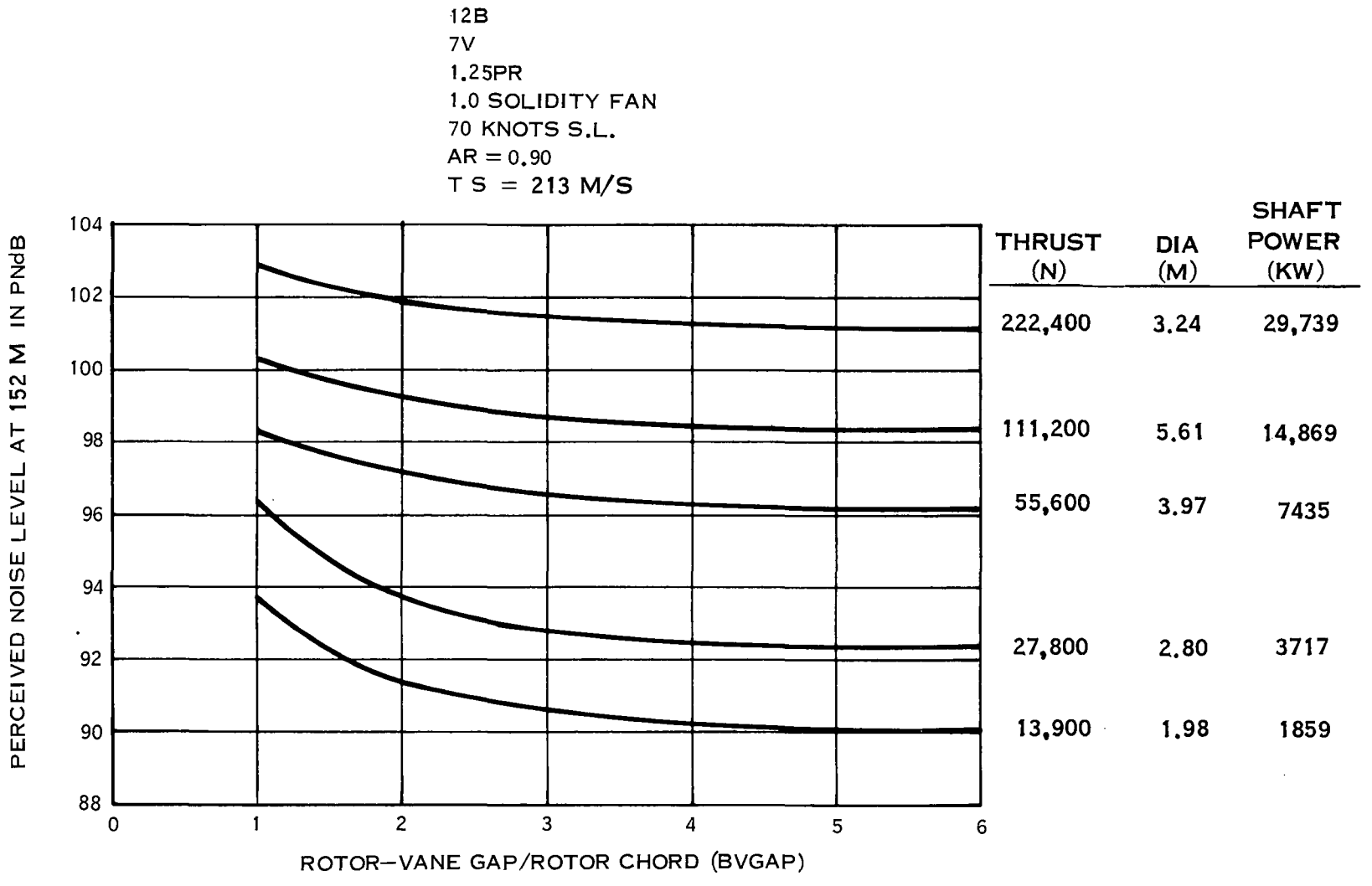

FIGURE 41. EFFECT OF BVGAP BLADE–VANE GAP AND THRUST ON NOISE AT 1.25 PRESSURE RATIO

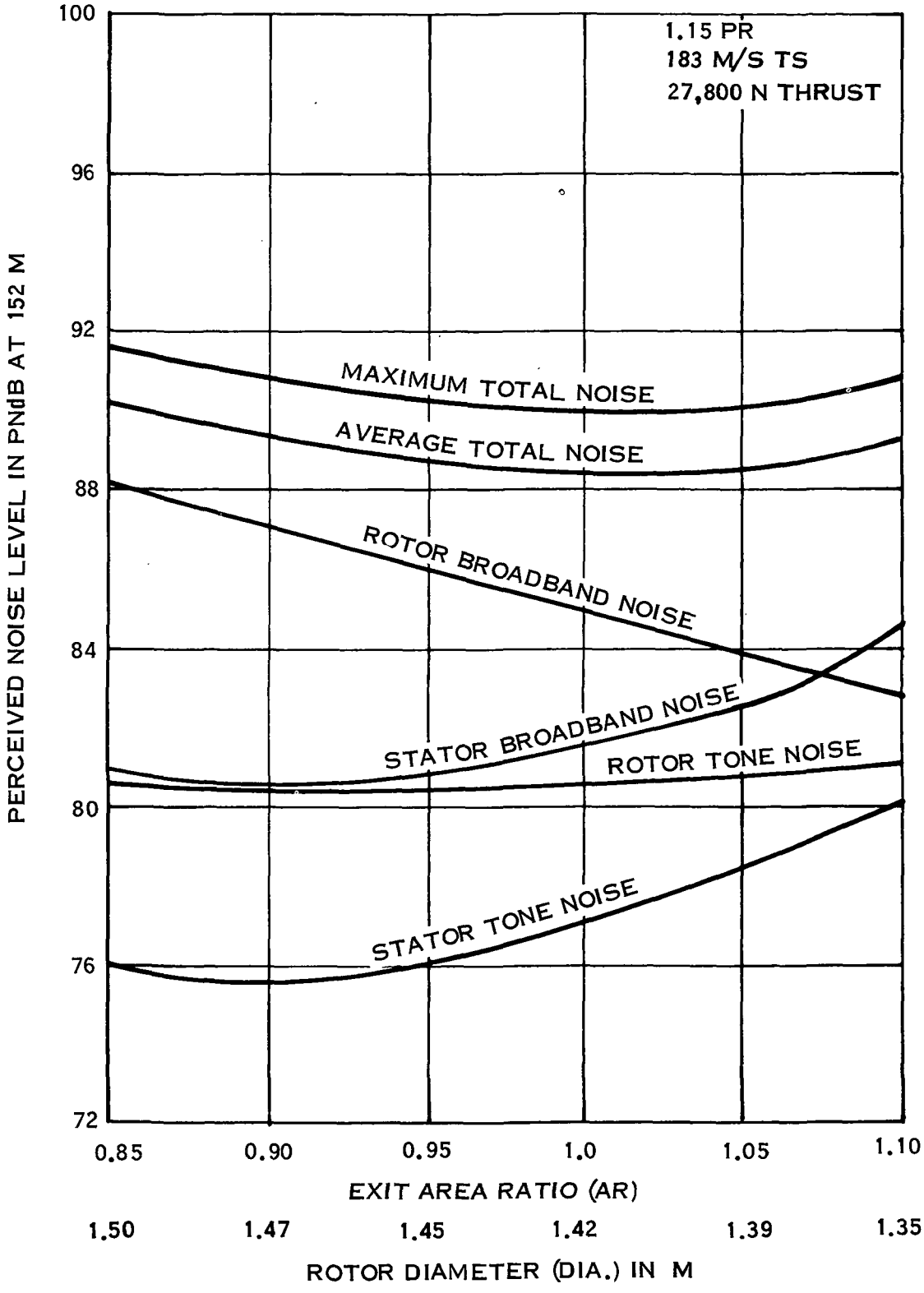

FIGURE 42. EFFECT OF EXIT AREA RATIO ON COMPONENT NOISE OF THE 1.0 SOLIDITY DESIGN

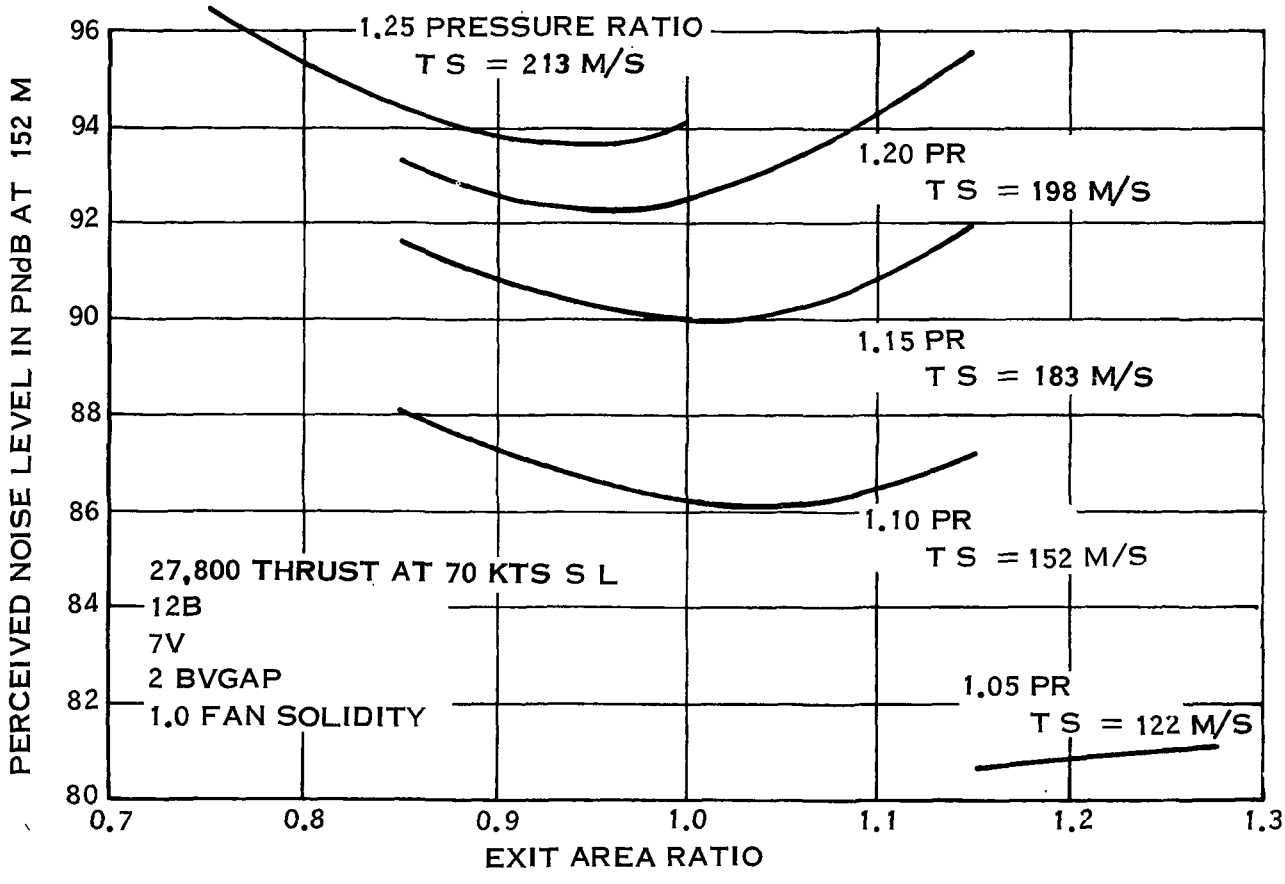

FIGURE 43. EFFECT OF EXIT AREA RATIO AND PRESSURE RATIO ON NOISE OF THE 1.0 SOLIDITY DESIGN

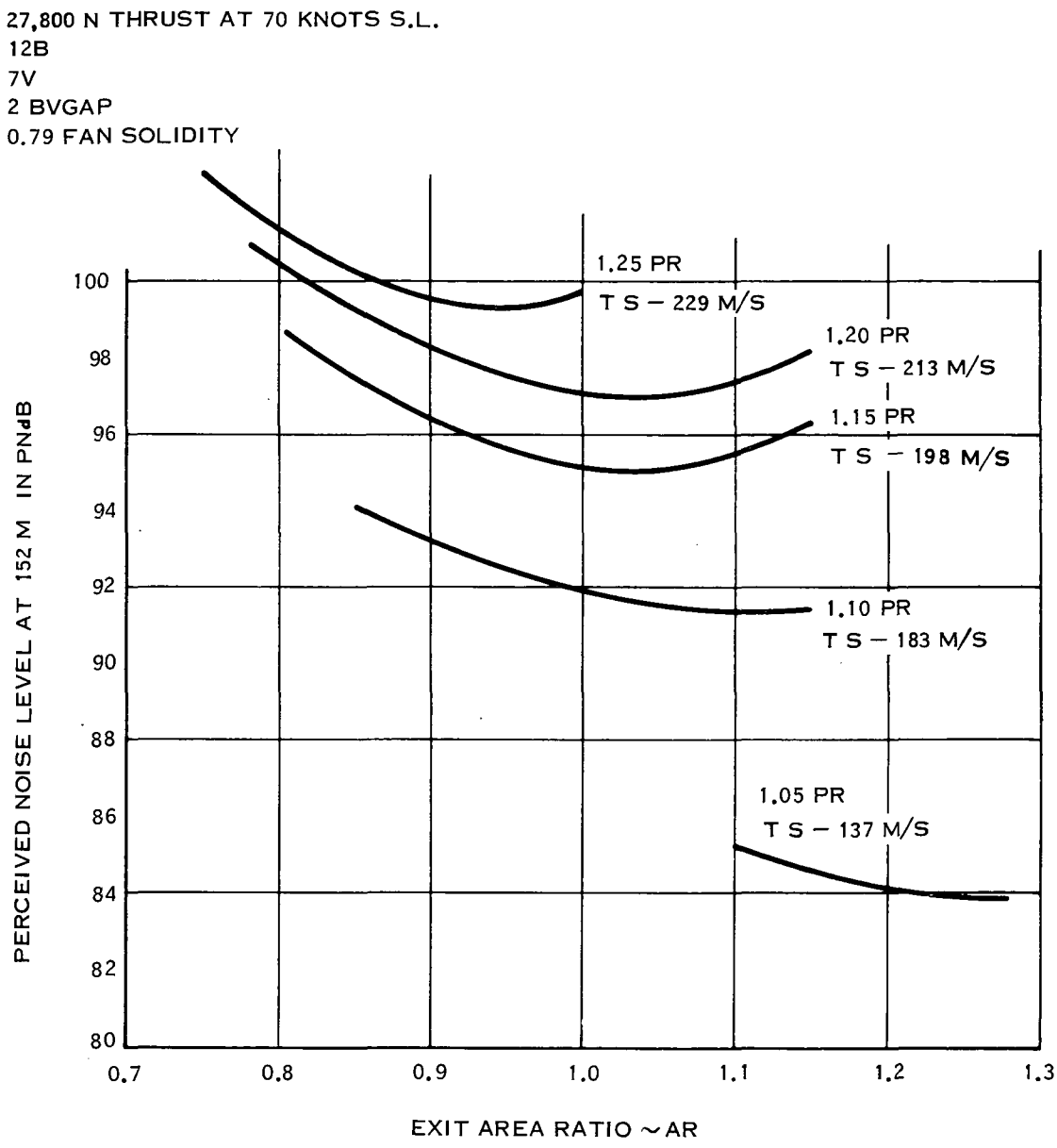

FIGURE 44. EFFECT OF EXIT AREA RATIO AND PRESSURE RATIO ON NOISE OF THE 0.79 SOLIDITY DESIGN

27,800 N THRUST AT 70 KNOTS S L
12B
7V
2 BVGAP
1.0 SOLIDITY FAN

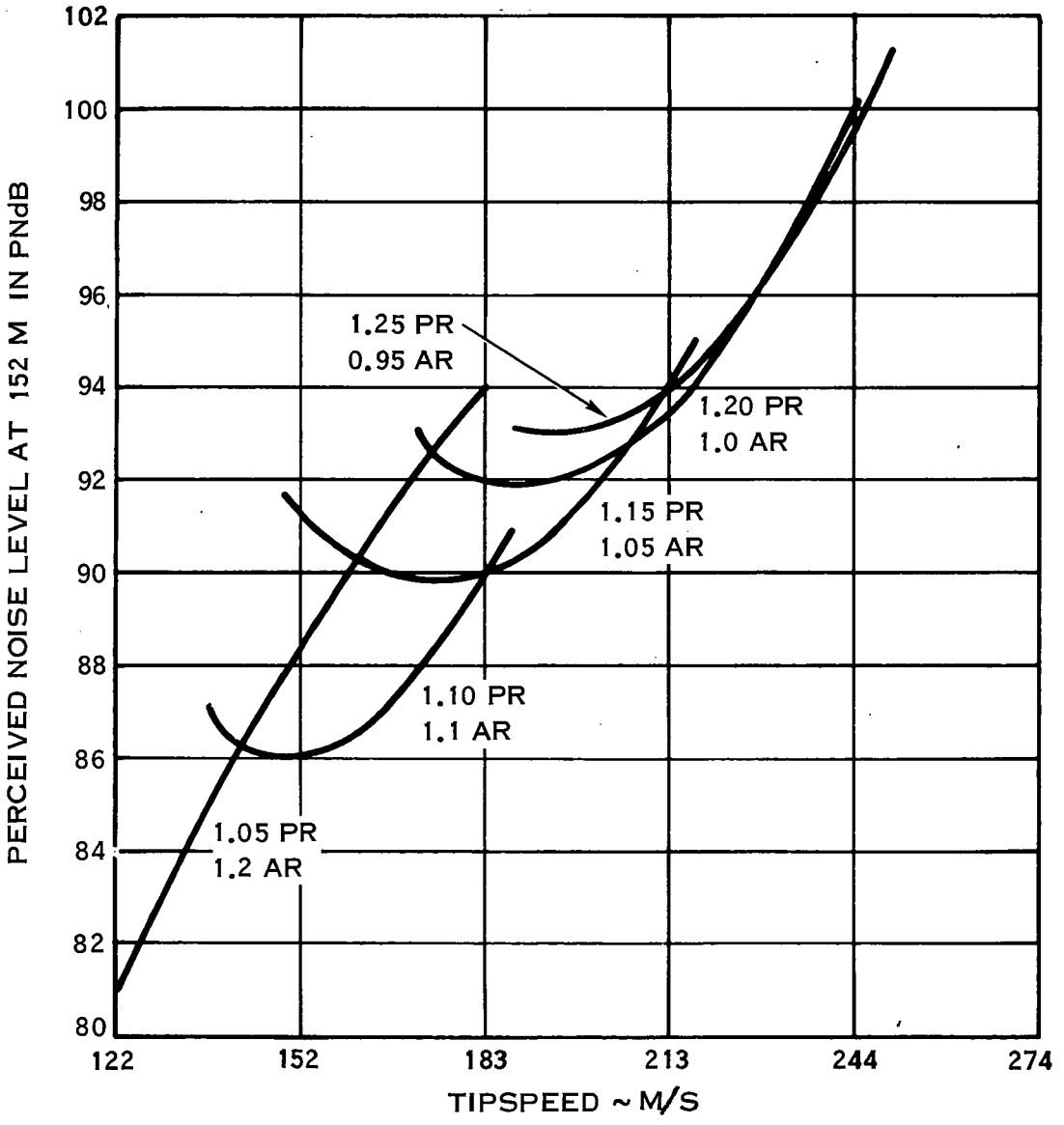

FIGURE 45. EFFECT OF TIP SPEED AND PRESSURE RATIO ON NOISE OF THE 1.0 SOLIDITY FAN

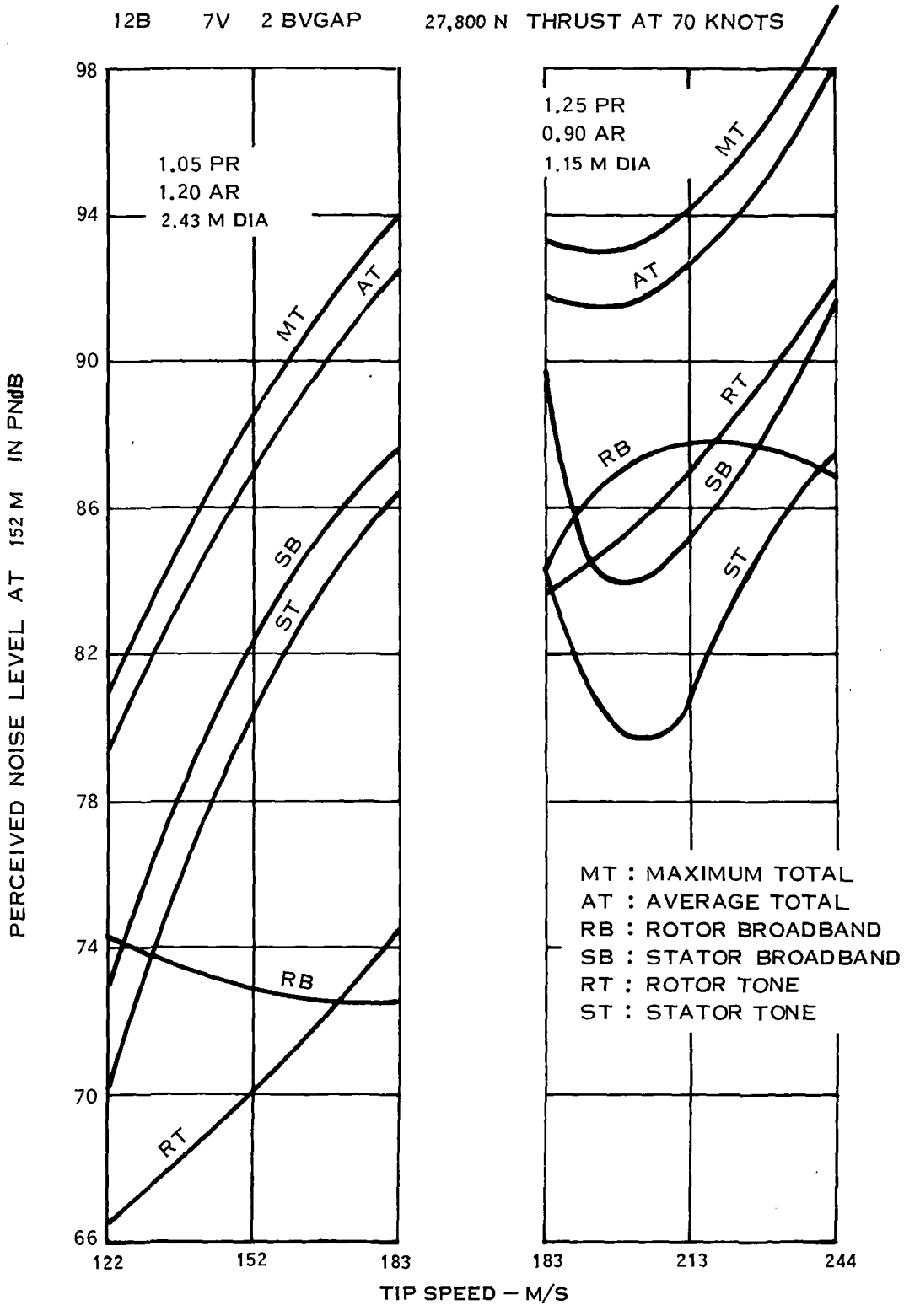

FIGURE 46. EFFECT OF TIP SPEED ON COMPONENT NOISE OF THE 1.0 SOLIDITY FAN

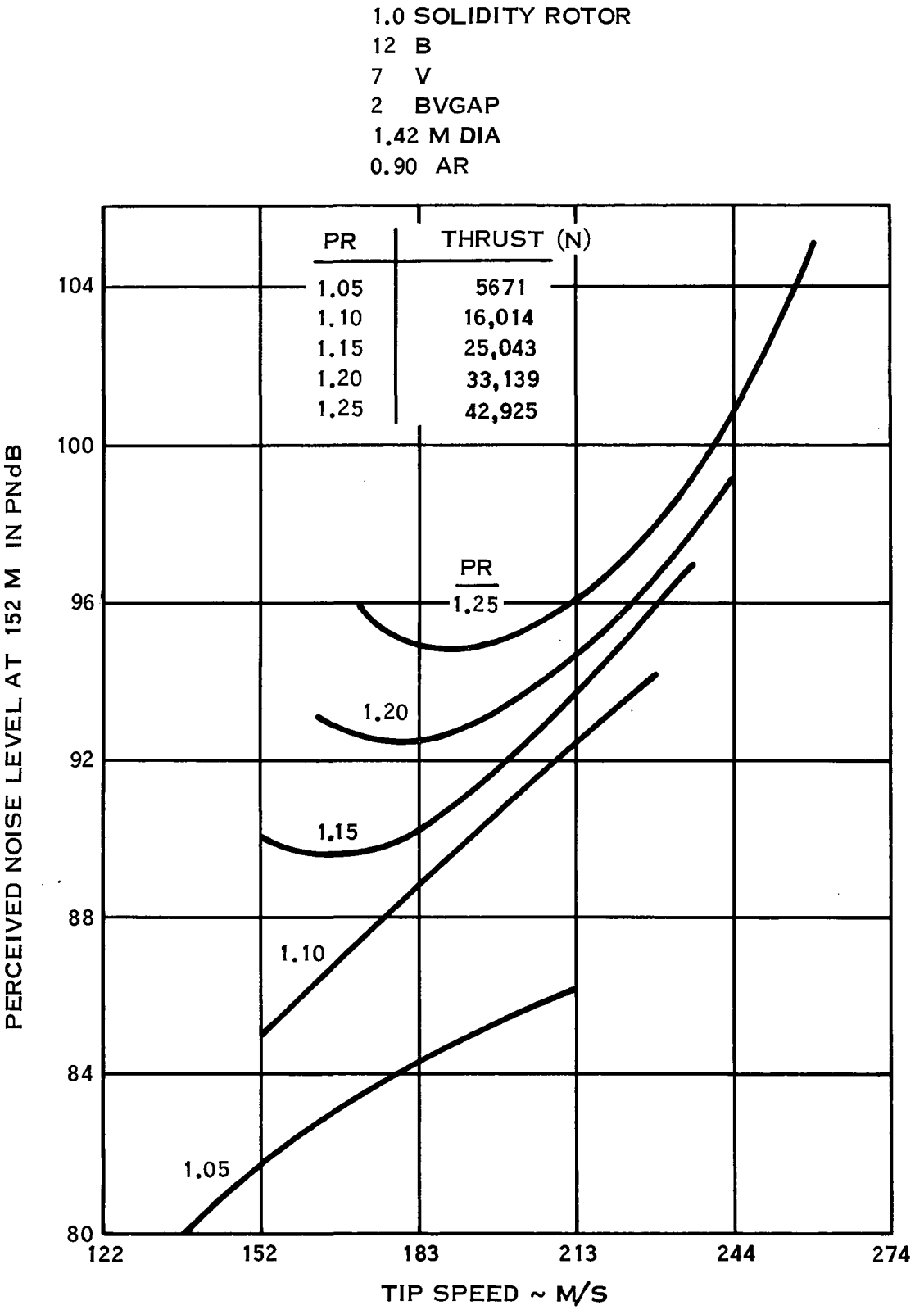

FIGURE 47. EFFECT OF TIP SPEED AND PRESSURE RATIO ON NOISE WITH CONSTANT AREA RATIO AND FAN DIAMETER

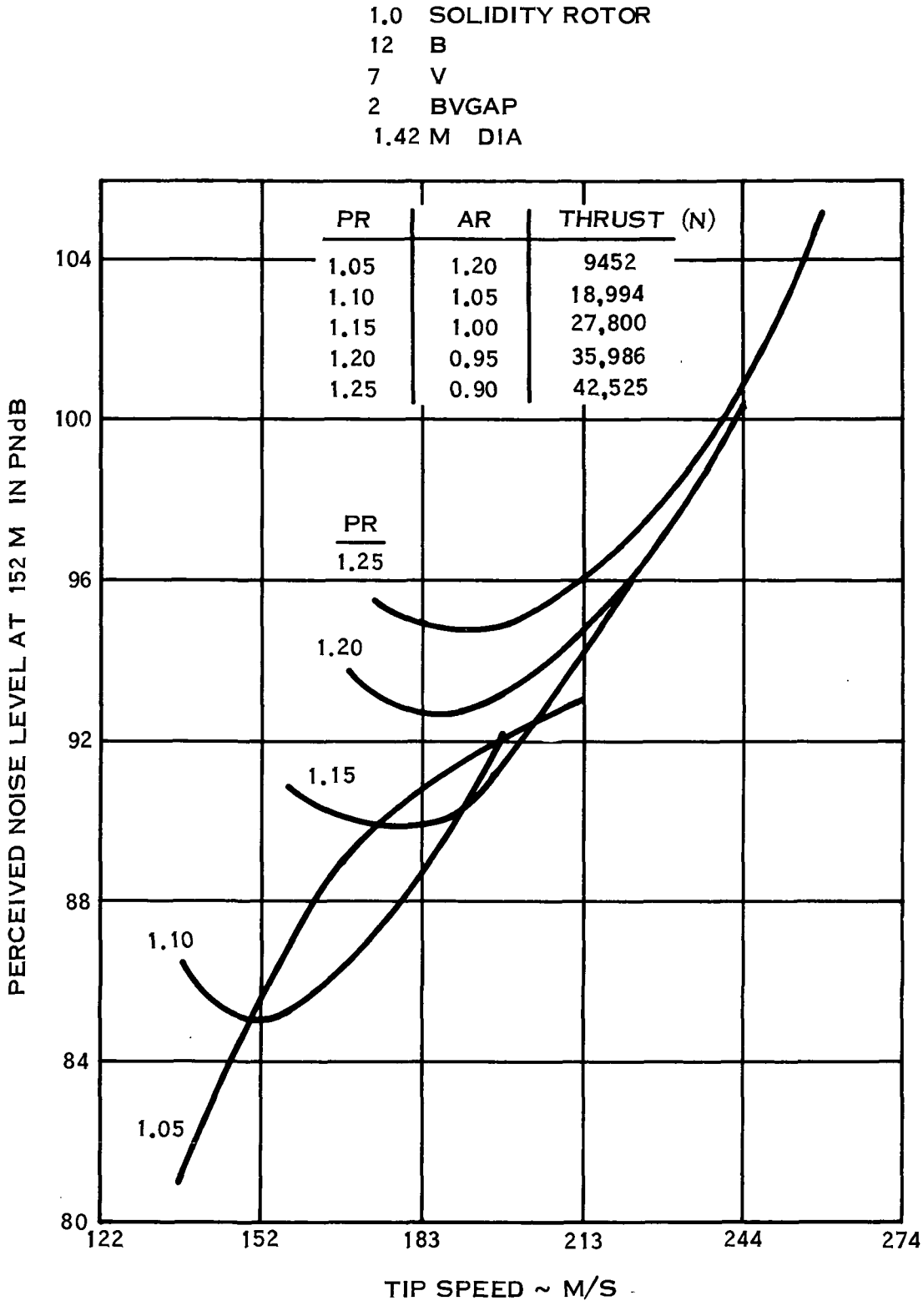

FIGURE 48. EFFECT OF TIP SPEED AND PRESSURE RATIO ON NOISE WITH OPTIMUM AREA RATIO AND CONSTANT FAN DIAMETER

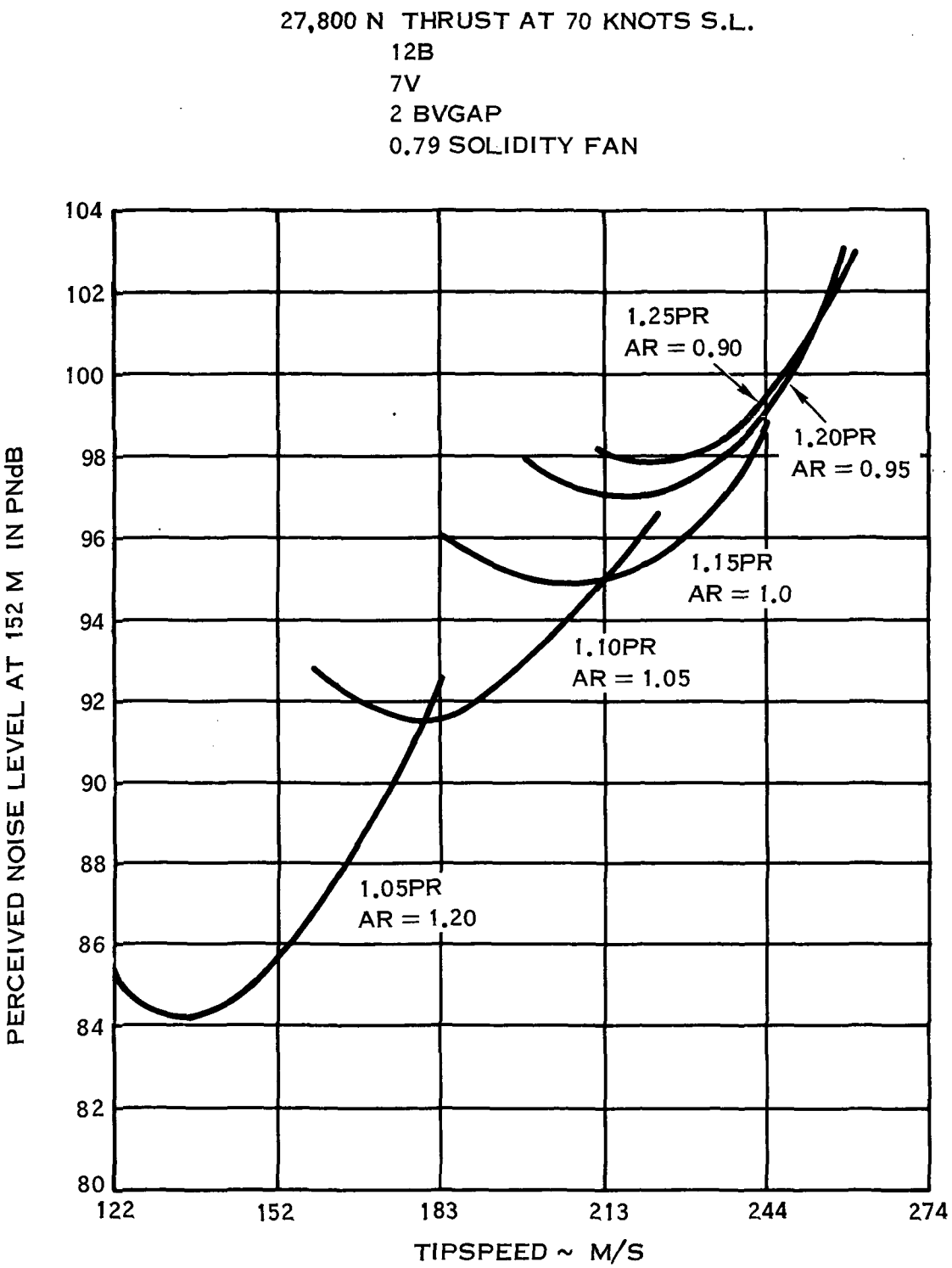

FIGURE 49. EFFECT OF TIP SPEED AND PRESSURE RATIO ON NOISE OF THE 0.79 SOLIDITY FAN

27,800 N THRUST AT 70 KNOTS S.L.
12 B
7 V
2 BVGAP
1.6 SOLIDITY FAN

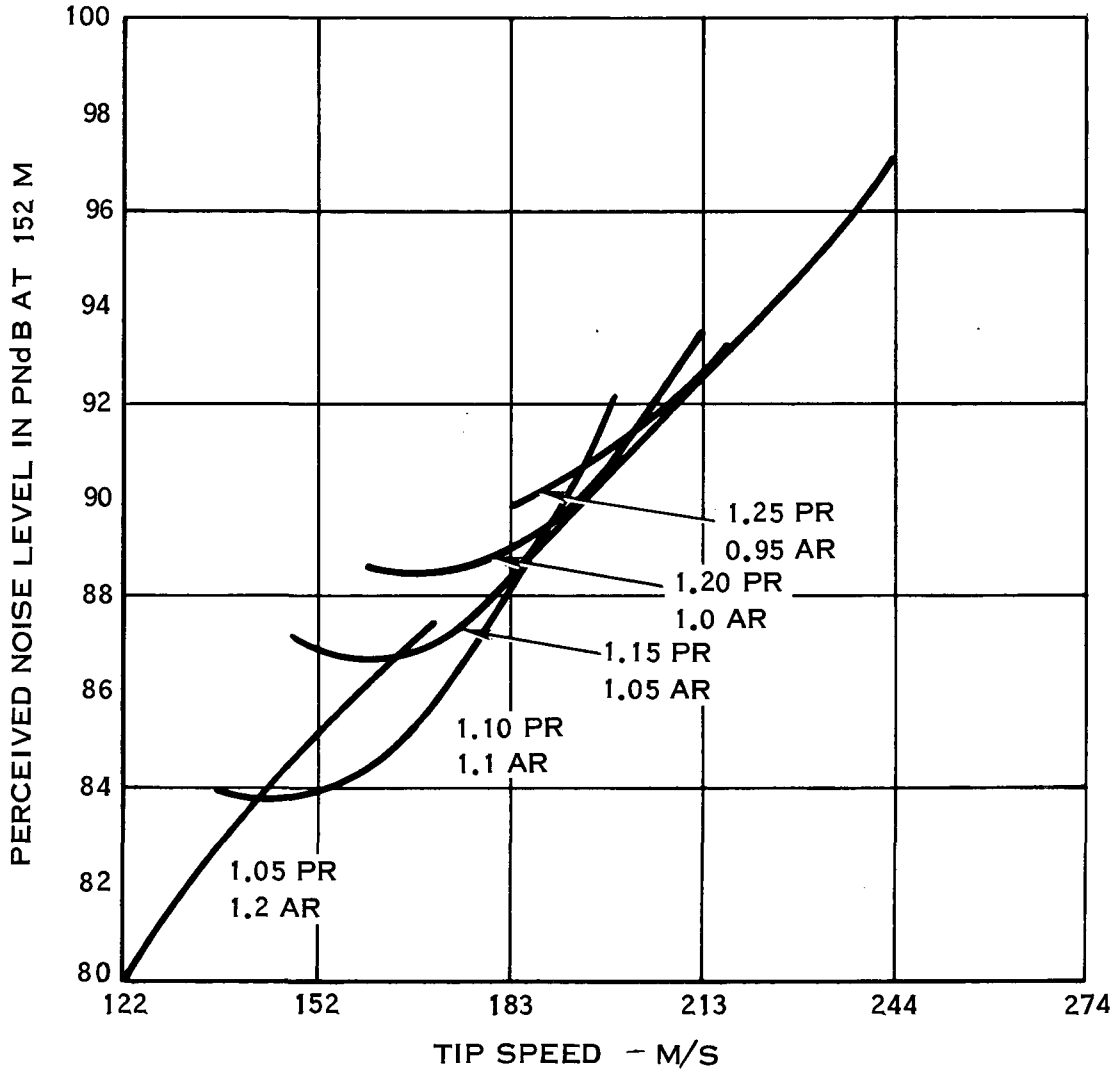

FIGURE 50. EFFECT OF TIP SPEED AND PRESSURE RATIO ON NOISE OF THE 1.6 SOLIDITY FAN

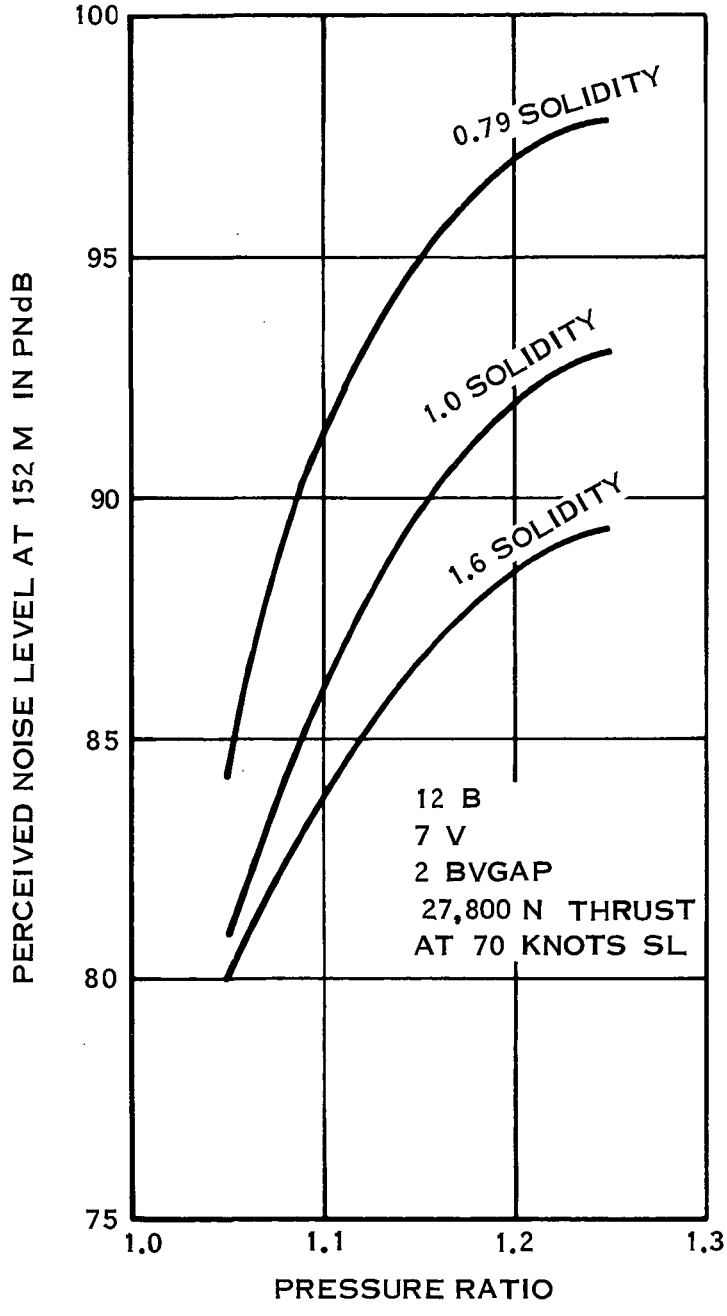

FIGURE 51. EFFECT OF PRESSURE RATIO AND FAN SOLIDITY ON NOISE

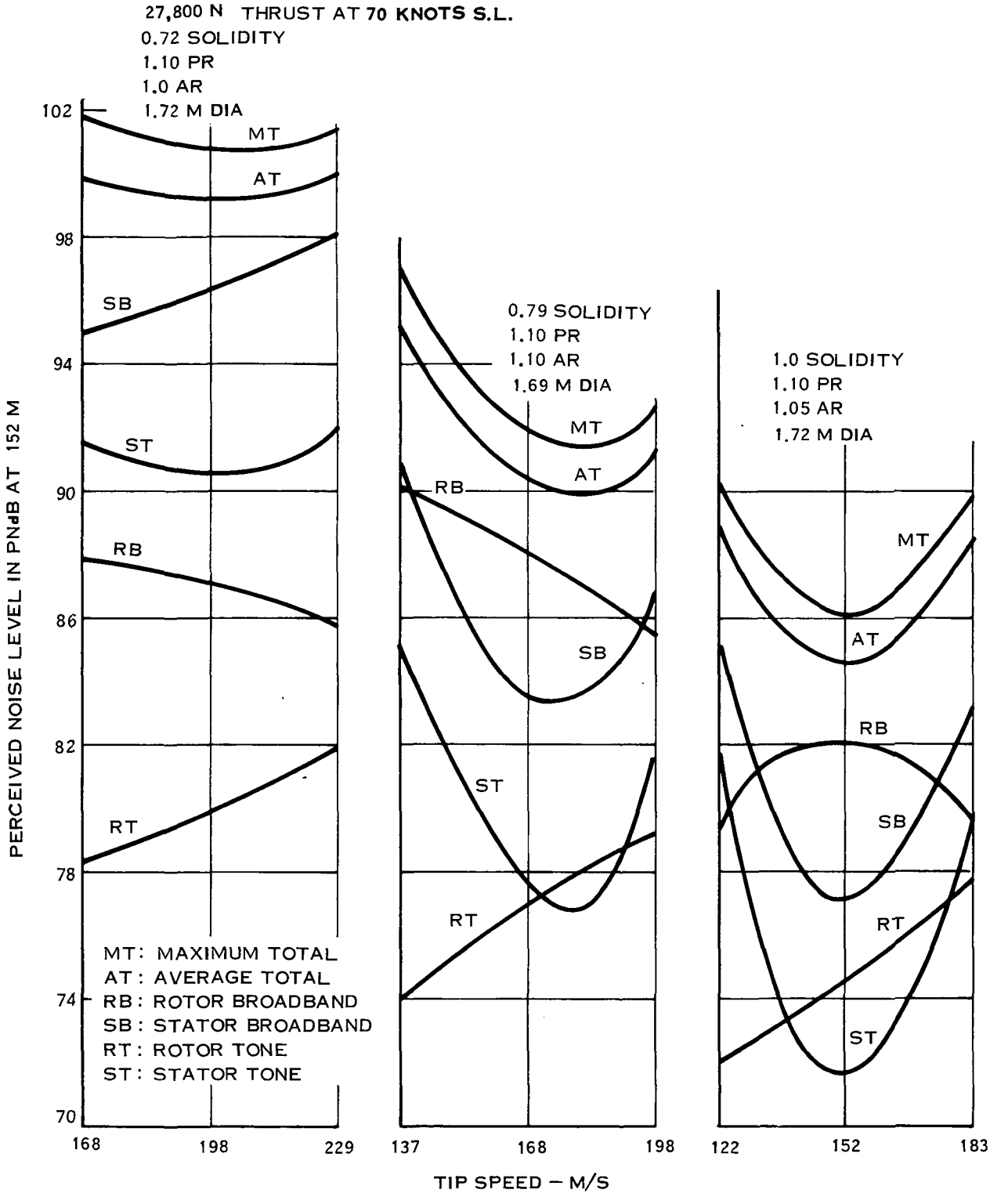

FIGURE 52. COMPONENT NOISE LEVELS AT 1.10 PRESSURE RATIO

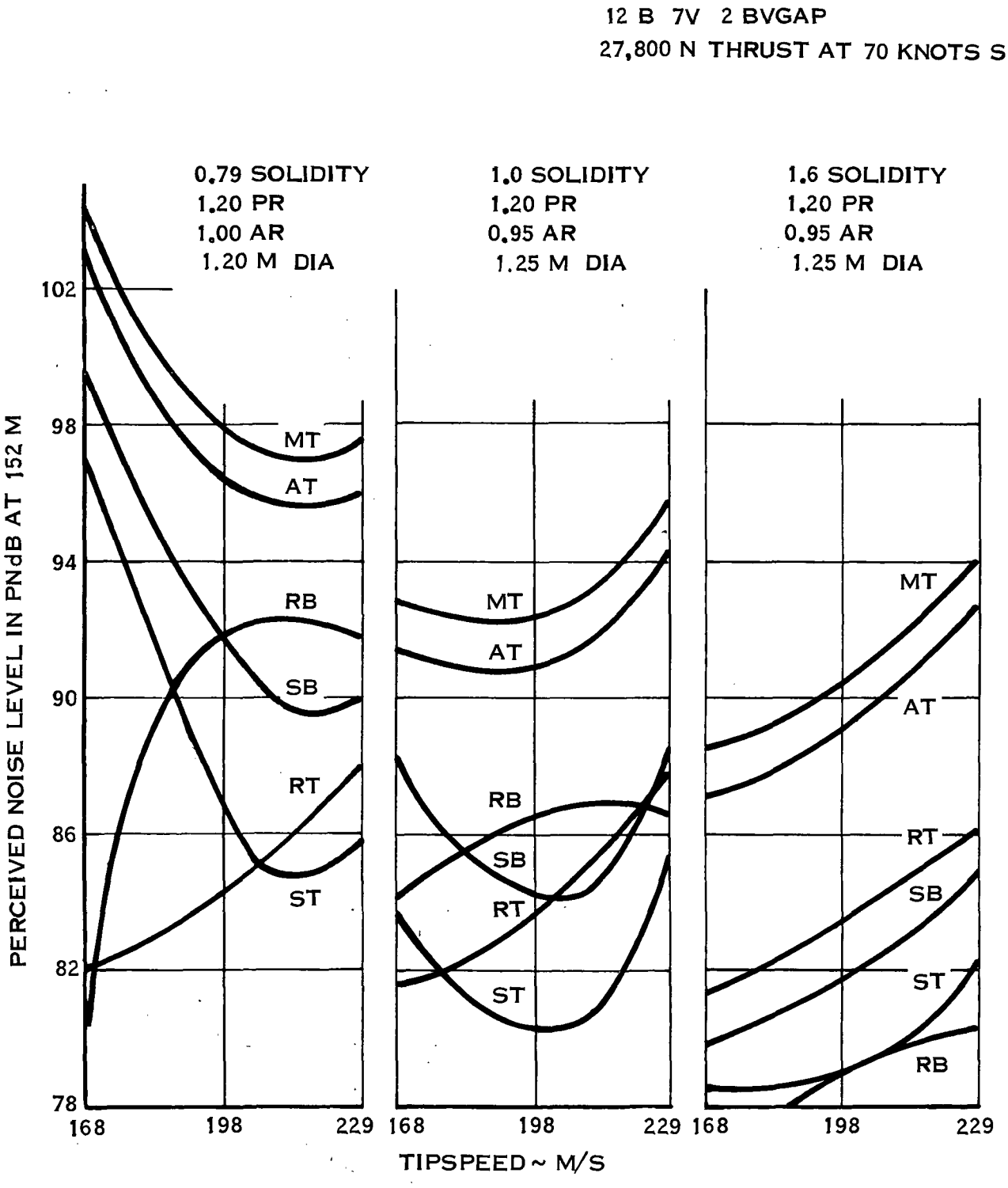

FIGURE 53. COMPARISON OF COMPONENT NOISE FOR THREE DIFFERENT ROTOR SOLIDITIES AT 1.20 PRESSURE RATIO

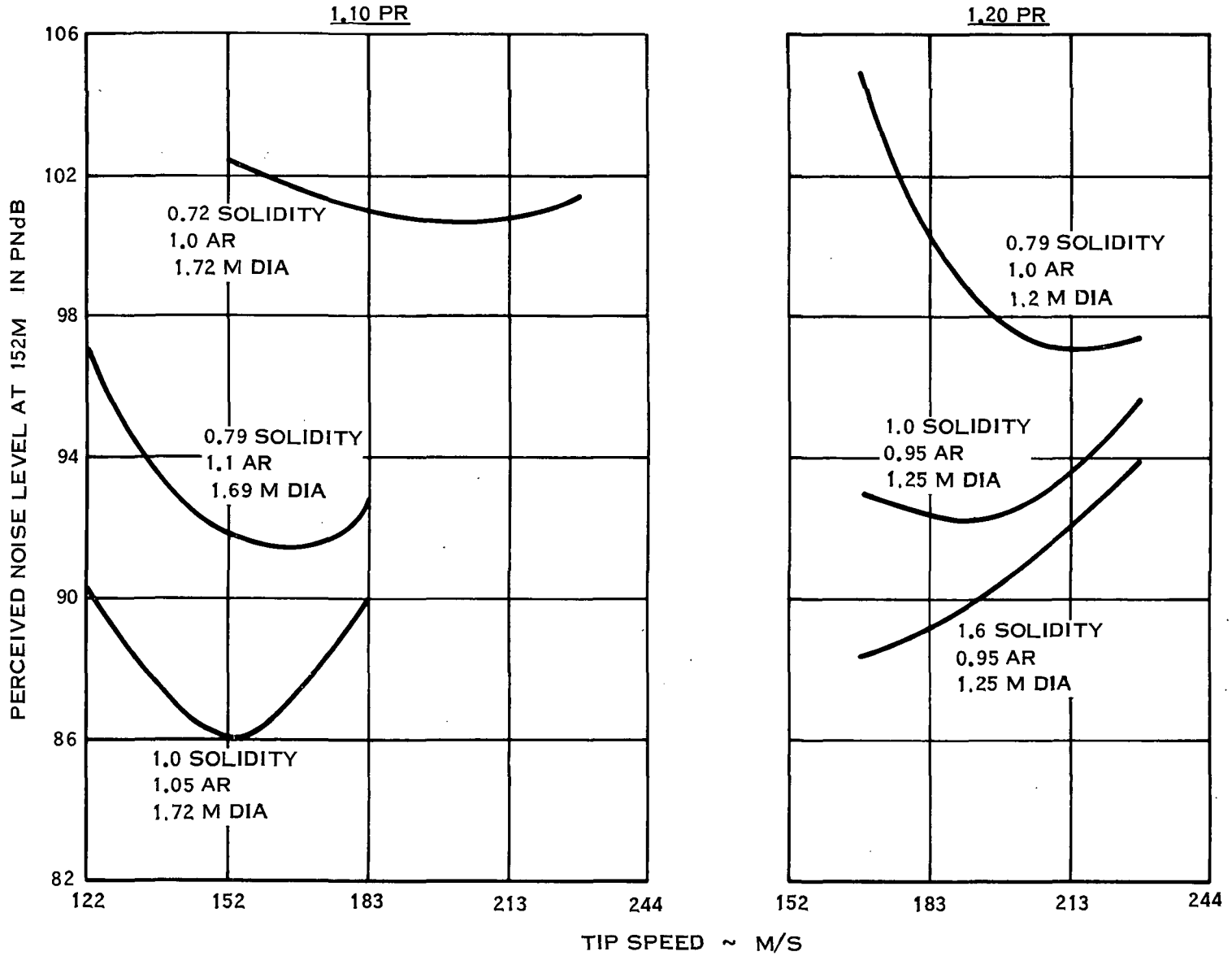

FIGURE 54. SUMMARY OF NOISE LEVELS AT 1.10 AND 1.20 PRESSURE RATIO AT 27,800 N THRUST

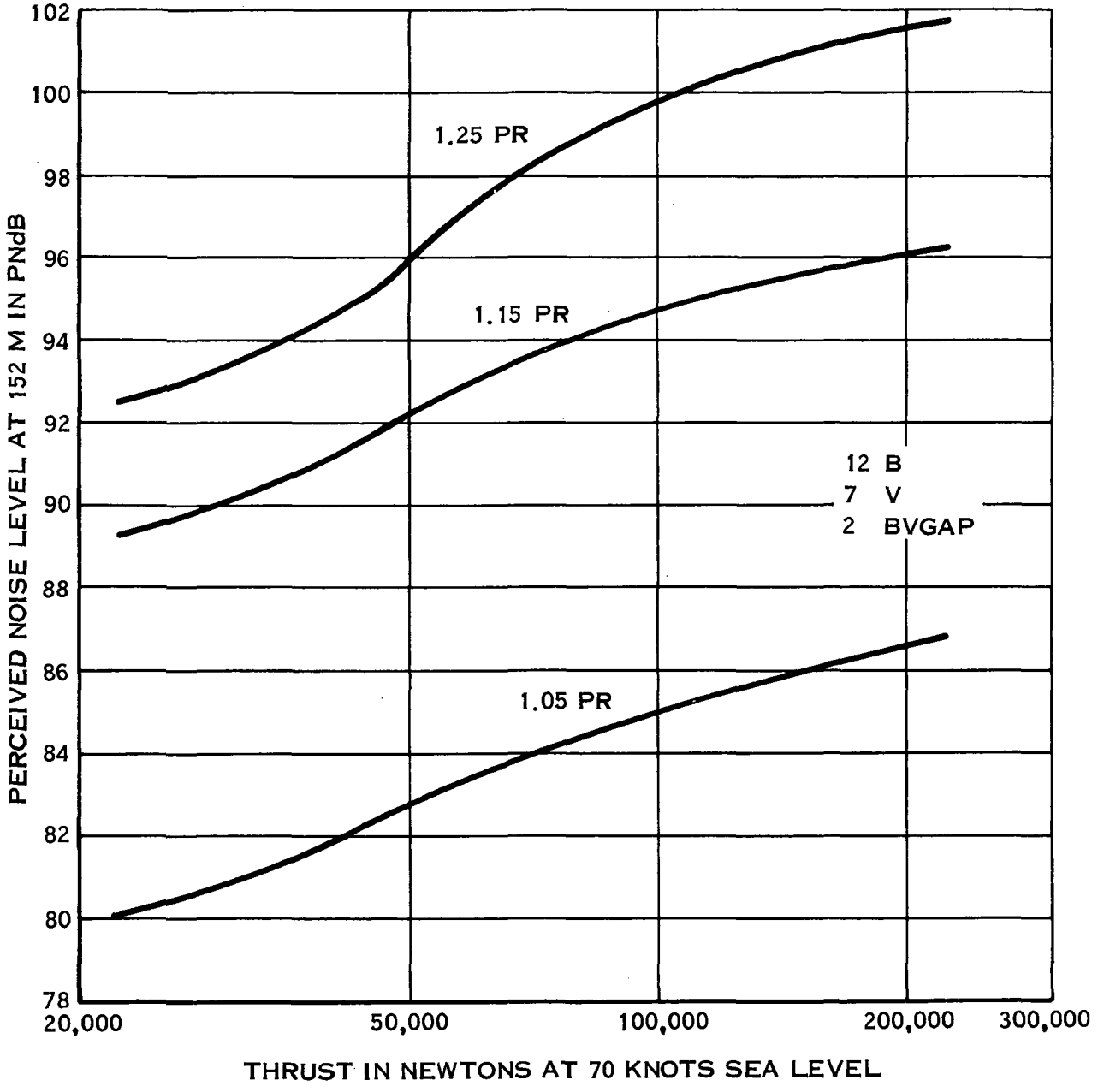

FIGURE 55. EFFECT OF THRUST AND PRESSURE RATIO ON NOISE OF A 1.0 SOLIDITY FAN

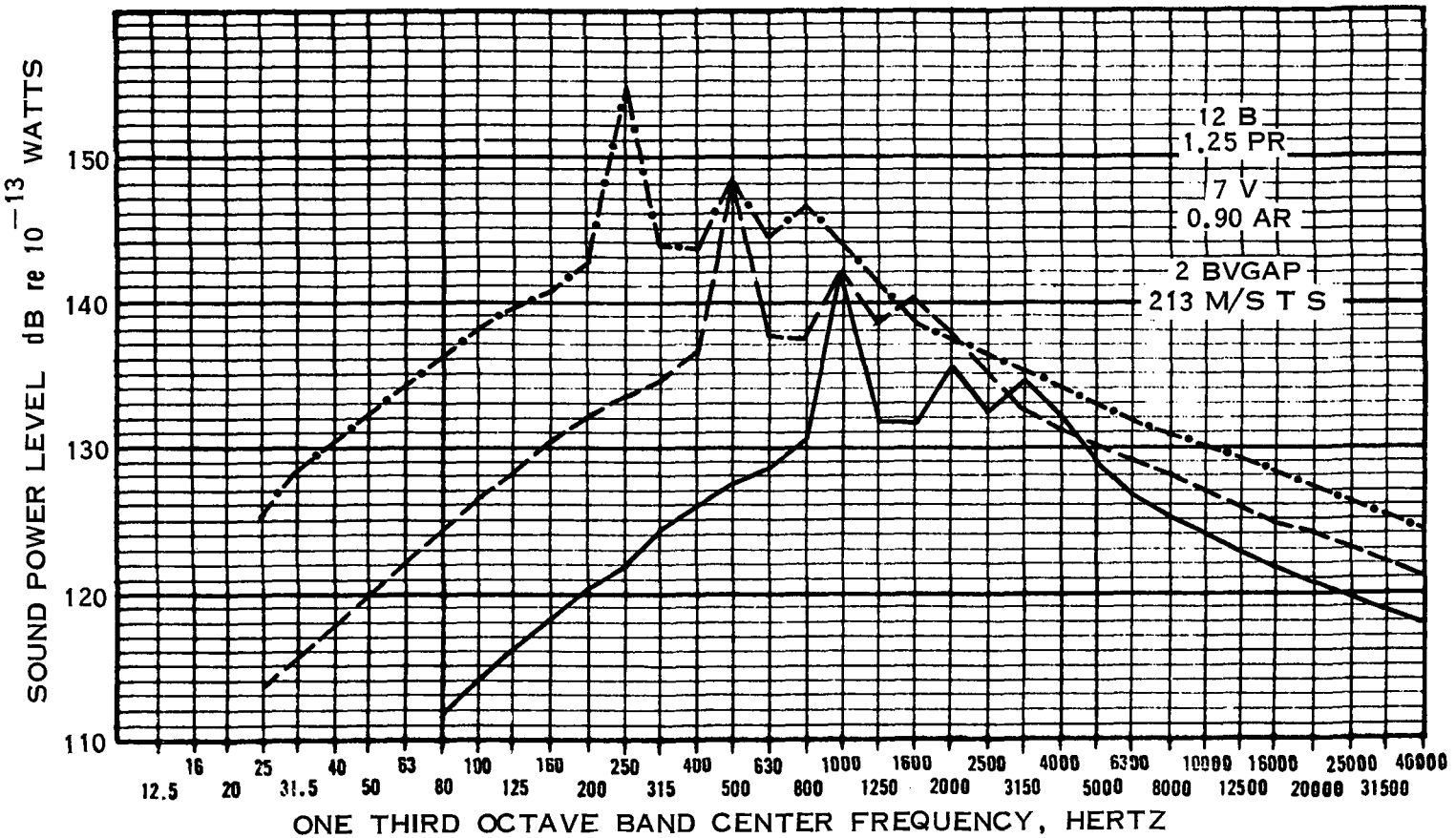

— 13,900 N THRUST AT 70 KNOTS S.L.	— — — 55,600 N THRUST AT 70 KNOTS S.L.	—·—·— 222,400 N THRUST AT 70 KNOTS S.L.
0.81 M DIA	1.62 M DIA	3.24 M DIA
91.3 PN dB	97.0 PN dB	101.8 PN dB

FIGURE 56. EFFECT OF THRUST ON NOISE SPECTRUM

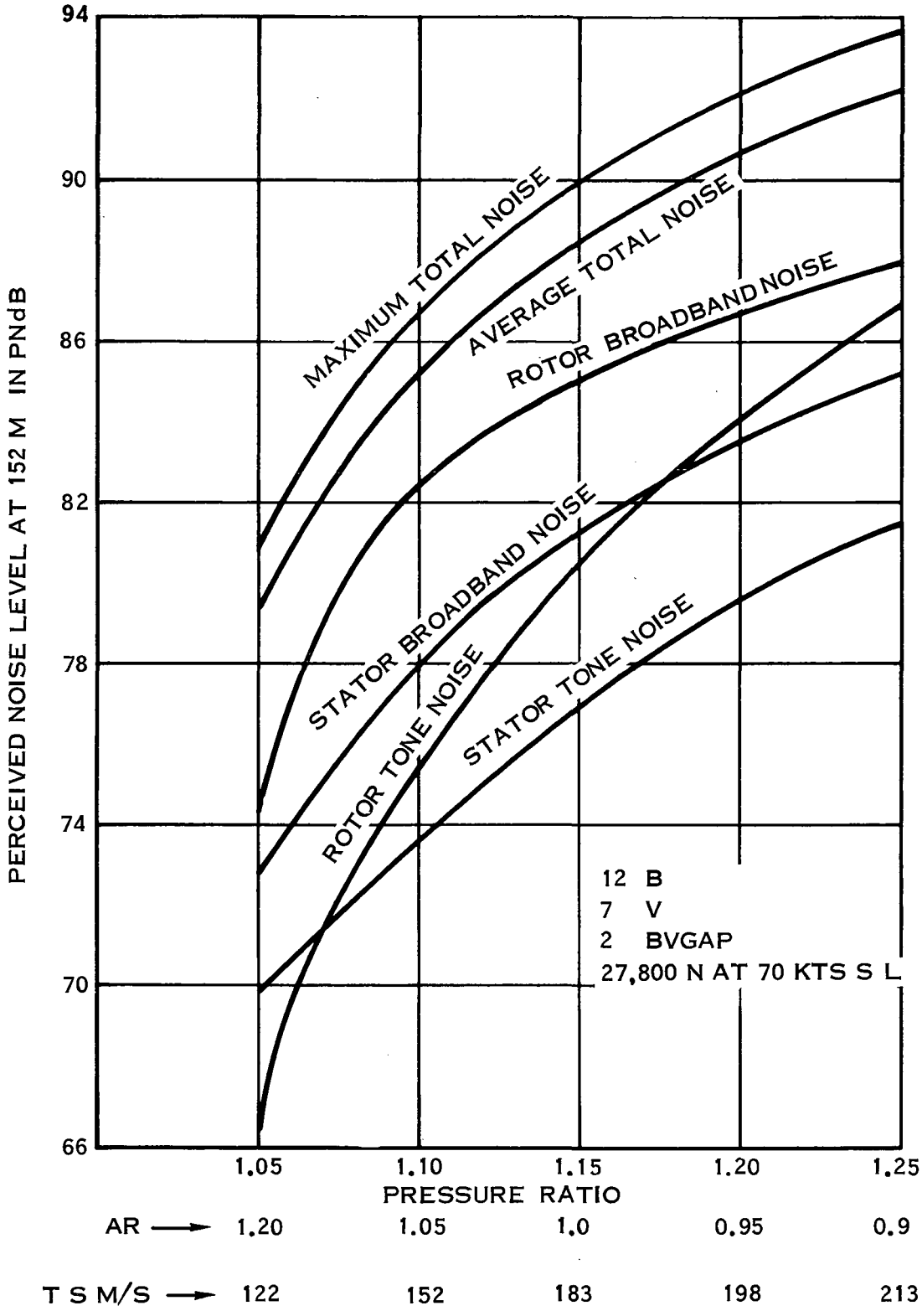

FIGURE 57. EFFECT OF PRESSURE RATIO ON COMPONENT NOISE OF A 1.0 SOLIDITY FAN

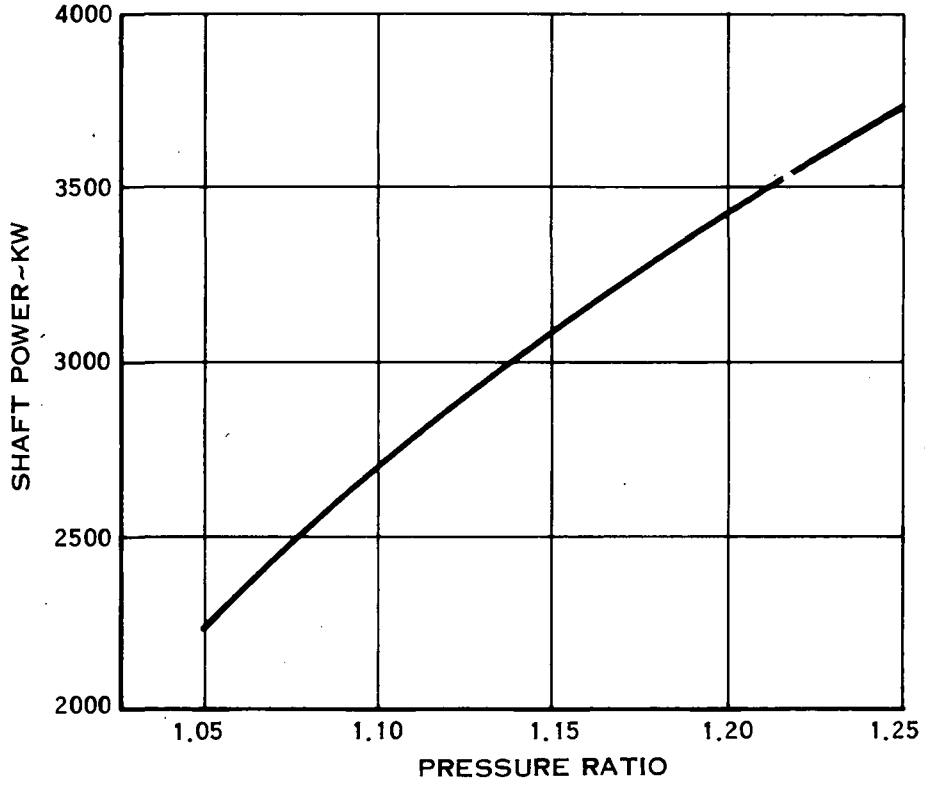

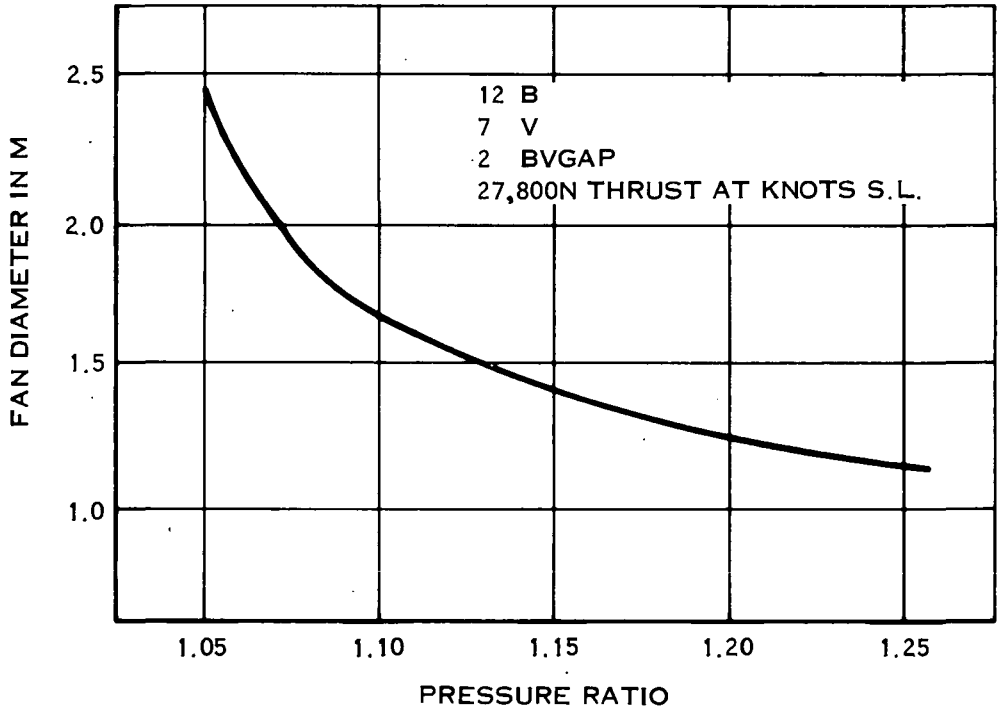

FIGURE 58. INFLUENCE OF PRESSURE RATIO ON SHAFT POWER AND FAN DIAMETER OF THE 1.0 SOLIDITY FAN

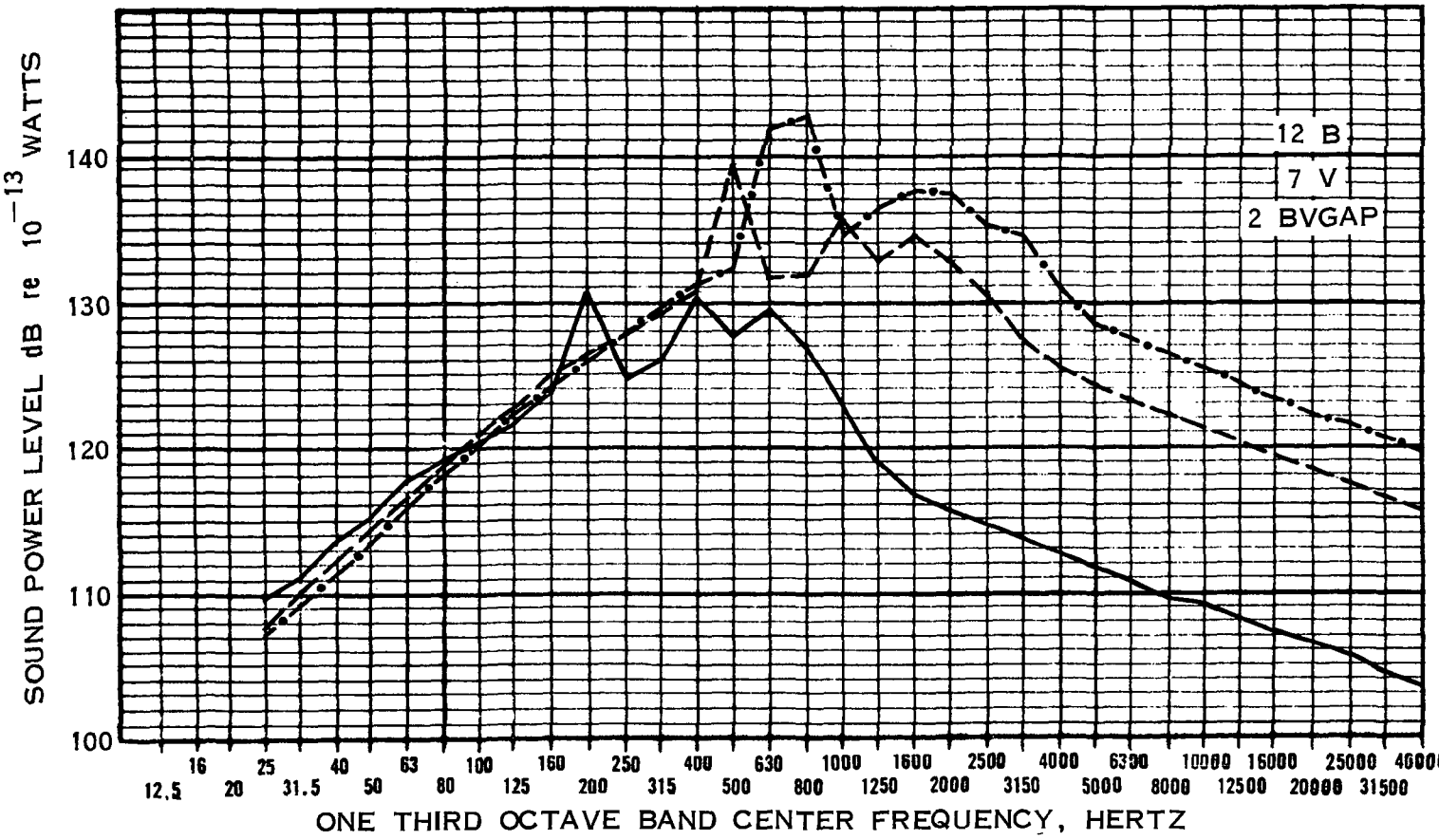

———	1.05 PR	27,800 N	– – –	1.15 PR	27,800 N	—•—	1.25 PR	27,800 N
	1.20 AR	THRUST AT		1.00 AR	THRUST AT		0.90 AR	THRUST AT
	2.43 M DIA	70 KNOTS		1.42 M DIA	70 KNOTS		1.15 M DIA	70 KNOTS
	122 M/S	S.L.		183 M/S	S.L.		213 M/S	S.L.
	T S	80.0 PNdB		T S	89.8 PNdB		T S	93.7 PNdB

FIGURE 59. EFFECT OF PRESSURE RATIO ON NOISE SPECTRUM

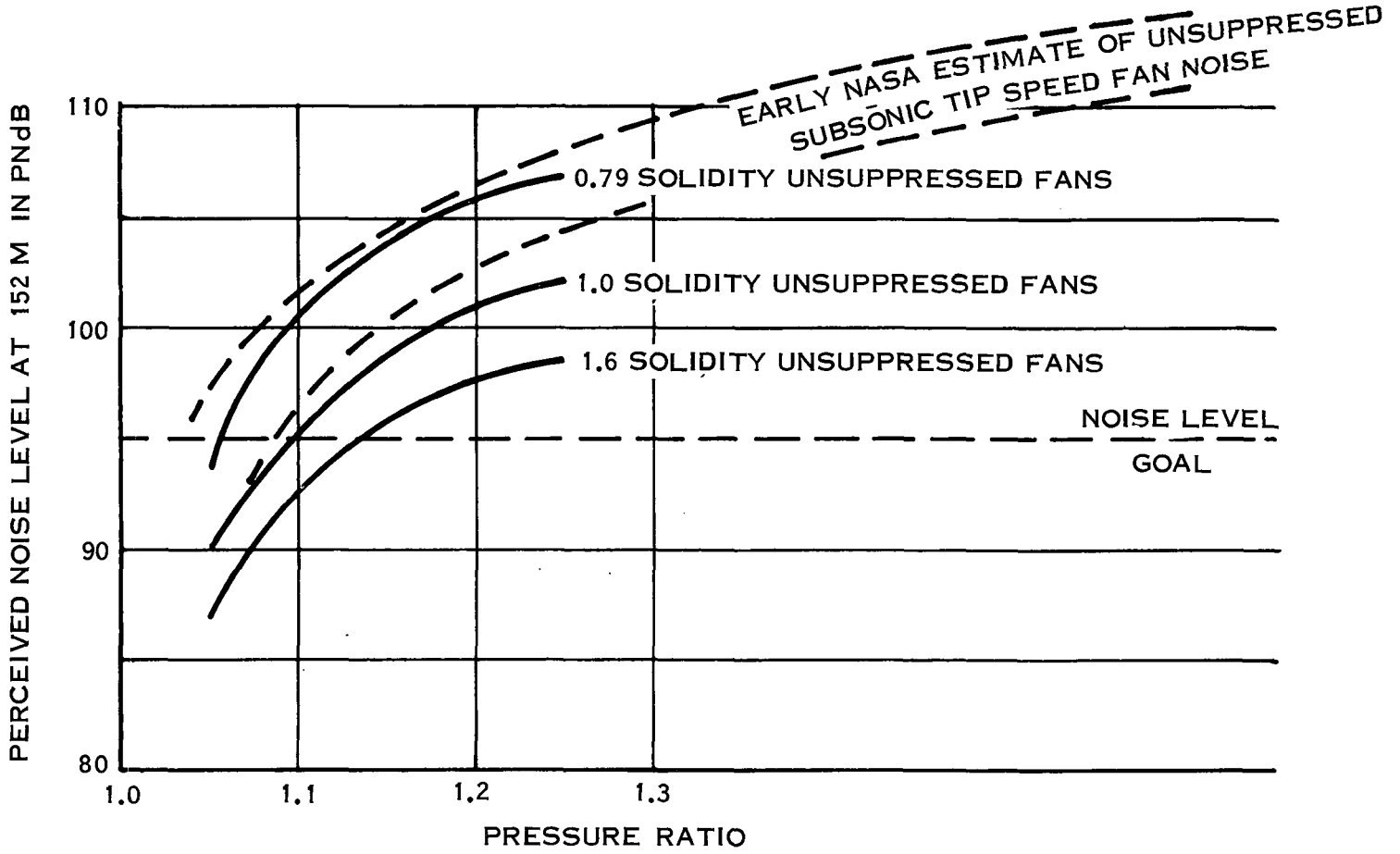

FIGURE 60. UNSUPPRESSED FAN NOISE FOR A 45,360 KG STOL AIRCRAFT

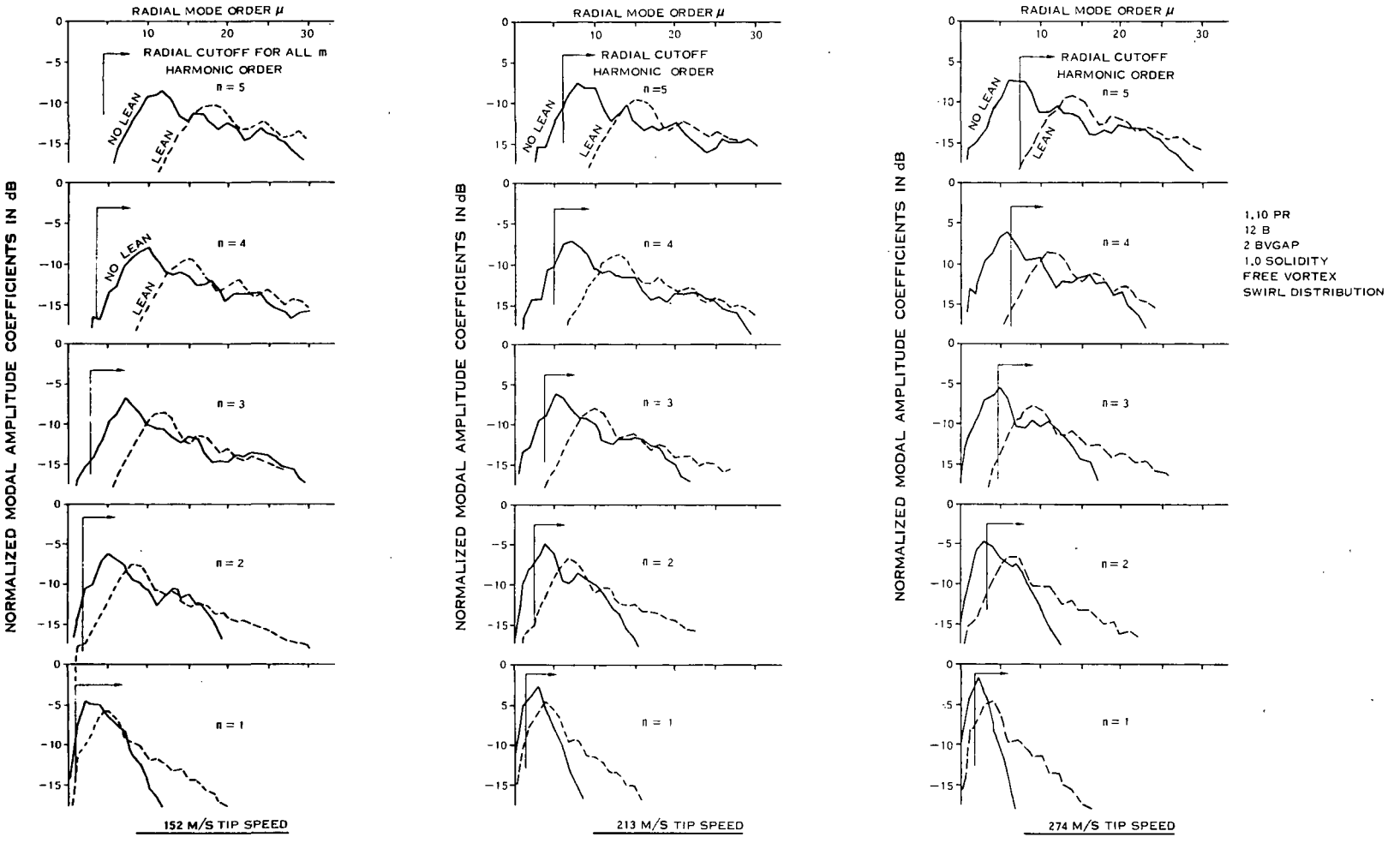

FIGURE 61. EFFECT OF VANE LEAN AS A FUNCTION OF TIP SPEED

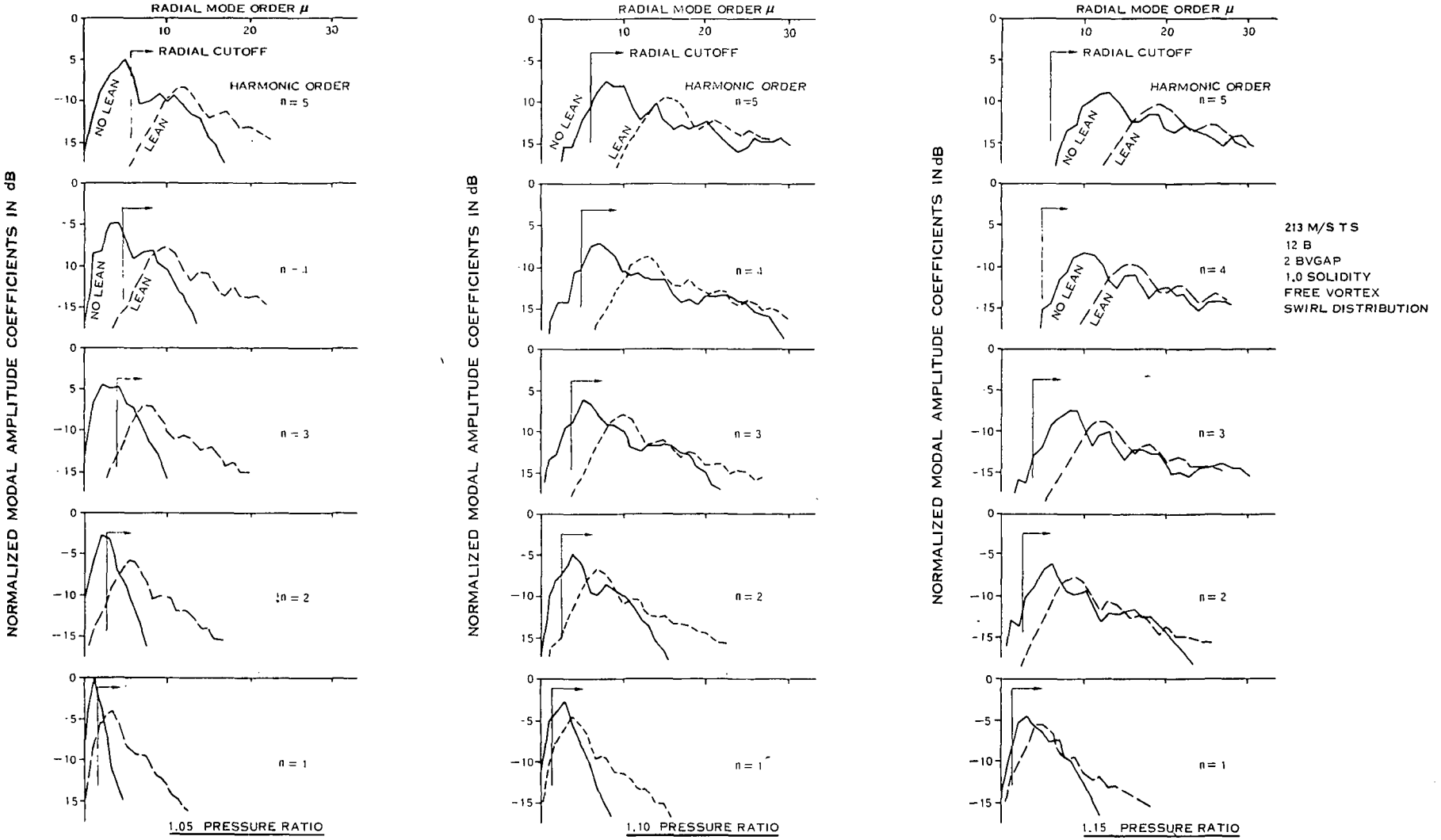

FIGURE 62. EFFECT OF VANE LEAN AS A FUNCTION OF PRESSURE RATIO

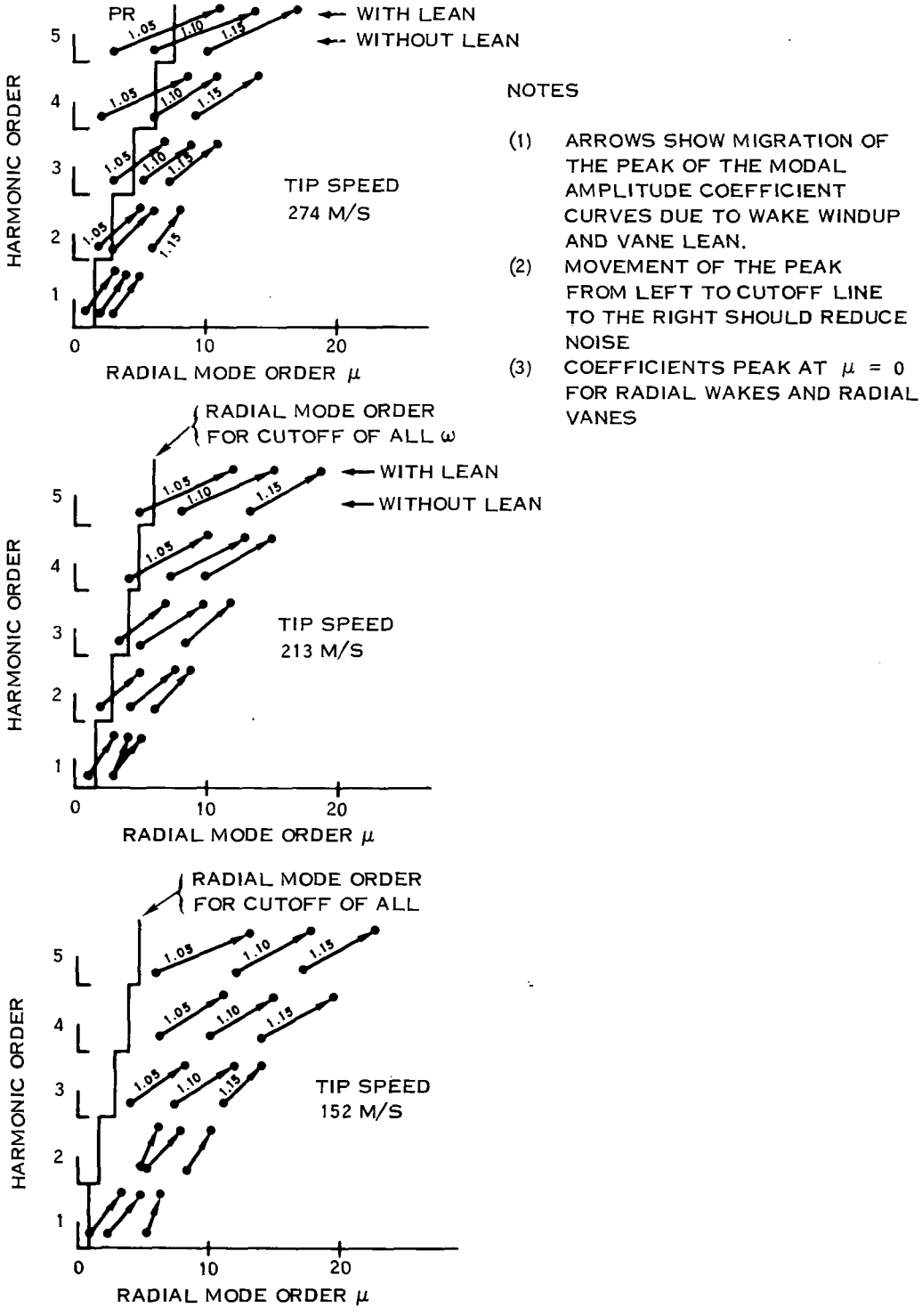

FIGURE 63. SUMMARY PLOT OF LEAN, TIP SPEED, AND PRESSURE RATIO EFFECTS

NOTE: RESULTS ARE SHOWN FOR 1.15 PR, 0.79 SOLIDITY FAN

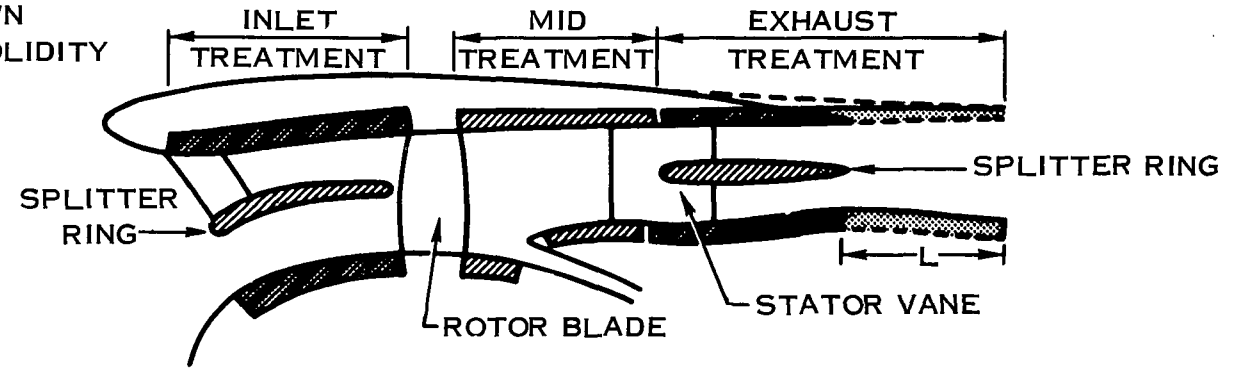

TREATMENT CONFIGURATION			REDUCTION IN PERCEIVED NOISE LEVEL
INLET	MID	EXHAUST	
NONE	NONE	WALLS	4.8
NONE	NONE	WALLS PLUS SPLITTER OR ONE L EXTENSION	5.0
NONE	WALLS	WALLS	5.7
WALLS	NONE	WALLS PLUS SPLITTER OR ONE L EXTENSION	7.4
NONE	WALLS	WALLS PLUS SPLITTER OR ONE L EXTENSION	8.0
WALLS	WALLS	WALLS PLUS SPLITTER OR ONE L EXTENSION	8.5
WALLS	WALLS	WALLS PLUS TWO SPLITTERS OR TWO L EXTENSION	9.5
WALLS	WALLS	WALLS PLUS THREE SPLITTERS OR THREE L EXTENSION	10.5
WALLS PLUS ONE SPLITTER	WALLS	WALLS PLUS THREE SPLITTERS OR THREE L EXTENSION	11.3

FIGURE 64. RESULTS OF INITIAL STUDY OF Q-FAN TREATMENT

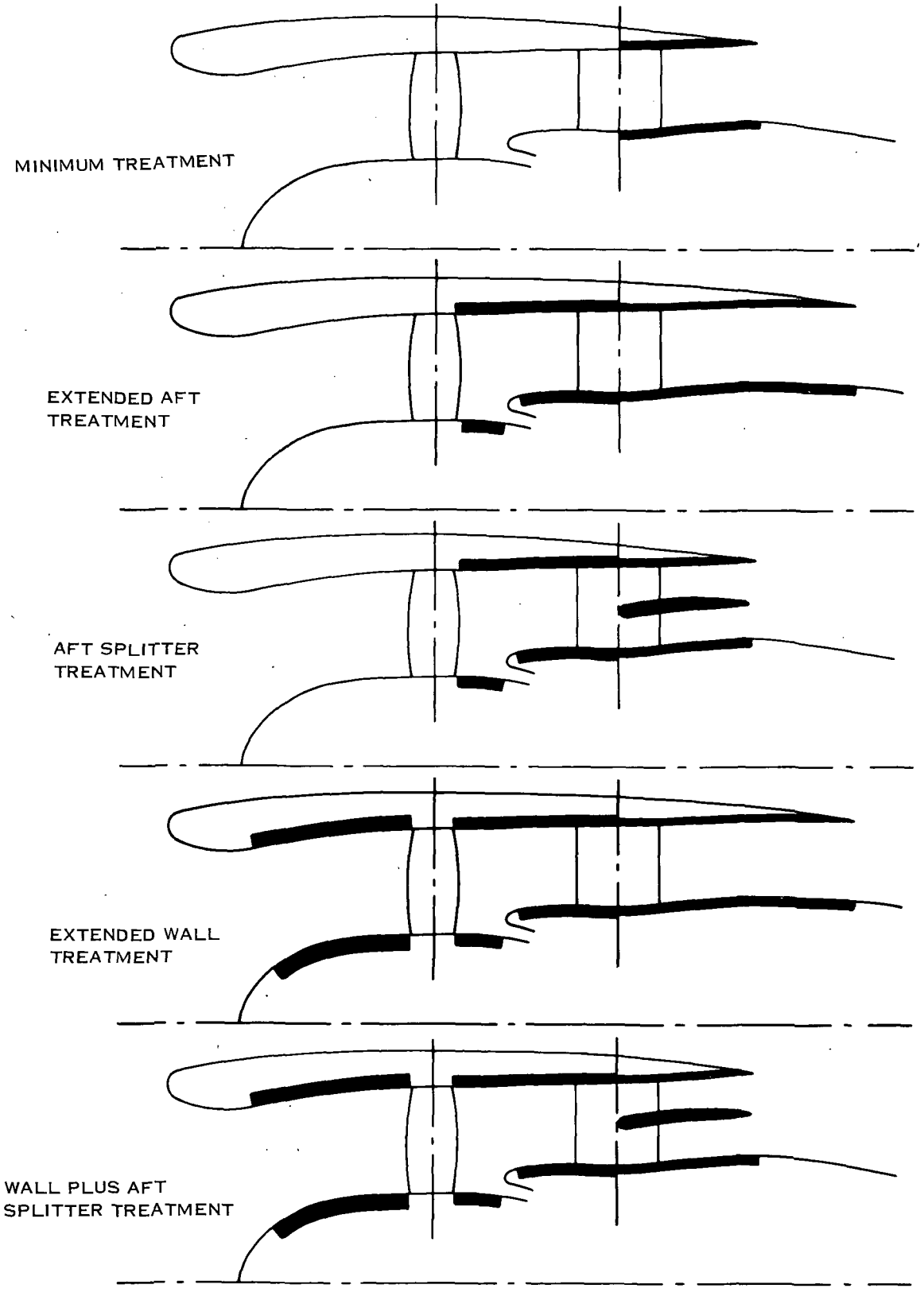

FIGURE 65. CONFIGURATIONS USED IN DETAILED TREATMENT STUDY

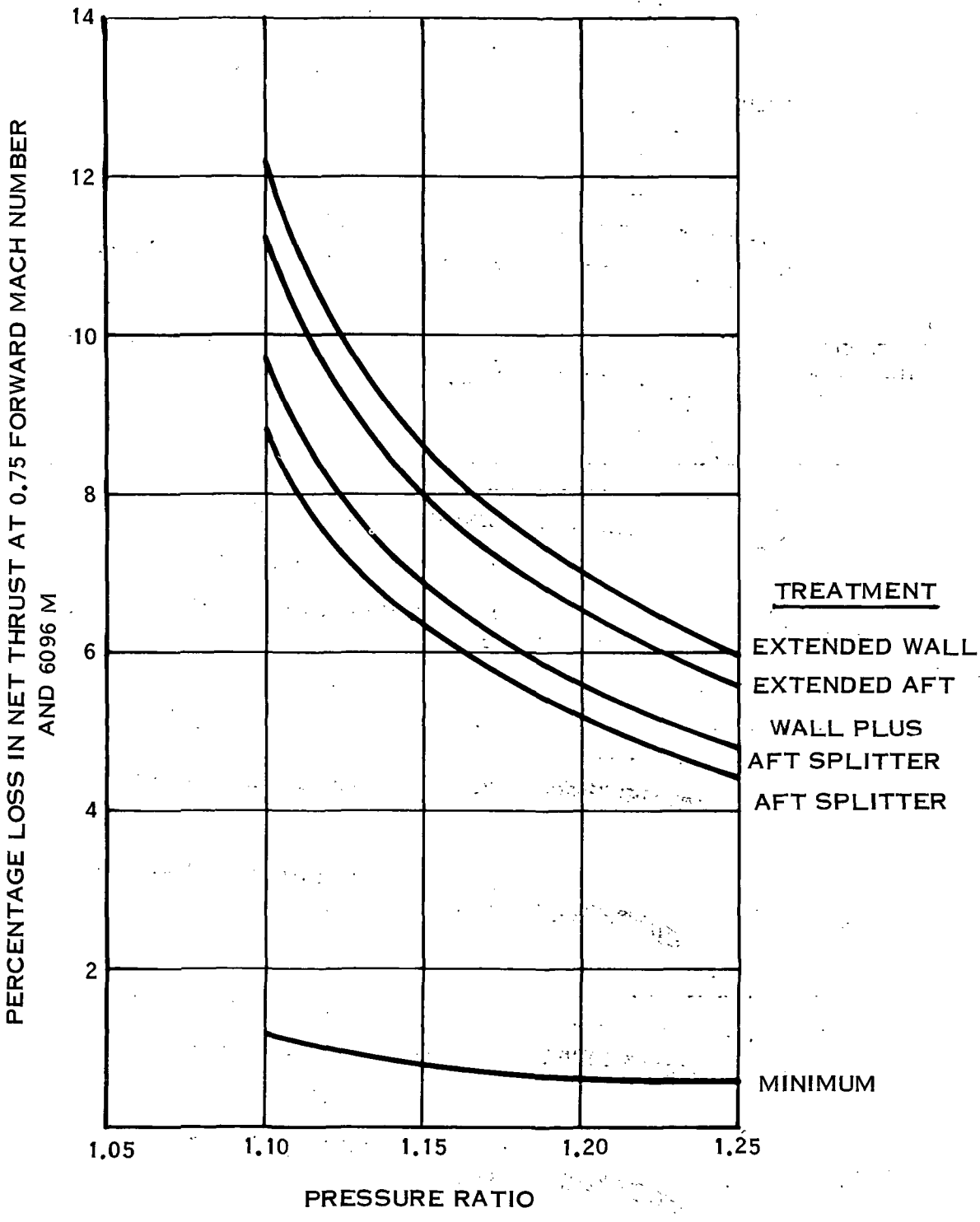

FIGURE 66. EFFECT OF DUCT TREATMENT ON CRUISE THRUST

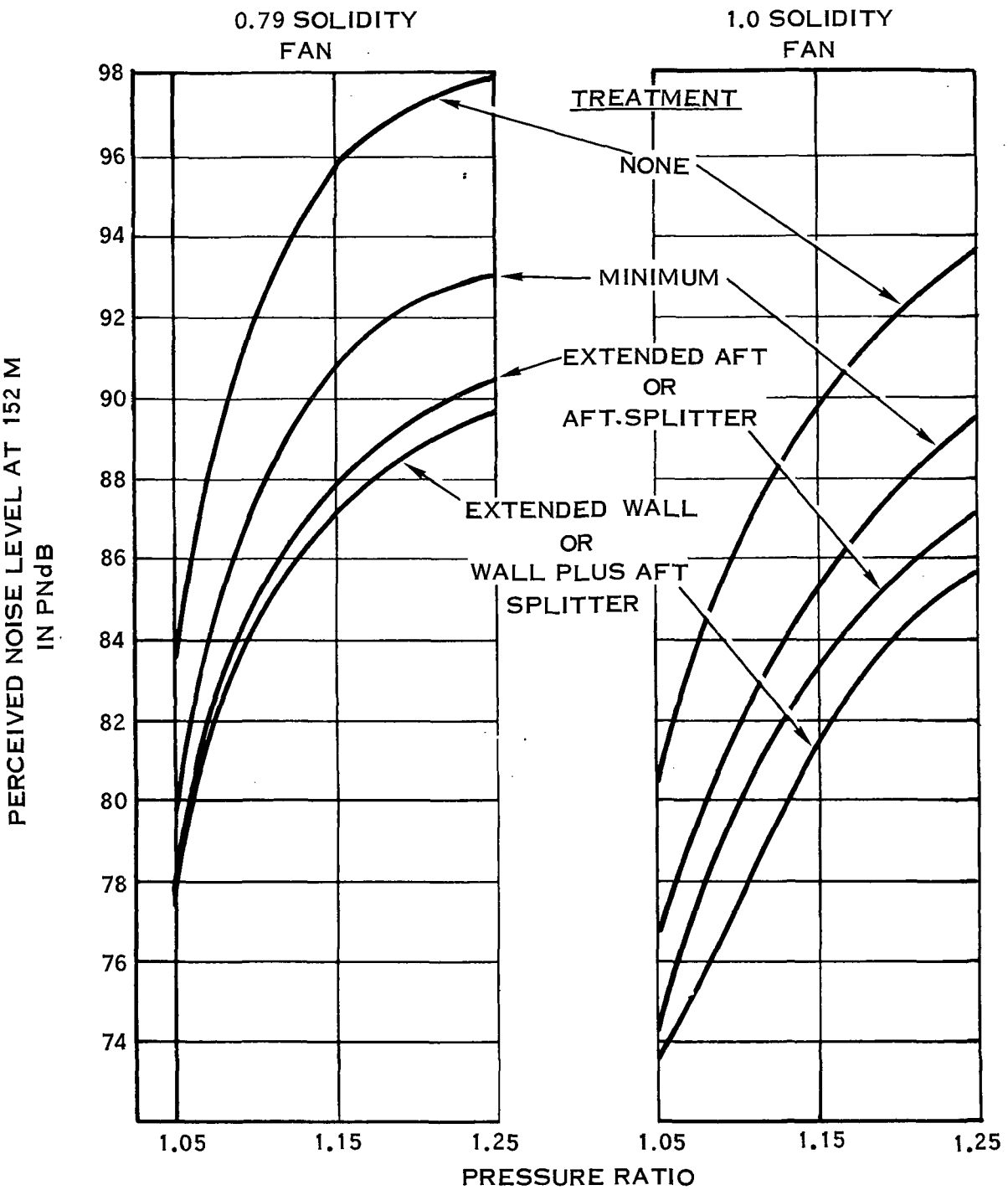

NOTE: BOTH CASES SHOWN FOR 27,800 N THRUST AT 70 KTS S L

FIGURE 67. EFFECT OF PRESSURE RATIO AND FAN SOLIDITY ON ATTENUATION

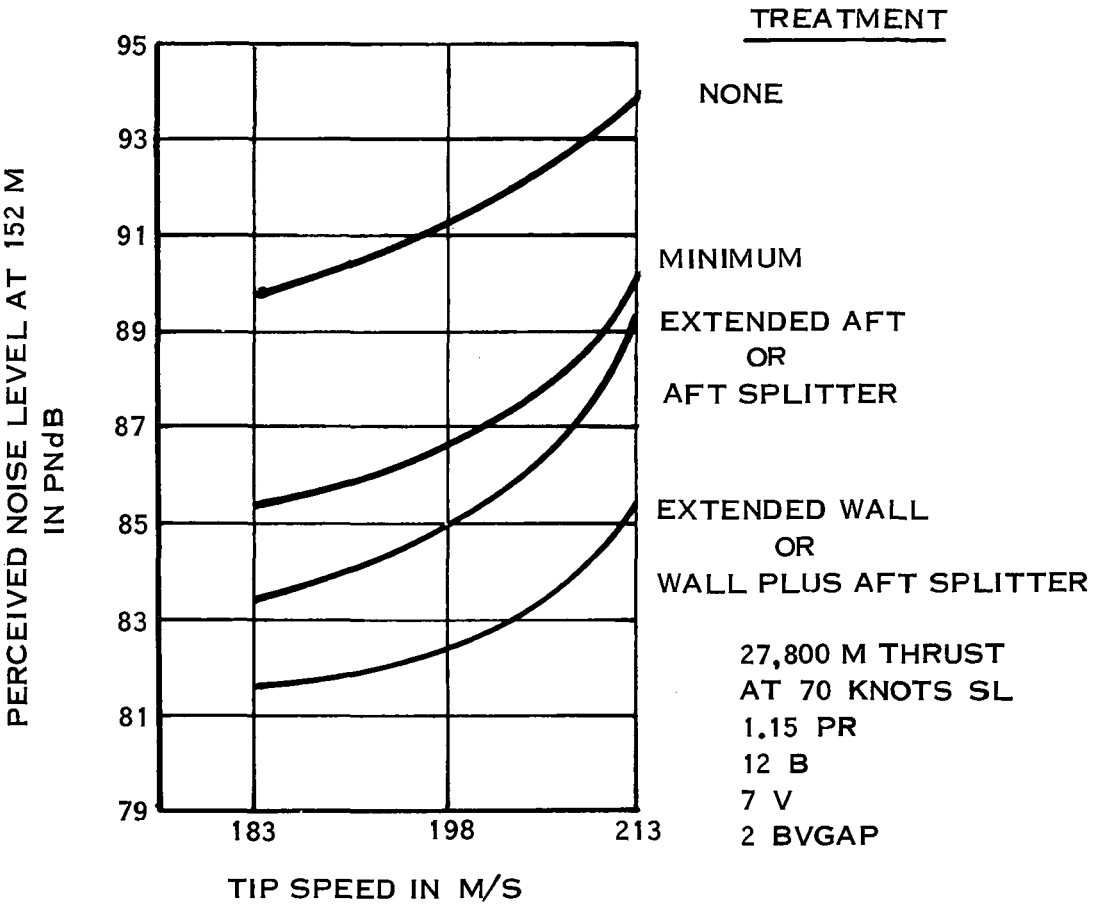

FIGURE 68. EFFECT OF TIP SPEED ON ATTENUATION FOR A 1.0 SOLIDITY FAN

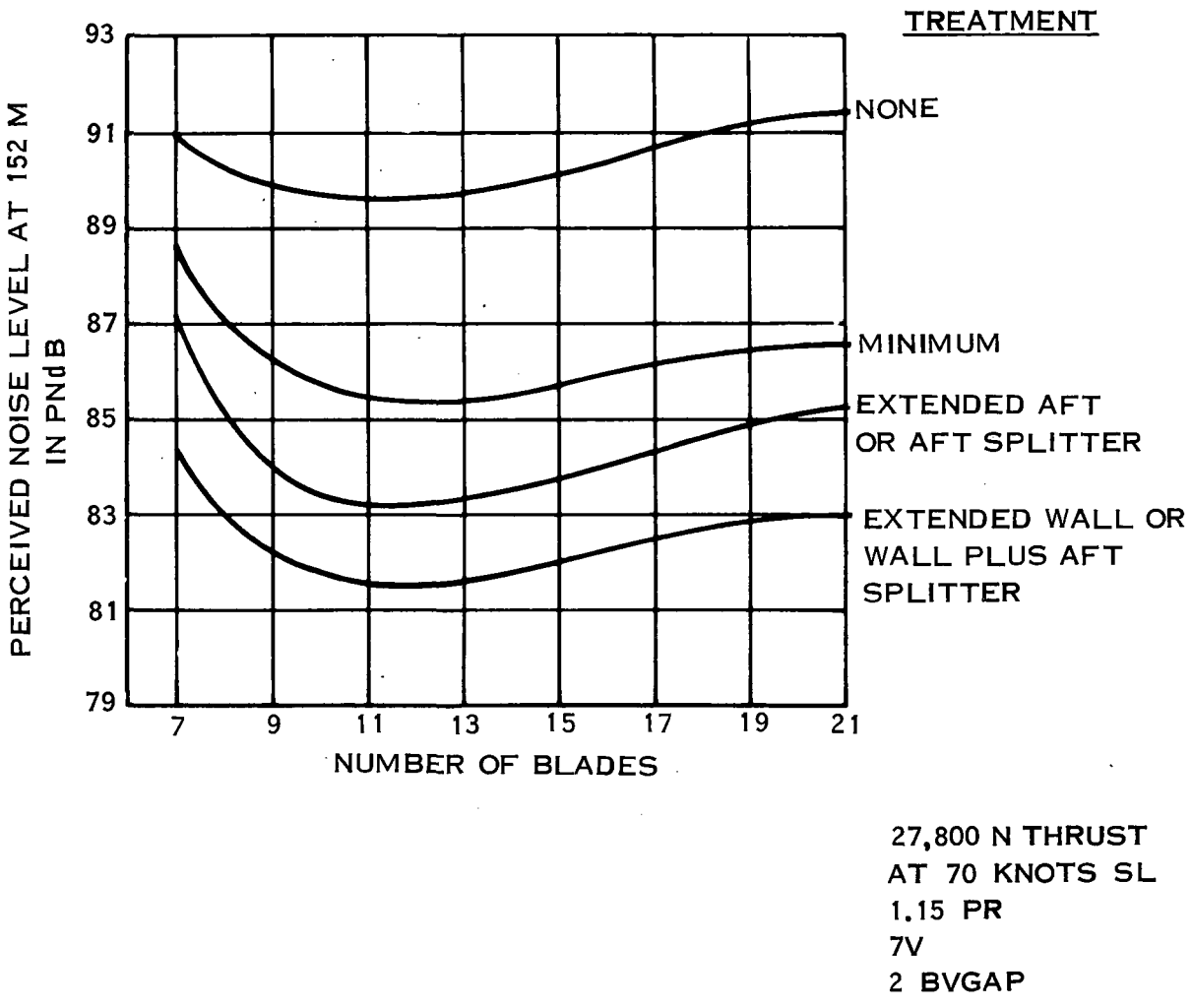

FIGURE 69. EFFECT OF NUMBER OF BLADES ON ATTENTUATION FOR A 1.0 SOLIDITY FAN

☆ U. S. GOVERNMENT PRINTING OFFICE: 1973—736-351

"The aeronautical and space activities of the United States shall be conducted so as to contribute . . . to the expansion of human knowledge of phenomena in the atmosphere and space. The Administration shall provide for the widest practicable and appropriate dissemination of information concerning its activities and the results thereof."

—NATIONAL AERONAUTICS AND SPACE ACT OF 1958

NASA SCIENTIFIC AND TECHNICAL PUBLICATIONS

TECHNICAL REPORTS: Scientific and technical information considered important, complete, and a lasting contribution to existing knowledge.

TECHNICAL NOTES: Information less broad in scope but nevertheless of importance as a contribution to existing knowledge.

TECHNICAL MEMORANDUMS: Information receiving limited distribution because of preliminary data, security classification, or other reasons. Also includes conference proceedings with either limited or unlimited distribution.

CONTRACTOR REPORTS: Scientific and technical information generated under a NASA contract or grant and considered an important contribution to existing knowledge.

TECHNICAL TRANSLATIONS: Information published in a foreign language considered to merit NASA distribution in English.

SPECIAL PUBLICATIONS: Information derived from or of value to NASA activities. Publications include final reports of major projects, monographs, data compilations, handbooks, sourcebooks, and special bibliographies.

TECHNOLOGY UTILIZATION PUBLICATIONS: Information on technology used by NASA that may be of particular interest in commercial and other non-aerospace applications. Publications include Tech Briefs, Technology Utilization Reports and Technology Surveys.

Details on the availability of these publications may be obtained from:

SCIENTIFIC AND TECHNICAL INFORMATION OFFICE

NATIONAL AERONAUTICS AND SPACE ADMINISTRATION

Washington, D.C. 20546